Journal of Medicinal Chemistry

pubs.acs.org/jmc

Open Access

This article is licensed under CC-BY-NC-ND 4.0

Article

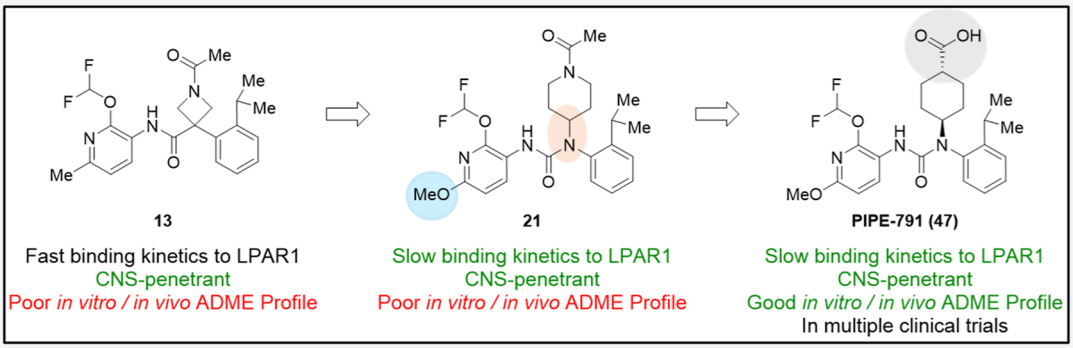
Discovery of PIPE-791, A Potent and Brain-Penetrant Lysophosphatidic Acid Receptor 1 Antagonist with Slow Tight Binding Characteristics for the Treatment of Neuroinflammatory Disorders

Austin Chen,* Christopher Baccei, Jill Baccei, Alexander Broadhead, Kym I. Lorrain, Michael M. Poon, Jeffrey Roppe, Thomas O. Schrader, Karin J. Stebbins, Lino Valdez, Yifeng Xiong, and Daniel S. Lorrain

Cite This: J. Med. Chem. 2026, 69, 15888−15927

Read Online

ACCESS | Metrics & More | Article Recommendations | Supporting Information



ABSTRACT: We describe the discovery and characterization of **PIPE-791**, a potent and brain-penetrant lysophosphatidic acid receptor 1 (LPAR1) antagonist with slow association and dissociation kinetics. SAR studies initiated from a literature lead (**13**) led to the identification of compound **21** that possessed a unique urea scaffold responsible for slow but tight binding to LPAR1. Further optimizations that improved PK and metabolic profiles led to the discovery of **PIPE-791**. **PIPE-791** efficiently traversed the BBB in multiple preclinical species and was efficacious in preclinical models of neuroinflammatory disorders. **PIPE-791** possessed excellent ADME properties and was well-tolerated in 28 day GLP (Good Laboratory Practice) toxicity studies in rats and minipigs at doses up to 1000 mg/kg/day. Based on these results and a comprehensive first-in-human enabling preclinical data package, **PIPE-791** was advanced into clinical development, including an ongoing trial in subjects with chronic osteoarthritis pain or chronic lower back pain (NCT6810245).

INTRODUCTION

Lysophosphatidic acids (LPAs), a family of signaling phospholipids where each member is distinguished by both the length and the degree of unsaturation of its fatty acid residue and by how this residue is linked to the glycerol backbone, are known to promote a host of cellular responses—including growth, differentiation, survival, and cytoskeletal rearrangement—through their activation of six cognate G protein coupled receptors (LPAR1−6).[1] LPAR1, LPAR2, and LPAR3 are members of the endothelial differentiation gene (EDG) subfamily, while LPAR4, LPAR5, and LPAR6 are members of the purinergic subfamily.[2]

Levels of circulating LPA, produced primarily from either autotaxin-catalyzed cleavage of lysophosphatidylcholine (LPC) or by phospholipase $A_{1/2}$-mediated hydrolysis of phosphatidic acid (PLA),[3] can become abnormally elevated in various human diseases. Increased LPA levels, when compared to healthy, age-matched controls,[4] have been detected in the serum of patients diagnosed with ovarian cancer,[5] hepatitis C infection,[6] or renal failure;[7] in the bronchoalveolar lavage fluid (BALF)[8] and exhaled breath condensates[9] of idiopathic pulmonary fibrosis (IPF) patients;[10] and in the CSF of patients with multiple sclerosis,[11] lumbar spinal canal stenosis (LSCS),[12] or traumatic brain injury.[13] While the inhibition of enzymes responsible for LPA production could represent an attractive avenue for the treatment of these diseases,[14,15] the challenges associated with sustaining full blockade of enzymes chronically and subsequent upregulation of other compensatory pathways have been

Received: April 1, 2026
Revised: June 8, 2026
Accepted: June 12, 2026
Published: June 29, 2026



© 2026 The Authors. Published by American Chemical Society

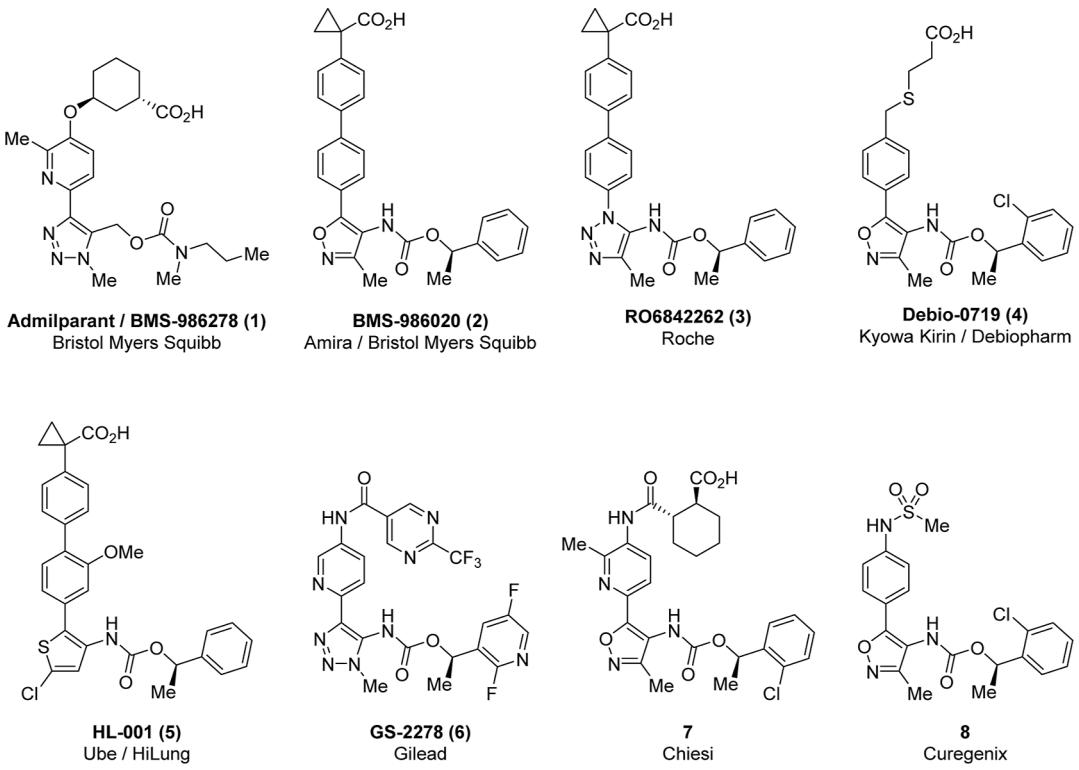


Figure 1. Selection of "L-shaped" LPAR1 antagonists in preclinical and clinical development.

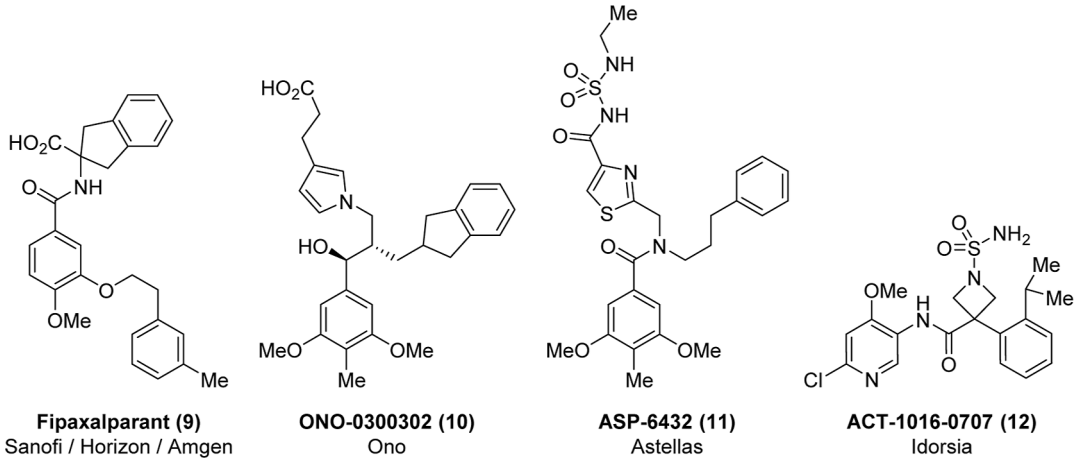


Figure 2. Selection of "T-shaped" LPAR1 antagonists in preclinical and clinical development.

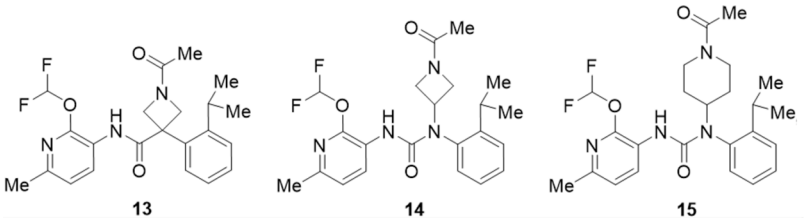
difficult to overcome in the clinic.[16] As such, modulation of the LPA-LPAR signaling axis, in particular LPAR1 which is expressed throughout various tissues and organs including the brain, spinal cord, heart, intestine, lung, kidney, spleen, and skeletal muscle,[1b] has emerged as a promising approach to the treatment of diseases in these tissues.[17] In particular, LPAR1 antagonists admilparant (**1**, Figure 1), a compound currently in Phase 3 clinical development for the treatment of idiopathic and progressive pulmonary fibrosis, and BMS-986020 (**2**, Figure 1) both demonstrated significant reduction in the forced vital capacity (FVC) decline of drug-treated patients.[18,19] It is worth noting that the development of BMS-986020, the first generation LPAR1 antagonist to enter clinical testing, was eventually halted due to the emergence of compound-specific hepatobiliary toxicity.[20]

RESULTS AND DISCUSSION

At the start of our medicinal chemistry program, despite the availability of studies that directly linked aberrant LPA-LPAR1 signaling to neurological dysfunction, we were not aware of a potent and selective LPAR1 antagonist that could effectively traverse the BBB. In fact, intrathecal or direct injection of LPAR1 antagonists into the brain was often necessary to evaluate the impact of LPAR1 antagonism in various animal models of CNS diseases.[21] To effectively target LPAR1 in the CNS space without needing to resort to such invasive procedures, we initiated a lead optimization campaign around the "L-shaped" bis-heteroaryl carbamate scaffold from which the most well-known LPAR1 antagonists (Figure 1), including admilparant, were derived.[22−29] This effort produced a series of potent and selective CNS-penetrant LPAR1 antagonists, including [^{18}**F**]-**OPC3497**;[30] a positron emission tomography

https://doi.org/10.1021/acs.jmedchem.6c01049
J. Med. Chem. 2026, 69, 15888−15927

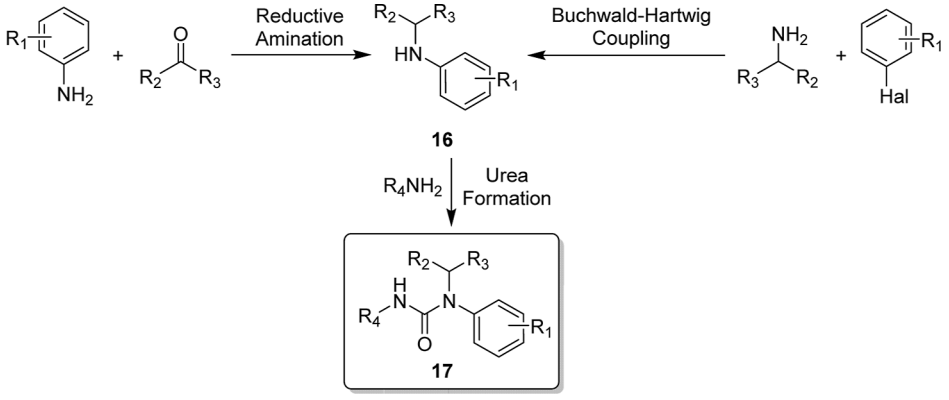
Table 1. Profiles of the Initial Promising Hits for Lead Optimization



	13	14	15
LPAR1 K_i (nM)[a]	12.6	45.0	2.1
LPAR1 Ca^{2+} mobilization assay IC_{50} (30 min preincubation, nM)[a]	45.9	1630	2094
LPAR1 Ca^{2+} mobilization assay IC_{50} (24 h preincubation, nM)[a]	48.9	58.9	7.1
rat PPB, brain tissue binding (% free)[b]	12.7, 2.5	13.4, 3.7	3.8, 1.2
rat PK @ 10 mpk PO and 2 mpk IV			
CL_{tot}, CL_u (mL/min/kg)	55,430	26,196	35,903
Vd (L/kg)	12.5	12.3	9.0
$T_{1/2,\ IV}$ (h)	9.3	15.9	10.2
F (%)	1.0	4.2	2.7
$K_{p,uu,\ brain,\ 2\ h}$[c]	0.48	0.47	0.30

[a]For number of replicates and standard error of the mean, see the Supporting Information. [b]PPB, plasma protein binding. [c]$K_{p,uu,brain,2h}$, unbound brain-to-plasma partition coefficient at 2 h postdose.

Scheme 1. Representative Synthetic Scheme to Access LPAR1 Antagonists with Urea Linker



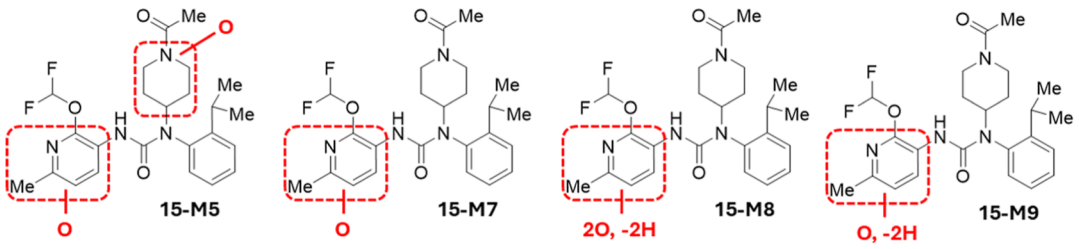
tracer that was successfully used in the clinic to assess LPAR1 target engagement in the brain.[31] However, the campaign was abandoned as it failed to deliver a development candidate with an acceptable therapeutic index and ADME properties sufficient to enable q.d. dosing.

Subsequent SAR studies carried out on other structurally distinct scaffolds that had previously afforded potent and selective peripherally restricted LPAR1 antagonists (Compounds **9**, **10**, and **11**, Figure 2)[22,32,33] proved to be similarly unproductive, until a series of patent applications from Idorsia where analogues of **ACT-1016−0707** (**12**), a potent LPAR1 antagonist with promising activity in preclinical models of fibrotic diseases, were disclosed.[34,35]

Amide **13** (Table 1), a compound disclosed in one of the patent applications from Idorsia,[34a] was a particularly promising starting point for our own medicinal chemistry optimization campaign. Despite its lack of an acidic headgroup or a lipophilic tail, structural features that were prevalent in most known LPAR1 antagonists (*vide supra*), **13** demonstrated high binding affinity for LPAR1 (K_i = 12.6 nM). Compound **13** also capably blocked LPA-induced calcium mobilization in B103 rat neuroblastoma cells that stably overexpressed human LPAR1 regardless of whether these cells were pretreated for 30 min (IC_{50} = 45.9 nM) or 24 h (IC_{50} = 48.9 nM) with the test article prior to the addition of 5 μM of 18:1 LPA (See Experimental Section for more details). Additionally, significant levels of **13** remained unbound when it was incubated for 6 h with either rat plasma (f_u = 0.127) or brain homogenate (f_u = 0.025). While amide **13** displayed moderate unbound clearance (CL_u = 430 mL/min/kg) and suboptimal oral bioavailability (F = 1.0%) when administered to rats as a suspension in conventional aqueous formulation, significant unbound concentrations of **13** could still be detected in both the brain and plasma 2 h post dose to give a calculated $K_{p,uu,\ brain}$ of 0.48. To enable rapid analoguing, we deliberately pivoted from the synthetically cumbersome spirocyclic amide scaffold in **13**[36] to one with a urea linker (**17**) where the requisite aniline precursor **16** could itself be readily assembled from commonly available starting materials using highly enabling transformations such as reductive amination or Buchwald−Hartwig coupling (Scheme 1).[37]

Among the initially synthesized compounds, urea **14** (Table 1) was profiled revealing anticipated similarities to its amide analogue **13** as well as noteworthy differences. Going from **13** to **14**, the insertion of a nitrogen atom led to a 2.2-fold improvement in unbound clearance and a concomitant increase

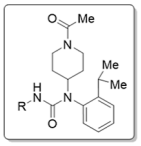
https://doi.org/10.1021/acs.jmedchem.6c01049
J. Med. Chem. 2026, 69, 15888−15927

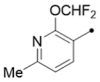
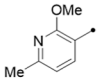
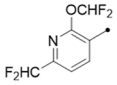
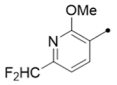
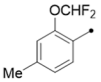
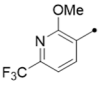
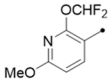
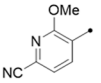
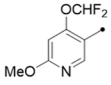
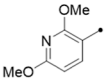
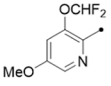


ID	Relative Peak Area from EIC of LM Samples @ 60 min[a]	
	Human	Rat
15-M5	4.6%	6.7%
15-M7	56.3%	69.6%
15-M8	5.1%	3.0%
15-M9	3.6%	4.0%
15-M10	1.7%	3.3%
15	25.3%	8.6%

Figure 3. LC−MS/MS analysis of metabolites formed after incubating 10 μM of compound **15** with 1 mg/mL of human and rat LM and 2 mM NADPH at 37 °C.

Table 2. Effects of Substituents and Pyridine Nitrogen on Western (Hetero)arene SAR[a]



Compound	R	LPAR1 Ca^{2+} IC_{50} 24 h pre-incubation (nM)[a]	HLM / RLM $T_{1/2}$ (min)[b]	Compound	R	LPAR1 Ca^{2+} IC_{50} 24 h pre-incubation (nM)[a]	HLM / RLM $T_{1/2}$ (min)[b]
15		2.1	8.9, 3.8	**24**		7.6	6.1, <2.5
18		39	5.6, 3.0	**25**		73	6.1, <2.5
19		45	12.6 , 5.0	**26**		77	14.6, 6.6
20		1.7	<2.5, <2.5	**27**		252	- , -
21		10	16.3, 11.0	**28**		899	- , -
22		159	- , -	**29**		49	10.3, 7.9
23		1,310	- , -	**30**		4,130	- , -

[a]For number of replicates and standard error of the mean, see the Supporting Information. [b]HLM, human liver microsome; RLM, rat liver microsome.

https://doi.org/10.1021/acs.jmedchem.6c01049
J. Med. Chem. 2026, 69, 15888−15927

in plasma half-life when these compounds were administered intravenously to rats. While their respective observed oral bioavailabilities were low, both compounds effectively partitioned into the brain. Compared to **13**, urea **14** exhibited a 3.6-fold drop in binding affinity to LPAR1, but the magnitude of its loss in functional potency (as measured by blockade of LPA-induced calcium mobilization) was context dependent. Specifically, when the preincubation time was limited to 30 min, **14** was a significantly (>35-fold) less potent LPAR1 antagonist than **13**. In contrast, when the preincubation time was extended to 24 h, these two compounds were found to be nearly equipotent. This unexpected potency dependence on incubation time was not unique to **14**, but a behavior shared by many other members of our urea series, including the ring expanded analogue **15**, where a 295-fold improvement in potency was observed after extending the incubation time to 24 h. This phenomenon, which was eventually ascribed to the slow binding kinetics of these urea compounds and the resulting long residence time on LPAR1 (*vide infra*), afforded us the opportunity to extend the duration of targeted pharmacodynamic effects beyond the limitations of PK properties.[38]

Although the LPAR1 potency of **15** satisfied our predefined development candidate profile, its high unbound plasma clearance (CL_u = 903 mL/min/kg) in rodents and the attendant low oral bioavailability (F = 2.7%) due to extensive first-pass metabolism proved unacceptable for further development. Incubation with human and rat liver microsomes (LM) revealed that the same set of metabolites were produced by both species, with the western aminopyridine ring being more metabolically labile than the piperidine ring (Figure 3). Additionally, the total relative peak area from extracted ion chromatogram (EIC) for metabolites associated with deacylation and/or oxidation of the eastern diisopropylaniline was less than 2% in both human and rat LM incubations. Furthermore, there were no detectable metabolites derived from the cleavage of the urea linker.

Considering the metabolic profile of compound **15**, we first focused our attention on optimizing the western aminopyridine ring. A limited selection of compounds that were exemplified are presented in Table 2. The parent masses and MS/MS fragmentation patterns of **15-M8** and **15-M9** metabolites suggested that the methyl substituent was efficiently oxidized by LM into a carboxylic acid and an aldehyde, respectively. However, deletion of this methyl group was not beneficial for stability in these LM incubations and was also accompanied by a 10-fold or more loss in LPAR1 potency (compare **15** vs **18**, and **24** vs **25**). It is possible that the *ortho*-methyl substitution may in fact be protecting the pyridine nitrogen from getting oxidized by providing steric hindrance. Therefore, other substituents *ortho* to the pyridine nitrogen with different electronic demands were examined. As was expected, given the well-trodden strategy of blocking metabolism with the installation of a C−F bond,[39] difluorination of the methyl group was accompanied by a quantifiable improvement in half-life (compare **15** vs **19**, and **24** vs **26**). Unfortunately, significant loss in potency (>10-fold) was also observed following difluorination of the methyl group. In fact, replacement of the methyl group *ortho* to the pyridine nitrogen by increasingly electron withdrawing substituents (**24**: Me, σ = −0.17; **26**: CHF_2, σ = 0.32; **27**: CF_3, σ = 0.54; vs **28**: CN, σ = 0.66)[40] resulted in a corresponding lowering of binding affinity to LPAR1. On the other hand, increasing the overall electron density of the aromatic ring through either the removal of the pyridine nitrogen (compare **15** vs **20**) or by switching out the difluoromethoxy substituent for methoxy (compare **15** vs **24**, **18** vs **25**, **19** vs **26**, and **21** vs **29**) did not significantly impact the LPAR1 functional potency. However, some of these modifications were accompanied by an unwanted drop in metabolic stability, with nonpyridine **20** being fully metabolized even at the first sampling time point (5 min) of both human and rat LM incubations. In this effort, the only structural permutation identified that resulted in an improvement over the starting point **15** was compound **21**, where the half-life extension in human and rat LM incubations did not come at an unacceptable cost in LPAR1 potency (2.1 nM vs 10 nM). A subsequent pyridine nitrogen walk carried out on **21** (compare **21** vs **22** and **23**) was similarly unproductive. In fact, compound **23** was prone to hydrolytic cleavage at the urea linker, especially when stored as a wet DMSO solution. This liability was also observed in all exemplified analogues where the pyridine nitrogen was situated *ortho* to the urea NH (data not shown). Finally, exemplified compounds with the pyridine nitrogen situated *para* to the urea NH (e.g., **30**) were accompanied by a significant loss in LPAR1 potency (compare **30** vs **25**).

Additional evaluations of compound **21** were carried out and summarized in Table 3. Compound **21** exhibited high affinity for LPAR1 in the membrane radioligand binding assay, with a K_i of 0.87 nM. As was observed with other analogues bearing the urea linker, significant improvement in the LPAR1 functional potency of **21** (354-fold) was achieved when the assay incubation time was extended from 30 min to 24 h. Consistent with the improved stability observed in rat LM incubation experiments, there was a decrease in first-pass metabolism that manifested as an increase in oral bioavailability going from **15** (F = 2.7%) to **21** (F = 48.5%). Although the clearance of **21** from plasma circulation was high in rat, the similarly high volume of

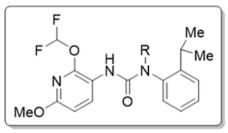
Table 3. Profile of Compound 21

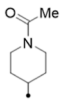
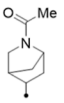
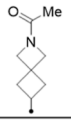
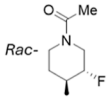
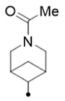
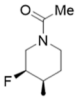
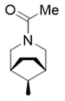
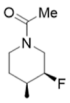
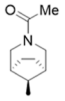
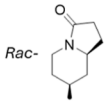
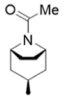
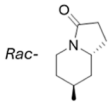
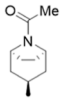
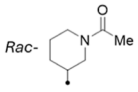
	21
LPAR1 K_i (nM)[a]	0.87
LPAR1 Ca^{2+} mobilization assay IC_{50} (30 min preincubation, nM)[a]	3540
LPAR1 Ca^{2+} mobilization assay IC_{50} (24 h preincubation, nM)[a]	10
rat PPB, brain tissue binding (% free)[b]	3.2, 2.2
rat PK @ 10 mpk PO and 2 mpk IV	
CL_{tot}, CL_u (mL/min/kg)	47, 1480
Vd (L/kg)	22.5
$T_{1/2,IV}$ (h)	11.9
F (%)	48.5
$K_{p,uu,brain,2h}$[c]	0.91
MDCK-MDR1 $P_{app,\ A\to B}/P_{app,\ B\to A}$ ($\times 10^{-6}$ cm/s), efflux ratio[d]	5.6/17.5, 3.1
CYP 1A2/2C9/2C19/2D6/3A4$_{mid}$ IC_{50} (μM)[e]	>30/>30/>30/24.8/11.8
manual patch clamp hERG IC_{50} (μM) @ 34 °C	>30
Eurofins SAFETYscan E/IC_{50} − 78 Assays	HTRA3 IC_{50} = 8.2 μM[f] nAChR(α4/β2) IC_{50} = 9.4 μM[g]

[a]For number of replicates and standard error of the mean, see the Supporting Information. [b]PPB, plasma protein binding. [c]$K_{p,uu,brain,2h}$, unbound brain-to-plasma partition coefficient at 2 h postdose. [d]MDCK-MDR1, Madin−Darby canine kidney cell transfected with human *MDR1* gene; $P_{app,A\to B}$, apparent permeability from apical to basolateral; $P_{app,B\to A}$, apparent permeability from basolateral to apical. [e]CYP3A4$_{mid}$, cytochrome P450 3A4 assay using midazolam as the probe substrate. [f]HtrA3, high-temperature requirement A serine peptidase 3. [g]nAChR, nicotinic acetylcholine receptor.

https://doi.org/10.1021/acs.jmedchem.6c01049
J. Med. Chem. 2026, 69, 15888−15927

Table 4. SAR of Piperidine Core Changes[a]



Compound	R	LPAR1 Ca^{2+} IC_{50} 24 h pre-incubation (nM)[a]	Compound	R	LPAR1 Ca^{2+} IC_{50} 24 h pre-incubation (nM)[a]
21		10	**37**		543
31		246	**38**		54
32		666	**39**		50
33		154	**40**		28
34		5,620	**41**		45
35		355	**42**		149
36		92	**43**		139

[a]For number of replicates and standard error of the mean, see the Supporting Information.

distribution indicated that the compound was well distributed into the tissues leading to a half-life of 11.9 h. In vitro, compound **21** was found to be moderately permeable across epithelial monolayers prepared from Madin−Darby canine kidney (MDCK) cells overexpressing P-gp transporters, with an acceptable efflux ratio of 3.1.[41] When the unbound concentrations of **21** in plasma and brain were quantified 2 h post oral dosing in rats, a $K_{p,uu,brain}$ of 0.91 confirmed that **21** readily partitioned into the CNS in vivo. The DDI risk of compound **21** as a perpetrator through its inhibition of CYP enzymes was also evaluated, and **21** was found to be a moderate inhibitor of CYP3A4 with midazolam as the probe substrate (IC_{50} = 11.8 μM). To assess the off-target promiscuity of compound **21**, it was tested against 78 assays using the Eurofins SAFETYscan E/IC_{50} ELECT service.[42] At a top testing concentration of 10 μM, **21** was found to only inhibit two off-targets, namely HtrA Serine Peptidase 3 (HTRA3) and nicotinic acetylcholine receptor α4/β2 (nAChR α4/β2), with an IC_{50} of 8.2 and 9.4 μM, respectively (see Supporting Information). Critically, compound **21** did not inhibit the activity of hERG at 30 μM in a manual patch-clamp assay.

Metabolite analysis from human and rat LM incubations had also implicated the central piperidine ring as a potential metabolic soft spot (see metabolites **15-M5** and **15-M10** in Figure 3). Having established **21** as a promising new lead, derivatives with substituted, spirocyclic, and bridged piperidine cores were exemplified, with a selection of these compounds presented in Table 4. While azaspiro[3.3]heptane has found success in drug discovery programs as a more soluble and metabolically stable bioisostere of piperidine,[43] its incorporation into our scaffold was not well tolerated for binding to LPAR1 (compare **21** vs **31**). Similarly, all bridged piperidine derivatives of **21**—regardless of the length of the alkylene bridge, the positional connectivity of the alkylene bridge with respect to the piperidine nitrogen, or the stereochemistry of the alkylene bridge with respect to the 4-piperidinyl carbon anchor—were also significantly less potent at antagonizing LPAR1 (compare **21** vs **32**, **33**, **34**, **35**, **36**, and **37**). Combined, these observations suggested that the LPAR1 binding pocket above and below the plane of compound **21**'s piperidine ring cannot readily accommodate rigid steric bulk. Even the incorporation of a single fluorine atom (compare **21** vs **38**, **39**, and **40**) was accompanied by a 3- to 5-fold loss in LPAR1 potency.

https://doi.org/10.1021/acs.jmedchem.6c01049
J. Med. Chem. 2026, 69, 15888−15927

Table 5. Effects of Increasing Polarity on Core SAR[a]

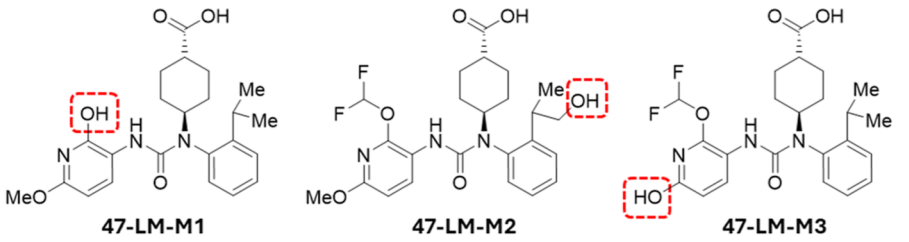
Compound	X	c Log D @ pH = 7.4	LPAR1 Ca^{2+} IC_{50} 24 h pre-incubation (nM)[a]	Rat PK @ 10 mpk PO and 2 mpk IV: PPB (% free)[b]	CL_u (mL/min/kg)	Vd (L/kg)	$T_{1/2,IV}$ (h)	F (%)	$AUC_{PO,free}$ (hr*μg/mL)	$C_{6h,free}$ (nM)	$C_{24h,free}$ (nM)	$K_{p,uu,brain,2h}$[c]
21		4.0	10	3.2	1,480	22.5	11.9	49	0.048	2.8 (0.28-fold over IC_{50})	1.1 (0.11-fold over IC_{50})	0.91
44		3.5	18	9.1	346	17.0	10.7	28	0.118	14 (0.76-fold over IC_{50})	0.52 (0.03-fold over IC_{50})	0.85
45		3.9	23	1.6	994	6.9	7.5	42	0.066	7.3 (0.32-fold over IC_{50})	1.9 (0.08-fold over IC_{50})	0.33
46		3.4	9.8	4.7	268	1.6	2.5	21	0.127	18 (1.9-fold over IC_{50})	0.58 (0.06-fold over IC_{50})	0.22
47		2.5	9.9	5.7	62	1.9	7.3	78	1.97	220 (22-fold over IC_{50})	86 (8.7-fold over IC_{50})	0.47
48		2.9	9.4	3.1	269	3.3	6.5	51	0.302	31 (3.3-fold over IC_{50})	6.2 (0.66-fold over IC_{50})	0.52
49		2.9	7.1	3.1	452	3.6	5.1	120	0.376	29 (4.2-fold over IC_{50})	7.9 (1.1-fold over IC_{50})	0.50

[a]For number of replicates and standard error of the mean, see the Supporting Information. [b]PPB, plasma protein binding. [c]$K_{p,uu,brain,2h}$, unbound brain-to-plasma partition coefficient at 2 h postdose.

Additionally, fluorination also failed to significantly extend the half-life of these compounds in human LM incubations ($T_{1/2}$ for **39** and **40** were determined to be 19.2 and 14.6 min, respectively). *Cis*- (**41**) and *trans*-fused (**42**) bicyclic γ-lactams, formally derived from the intramolecular cyclization of the acyl group onto the piperidine ring, were both less potent than **21**, with the *cis* stereochemistry being better tolerated for LPAR1 potency. While **41** was prepared as a racemic mixture, attempts to resolve it into its optically pure antipodes were unsuccessful. Compound **43**, the 3-piperidinyl constitutional isomer of **21**, was also determined to be inferior.

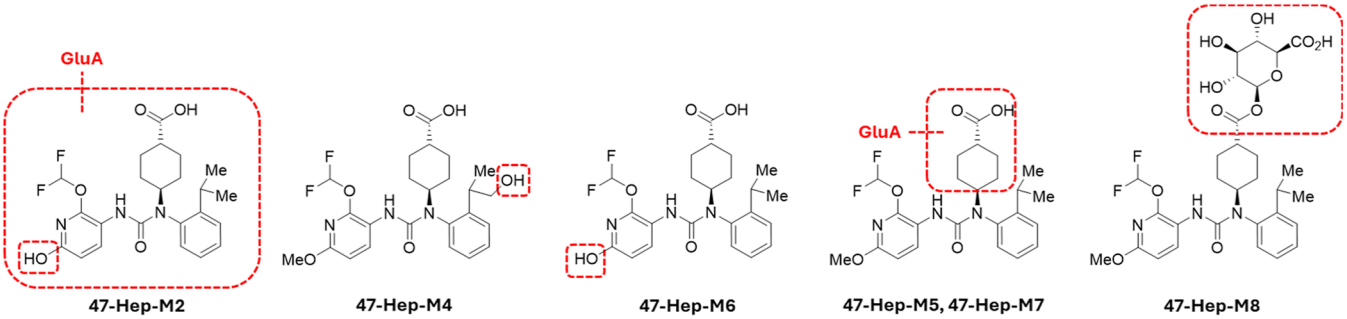
Higher lipophilicity is known to increase drug clearance.[44] With a calculated log D of 4.0 for compound **21**,[45] a campaign aimed at substituting the *N*-acetamide cap with more polar groups was conducted. In this effort, we were cognizant that lipophilicity-based optimization of unbound clearance could become counterproductive if one neglected to also account for its impact on volume of distribution.[46] Rat PK was therefore utilized to drive this late phase optimization, with the conservative assumption that the desired efficacy would be dictated by fold of unbound C_{min} over the LPAR1 functional IC_{50}. In this regard, both rat $C_{6h,free}$ and $C_{24h,free}$ could be treated as markers for unbound C_{min} since single-species allometric scaling would suggest that the half-life of human is approximately 4-times the half-life of rat.[47] Additionally, because unchecked increase in polarity is known to be detrimental for permeation across the BBB[48] and we were focused on antagonizing LPAR1 in the CNS, priority was given to the design and synthesis of compounds with a calculated log *D* between 1 and 4. For brevity, only profiles of compounds with $K_{p,uu,brain} > 0.1$ at 2 h post oral dose are shown in Table 5. It was apparent that this region of the LPAR1 pocket was tolerant of both polarity as well as steric bulk. Replacement of the acyl terminus in **21** with an oxetane, a known carbonyl bioisostere,[49] in **44** (calculated log *D* = 3.5) was accompanied by a 1.8-fold decrease in LPAR1 potency and a 2.8-fold increase in plasma free fraction. The drop in lipophilicity improved unbound clearance from plasma, but this did not translate into an extension of terminal half-life. While the overall unbound plasma exposure of **44** was improved over **21**, it was not sufficient to overcome the LPAR1 potency loss. Switching the *N*-acetamide in **21** for *N*-sulfonamide in **45** did not significantly alter the calculated log *D* and afforded a compound with a very similar profile. One key difference, a significant reduction in brain partitioning ($K_{p,uu,brain,2h}$ = 0.33 for **45** vs $K_{p,uu,brain,2h}$ = 0.91 for **21**) was a consequence of **45** being a substrate of P-gp mediated efflux (efflux ratio = 9.2 in the NIH MDCK-MDR1 assay). Substituting the piperidine nitrogen in **45** with a CH group afforded a pair of *cis*- and *trans*-cyclohexyl methyl sulfone diastereomers. The significantly more potent *cis* isomer **46** (9.8 nM vs 299 nM for the *trans* isomer, not shown) was further profiled. While the additional polarity had the intended beneficial effect on unbound plasma clearance (CL_u = 268 mL/min/kg), sulfone **46** was not deeply distributed into the tissues, including the brain ($K_{p,uu,brain,2h}$ = 0.22), and exhibited an unacceptably short half-life of 2.5 h. A key breakthrough was realized when a carboxylic acid was tethered onto the cyclohexane core. In this permutation, the *trans* isomer **47** was the more potent LPAR1 antagonist (9.9 nM vs 112 nM for the *cis* isomer, not shown). Across all key parameters under consideration, acid **47** was found to be superior to all other compounds exemplified in the urea series, including having the lowest unbound plasma clearance as well as the highest overall unbound plasma exposure in rats. At 6 and 24 h post a single 10 mg/kg oral dose, the unbound plasma concentrations of **47** in rat were 22- and 8.7-fold over its LPAR1 functional potency, respectively. Additionally, despite being an alkyl carboxylic acid, **47** was not extensively plasma protein-bound (f_u = 0.057) and was CNS penetrant ($K_{p,uu,brain,2h}$ = 0.47).[50] The latter was consistent with the finding that, in the NIH MDCK-MDR1 assay, **47** was highly permeable ($P_{app,A\rightarrow B} = 11 \times 10^{-6}$ cm/s; $P_{app,B\rightarrow A} = 26 \times 10^{-6}$ cm/s) and not a substrate of P-gp mediated

https://doi.org/10.1021/acs.jmedchem.6c01049
J. Med. Chem. 2026, 69, 15888−15927



ID	Relative Peak Area from EIC of LM Samples @ 60 min[a]		LPAR1 Ca^{2+} IC_{50} 24 h pre-incubation(nM)[b]
	Human	Rat	
47-LM-M1	0.6%	Not detected	2,130
47-LM-M2	1.0%	Not detected	233
47-LM-M3	3.3%	0.4%	69
47	95.1%	99.7%	9.9

Figure 4. LC−MS/MS analysis of metabolites formed after incubating 10 μM of compound **47** with 1 mg/mL of human and rat liver microsomes and 2 mM NADPH at 37 °C, and their respective LPAR1 inhibitory potencies.



GluA, glucuronic acid.

ID	Relative Peak Area from EIC of Hepatocyte Samples @ 240 min[a]				
	Human	Monkey	Minipig	Dog	Rat
47-Hep-M2	0.7%	1.5%	Not detected	0.3%	0.5%
47-Hep-M4	1.8%	2.9%	0.3%	Not detected	Not detected
47-Hep-M5	0.2%	1.2%	1.2%	0.5%	Not detected
47-Hep-M6	2.3%	2.7%	0.7%	1.0%	0.4%
47-Hep-M7	0.5%	2.1%	1.6%	1.0%	0.2%
47-Hep-M8	6.6%	15.6%	9.6%	10.4%	8.8%
47	87.9%	72.8%	86.8%	86.8%	90.2%

Figure 5. LC−MS/MS analysis of metabolites formed after incubating 10 μM of compound **47** with 1 × 10^6 cells/mL of hepatocytes at 37 °C.

efflux (efflux ratio = 2.4). Surprisingly, compound **48** and its epimer **49** were both potent antagonists of LPAR1, but neither of these two methylene homologated carboxylic acids offered any advantage in their respective rat PK profile over compound **47** and thus were not profiled further.

To determine whether the substantial improvements in rat PK realized with compound **47** were translatable to human, incubations with rat and human LM were carried out (Figure 4). In stark contrast to what was observed with **15** (Figure 3), under identical experimental conditions, 95.1% and 99.7% of **47** were recovered unchanged after 60 min of incubation with human and rat LM, respectively. In this setting, one metabolite (**47-LM-M3**) derived from demethylation of the methoxy group was formed in both rat and human whereas two additional metabolites—one from dedifluoromethylation of the difluoromethoxy group (**47-LM-M1**) and another from oxidation of the terminal methyl of the isopropyl substituent (**47-LM-M2**)—were only observed in humans. The structures of all three metabolites were confirmed through independent synthesis (*vide infra*) and their respective functional LPAR1 potencies were determined and found to be significantly less potent than parent **47**.

To accurately assess the impact of combined Phase I and Phase II metabolism on **47**, the compound was incubated with cryopreserved hepatocyte suspensions from Sprague−Dawley rats, Beagle dogs, Göttingen minipigs, Cynomolgus monkeys, and humans (Figure 5). Six distinct metabolites were produced by human hepatocytes, two of which were also detected in human LM incubations and formed in comparable quantities (**47-LM-M2** is **47-Hep-M4:** 1.0% in LM vs 1.8% in hepatocytes;

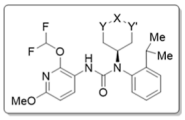
https://doi.org/10.1021/acs.jmedchem.6c01049
J. Med. Chem. 2026, 69, 15888−15927

Table 6. Higher Order Preclinical Species PK of Compound 47 and Select In Vitro ADME Profile

						PK @ 5 mpk PO and 2 mpk IV				
species	PPB (% free)[a]	Hep $T_{1/2}$ (min)[b]	CL_{tot}, CL_u (mL/min/kg)	Vd (L/kg)	$T_{1/2,IV}$ (h)	F (%)	$AUC_{PO\ free}$ (hr*μg/mL)	$C_{max,free}$ (nM)	$C_{24h,free}$ (nM)	$K_{p,uu,brain,2h}$[c]
dog	0.8	862	0.48, 60	0.39	15	39	0.451	97 @ 1.7 h	34	0.80
minipig	2.8	195	5.2, 186	3.2	14	54	0.187	27 @ 4.0 h	14	not determined
monkey	3.5	468	3.0, 86	1.5	9.6	66	0.575	193 @ 1.7 h	25	not determined
human	1.5	1150								

[a]PPB, plasma protein binding. [b]Determined using the hepatocyte incubation assay (refer to Experimental Section for detailed protocol). [c]$K_{p,uu,brain,2h}$, unbound brain-to-plasma partition coefficient at 2 h postdose.

Table 7. Effects of Alpha Substitution to the Carboxylic Acid Headgroup of Compound 47[a]



							Rat PK @ 10 mpk PO and 2 mpk IV						
Compound	Y-X-Y'	c Log D @ pH = 7.4	LPAR1 Ca^{2+} IC_{50} 24 h pre-incubation (nM)[a]	PPB (%)[b]	CL_u (mL/min/kg)	Vd (L/kg)	$T_{1/2,IV}$ (h)	F (%)	$AUC_{PO,free}$ (hr*μg/mL)	$C_{6h,free}$ (nM)	$C_{24h,free}$ (nM)	$K_{p,uu,brain,2h}$[c]	PXR Activation @ 10 μM[d]
47		2.5	9.9	5.7	62	1.9	7.3	78	1.97	220 (22-fold over IC_{50})	86 (8.7-fold over IC_{50})	0.47	2.2-fold
50		2.8	26	2.1	378	2.8	5.3	36	0.153	14 (0.77-fold over IC_{50})	2.9 (0.11-fold over IC_{50})	0.46	4.9-fold
51		3.1	3.6	2.6	428	2.3	7.1	54	0.216	2.6 (0.71-fold over IC_{50})	0.45 (0.13-fold over IC_{50})	0.50	8.3-fold
52		3.1	1.9	2.2	409	2.4	7.2	60	0.236	23 (12-fold over IC_{50})	1.1 (0.57-fold over IC_{50})	0.69	8.0-fold

[a]For number of replicates and standard error of the mean, see the Supporting Information. [b]PPB, plasma protein binding. [c]$K_{p,uu,brain,2h}$, unbound brain-to-plasma partition coefficient at 2 h postdose. [d]PXR, pregnane X receptor.

47-LM-M3 is **47-Hep-M6:** 3.3% in LM vs 2.3% in hepatocytes). The other four metabolites were derived from direct glucuronidation of **47** (**47-Hep-M8**: 6.6%, structure confirmed through independent synthesis, *vide infra*) and subsequent isomerization (**47-Hep-M5**: 0.2%; **47-Hep-M7**: 0.5%), or from glucuronidation of metabolite **47-Hep-M6** (**47-Hep-M2**: 0.7%). However, it is notable that the main peak in the EIC was parent **47**, with 87.9% remaining unchanged after 240 min of incubation with human hepatocytes. Across all the preclinical species examined, acid **47** was recovered mainly intact with the compound being most stable in rat (90.2% parent remaining) and least stable in monkey (72.8% parent remaining). Additionally, no unique human metabolites were detected in vitro using hepatocyte incubations.

The PK profiles of compound **47** in higher order preclinical species are shown in Table 6. As was observed previously in rats, compound **47** was found to be orally bioavailable in dogs, minipigs and monkeys, with *F* ranging from 39% in dogs to 66% in monkeys. Additionally, significant quantities of unbound **47** were found in the plasma and brain of dogs 2 h-post oral dose with a calculated $K_{p,uu,brain,2h}$ of 0.80 thereby confirming that efficient CNS penetration was achieved with **47** in higher order species as well. The in vivo unbound clearance of compound **47** was low across all three species evaluated but was highest in minipig (CL_u = 186 mL/min/kg) and lowest in dog (CL_u = 60 mL/min/kg), and consistent with what was observed in the in vitro hepatocyte stability experiments. The PK curves of all three species exhibited signs of enterohepatic recirculation (see Supporting Information), which effectively prolonged the apparent drug half-life of **47** (ranging from 9.6 h in monkey to 15 h in dog) while blunting its peak-to-trough ratio. This behavior suggested that the acyl glucuronide metabolite(s) formed in the liver—and observed in vitro in the corresponding hepatocyte incubations—were being excreted via bile into the intestine and either (1) cleaved back into parent **47** by bacterial β-glucuronidase and reabsorbed, or (2) directly retaken up by the intestinal enterocytes before being cleaved back into parent **47** by enteric β-glucuronidase. In rats and minipigs, we confirmed that the acyl glucuronide metabolite **47-Hep-M8** was the major metabolite found circulating in the plasma in an amount that was dependent on both the species and the route of drug administration. In rats, the total $AUC_{0\rightarrow 24h}$ of **47-Hep-M8** were 4.0% and 2.1% of unchanged **47** for PO- and IV-administered animals, respectively. In minipigs, the total $AUC_{0\rightarrow 24h}$ of **47-Hep-M8** were 60.4% and 29.0% of unchanged **47** for PO- and IV-administered animals, respectively.

While carboxylic acid-containing molecules are well represented in FDA-approved drugs, some have received black box warnings or were withdrawn due to the risk of idiosyncratic drug toxicity (IDT).[51] Although the causes of IDT can be complex and multifactorial in nature, one important contributor involves the triggering of an immune cascade in response to haptens formed from the covalent binding of reactive metabolites to proteins. In case studies involving withdrawn carboxylic acid-

https://doi.org/10.1021/acs.jmedchem.6c01049
J. Med. Chem. 2026, 69, 15888−15927

Table 8. Induction of Major CYP Isozymes in Cryopreserved Human Hepatocytes Following 3 Day Incubation with PIPE-791

CYP	average fold Induction of CYP in hepatocytes from 3 donors as measured by mRNA or enzyme activity						apparent E_{max}(fold)	apparent EC_{50}(μM)	fold induction of PC[a]
	0.1 μM PIPE-791	0.75 μM PIPE-791	1.5 μM PIPE-791	5 μM PIPE-791	15 μM PIPE-791	50 μM PIPE-791			
1A2	1.00	1.00	0.98	0.95	0.87	0.73	-	-	61.4
2B6	1.07	1.14	1.11	1.22	1.57	2.89	-	-	5.75
2C8	1.15	1.17	1.39	1.51	2.28	3.31	-	-	4.97
2C9	1.11	1.16	1.18	1.32	1.46	1.63	-	-	3.44
2C19	0.95	1.00	0.99	1.01	1.12	1.30	-	-	2.97
3A4	1.28	1.69	1.71	3.02	9.99	21.7	28.9	25.6	57.4

[a]Positive control (PC) used: 50 μM of Omeprazole (CYP1A2), 750 μM of Phenobarbital (CYP2B6), and 25 μM Rifampin (CYP 2C8, 2C9, 2C19, and 3A4).

Table 9. Direct and Time-dependent Inhibition of PIPE-791 on Major Human CYP Isozymes

CYP	marker substrate(concentration)	isoform-catalyzed reaction	CYP inhibition with PIPE-791		
			no pre-incubation (IC_{50}, DI, μM)[a]	30 min pre-incubation (IC_{50}, TDI, μM)[b]	TDI shift (fold)[b]
1A2	phenacetin (50 μM)	O-deethylation	>100	>100	-
2B6	bupropion (50 μM)	hydroxylation	>100	>100	-
2C8	amodiaquine (2 μM)	*N*-deethylation	17.4	7.73	2.25
2C9	diclofenac (5 μM)	4′-hydroxylation	>100	>100	-
2C19	*S*-mephenytoin (20 μM)	4′-hydroxylation	>100	>100	-
2D6	bufuralol (5 μM)	1′-hydroxylation	>100	>100	-
3A	midazolam (2 μM)	1′-hydroxylation	>100	86.8	>1.15
3A	testosterone (50 μM)	6β-hydroxylation	>100	80.5	>1.24

[a]DI, direct inhibition. [b]TDI, time-dependent inhibition.

containing drugs such as benoxaprofen, ibufenac, and zomepirac, the proposed culprit had been their respective reactive acyl glucuronide metabolites.[52] From these investigations, for a given total body burden,[53] the reactivity of the acyl glucuronide in question—whether by the direct displacement of the acyl residue with nucleophiles or by acyl migration followed by ring opening to reveal an aldehyde warhead—was found to correlate well with risk for IDT.[52,54] In this regard, the experimentally determined half-life of acyl glucuronide **47-Hep-M8** in 100 mM pH 7.4 potassium phosphate buffer at 37 °C was 149 min or 2.5 h (see Supporting Information). Additionally, its acyl migration rate—a ratio of the combined peak areas of all rearranged isomers of **47-Hep-M8** over the total peak area of all acyl glucuronide peaks (including unchanged **47-Hep-M8**) at the end of the 240 min incubation time—was determined to be 4.3% (see Supporting Information). Although the half-life of **47-Hep-M8** in KPB was slightly shorter than the recommended 3.6 h threshold separating safe drugs (half-lives of 7.2 h or longer) from withdrawn drugs (half-lives of 1.7 h or shorter),[52] when this value was considered in combination with its low acyl migration rate (less than 10%),[54] the potential of **47** to cause IDT in humans was assessed to be low.

Concurrently, we also investigated whether the formation of an acyl glucuronide metabolite could be completely obviated by disfavoring its formation through the judicious addition of bulk adjacent to the carboxylic acid headgroup (Table 7). α-Methylated analog **50** was found to be 2.6-fold less potent on LPAR1 than **47**. We were pleased to see that a cyclopropane ring spanning the α- and β-carbons to the carboxylic acid was in fact beneficial for LPAR1 potency (compare **47** vs **51** and **52**). However, while no peaks associated with the acyl glucuronide metabolite mass of **50**, **51**, and **52** were detected by LC−MS/MS in the plasma of rats dosed with these sterically encumbered acids at all the time points sampled, the overall unbound oral exposures of the circulating parent compound in each of these cases (**50**: $AUC_{PO,free}$ = 0.153 h*μg/mL; **51**: $AUC_{PO,free}$ = 0.216 h*μg/mL; **52**: $AUC_{PO,free}$ = 0.236 h*μg/mL) were all significantly less than that of compound **47** ($AUC_{PO,free}$ = 1.97 h*μg/mL). Additionally, at a nominal testing concentration of 10 μM, compounds **50**, **51**, and **52** were found to be moderate (**50**: 4.9-fold) to strong (**51**: 8.3-fold; **52**: 8.0-fold) activators of the PXR, a potentially significant DDI liability that was also shared by **ACT-1016−0707** (**12**: 5.6-fold PXR activation at 1 μM, 12.1-fold PXR activation at 10 μM). The sum of these data indicated that acid **47** remained the most promising compound for additional profiling and it was subsequently designated as clinical development candidate **PIPE-791**.

To identify the human UDP-glucuronosyltransferase (UGT) enzymes responsible for the formation of acyl glucuronide metabolite **47-Hep-M8**, **PIPE-791** was independently incubated with a panel of recombinant UGT isozymes—UGT 1A1, 1A3, 1A4, 1A6, 1A9, 2B7, and 2B15, in the presence of UDP glucuronic acid (UDPGA) at 37 °C for up to 60 min. Time dependent increases in the area ratio of **47-Hep-M8**, albeit small, were only observed in incubations with UGT 1A1 (0.5% of parent **PIPE-791** at 60 min) and 1A3 (4.3% of parent **PIPE-791** at 60 min). Similarly, minimal metabolic turnover was observed after **PIPE-791** was incubated with 0.6 mg/mL of human LM and an NADPH regenerating system at 37 °C for 60 min (91.4% of **PIPE-791** was recovered unchanged at the end of the incubation period). This result necessitated the use of recombinant human CYP enzymes for our reaction phenotyping study with **PIPE-791**. Of the panel of eight recombinant human CYPs screened, significant metabolic conversion was only achieved when **PIPE-791** was incubated with 50 pmol/mL of CYP2C8 (half-life = 13.2 min, see Supporting Information). Recombinant human CYP3A4 also contributed to a small extent to the Phase I metabolism of **PIPE-791** (12.1% conversion was

https://doi.org/10.1021/acs.jmedchem.6c01049
J. Med. Chem. 2026, 69, 15888−15927

achieved after 60 min of incubation), although a half-life could not be calculated. Additionally, it is unlikely that human transporters will play a significant role in the elimination or distribution of **PIPE-791** as it was not found to be a substrate of MDR1, BCRP, BSEP, MATE1, MATE2-K, OAT1, OAT3, OATP1B1, OATP1B3, OCT1, and OCT2 transporters (see Supporting Information). Therefore, it is anticipated that, in human, **PIPE-791** will be well distributed throughout the body—including into the CNS—and mainly excreted unchanged as the parent.

The potential of compound **PIPE-791** to induce (Table 8) or inhibit, both directly and in a time-dependent manner (Table 9), major drug-metabolizing human CYP enzymes was subsequently determined. In CYP induction studies carried out with cryopreserved hepatocytes from three separate human donors, nominal testing concentrations of up to 50 μM of **PIPE-791** could be used. It was confirmed that at 50 μM, **PIPE-791** (1) remained fully soluble in the incubation media, (2) was not metabolized to an appreciable extent (98.1% recovery), and (3) had no significant impact on the viability of these hepatocytes (98.9% viability relative to solvent-treated control) after 3 days of incubation. Incubating with 50 μM of **PIPE-791** did not lead to greater than 2-fold induction of CYP1A2 and CYP2C9, as measured by mRNA expression, nor of CYP2C19, as measured by enzyme activity. Additionally, less than 2-fold induction of CYP2B6 and CYP2C8 mRNA was seen when these hepatocytes were incubated with 15 and 5 μM of **PIPE-791**, respectively. **PIPE-791** was however found to be an inducer of CYP3A4, with an apparent EC_{50} of 25.6 μM and an apparent E_{max} of 28.9-fold. On the other hand, using human liver microsomes, **PIPE-791** showed no or limited direct and time-dependent inhibition (TDI) effects on CYP 1A2, 2B6, 2C9, 2C19, and 2D6 (Table 9) at a nominal testing concentration of 100 μM, the top concentration evaluated. While <50% direct inhibition of either CYP3A-mediated midazolam 1′-hydroxylation or testosterone 6β-hydroxylation was observed with 100 μM of **PIPE-791**, a time-dependent increase in the inhibition of this isozyme was seen after human LM were preincubated with **PIPE-791** for 30 min in the presence of NADPH ($IC_{50,TDI}$ = 86.8 μM for midazolam 1′-hydroxylation; $IC_{50,TDI}$ = 80.5 μM for testosterone 6β-hydroxylation). Since **PIPE-791** was previously found to be a CYP2C8 substrate during our CYP reaction phenotyping studies (*vide supra*), it was, as anticipated, also a direct and a time-dependent inhibitor of CYP2C8 with an apparent IC_{50} of 17.4 and 7.73 μM, respectively. Since the overall risk of a given compound to precipitate CYP-mediated DDI at its anticipated therapeutic dose needs to be interpreted in the context of its projected steady state exposure in the liver, it is worth noting that the liver-to-plasma partitioning ratio of **PIPE-791** was determined to be 4.3 in rats.

To assess the risk of **PIPE-791** to act as a perpetrator of transporter-mediated DDI, its ability to inhibit a panel of human transporters was also quantified (Table 10). At a top testing concentration of 30 μM, **PIPE-791** minimally inhibited MDR1-mediated bidirectional transport of digoxin (15.6% inhibition), BCRP-mediated bidirectional transport of prazosin (11.4% inhibition), as well as MATE1- and MATE2-K-mediated uptake of metformin (9.1% inhibition and −18.0% inhibition, respectively) in MDCK cell lines that overexpressed these transporters. Similarly, at 30 μM, **PIPE-791** did not significantly inhibit OAT1-mediated uptake of *p*-aminohippuric acid (13.3% inhibition), or OCT1- and OCT2-mediated uptake of tetraethylammonium (−18.1% inhibition and −7.0% inhibition, respectively) in CHO cell lines that overexpressed these transporters. However, **PIPE-791** did dose-dependently inhibit OAT3-mediated uptake of estrone-3-sulfate (IC_{50} = 23.0 μM), OATP1B1-mediated uptake of estradiol-17β-glucuronide (IC_{50} = 3.5 μM), and OATP1B3-mediated uptake of cholecystokinine-8 (IC_{50} = 20.7 μM). With the toxic buildup of hepatic bile acids having been identified as the primary cause of hepatobiliary toxicity seen with LPAR1 antagonist **BMS-986020** (**2**) in the clinic,[20,24] whether **PIPE-791** similarly inhibited BSEP, a key transporter involved in maintaining bile acid homeostasis, was of particular interest. Gratifyingly, using inside-out membrane vesicles prepared from HEK293 cells overexpressing BSEP, **PIPE-791** only weakly inhibited BSEP-mediated transport of taurocholate in the presence of ATP with an IC_{50} of 24.4 μM.

Table 10. Inhibition of Major Human Transporters with PIPE-791

transporter[a]	probe substate (concentration)	apparent IC_{50}(μM)
MDR1	digoxin (1 μM)	>30
BCRP	prazosin (1 μM)	>30
MATE1	metformin (2 μM)	>30
MATE2-K	metformin (10 μM)	>30
OAT1	aminohippuric acid (0.4 μM)	>30
OAT3	estrone-3-sulfate (1 μM)	23.0
OATP1B1	estradiol-17β-glucuronide (1 μM)	3.5
OATP1B3	cholecystokinine-8 (0.1 μM)	20.7
OCT1	tetraethyl-ammonium (5 μM)	>30
OCT2	tetraethyl-ammonium (5 μM)	>30
BSEP	taurocholate (2 μM)	24.4

[a]BCRP, breast cancer resistance protein; BSEP, bile salt export pump; MATE, multidrug and toxin extrusion protein; MDR, multidrug resistance; OAT, organic anion transporter; OATP, organic anion transporting polypeptide; OCT, organic cation transporter.

In light of a recent study that questioned whether the in vivo hepatobiliary toxicity potential of a given compound can be sufficiently derisked with just an in vitro biochemical assay that quantified the direct inhibition of an isolated bile acid transporter like BSEP,[28] we decided to evaluate **PIPE-791** in a more predictive in vitro system that assessed the dose-dependent impact of **PIPE-791** on sandwich-cultured human hepatocytes (SCHH) with fully functional transporters that had been challenged with a physiological mixture of bile acids.[55] In this setup, a sufficient concentration of bile acids (250 μM) was used to unbalance the bile acid homeostasis without inducing hepatotoxicity unless the adaptive mechanisms of the cultured hepatocytes were also disrupted by the test article. As expected, treatment of SCHH with 50 μM of imatinib, a known hepatotoxic compound, led to extensive lactate dehydrogenase (LDH) leakage (280% of solvent control) and ATP depletion (4.3% of solvent control) even in the absence of additional bile acids. On the other hand, increases in LDH leakage (219% of solvent control) and decreases in ATP content (3.4% of solvent control) were only observed when SCHH were challenged with both 75 μM of troglitazone, a potent inducer of hepatic cholestasis,[56] and a media containing additional bile acids. Most importantly, at all concentrations examined, **PIPE-791** demonstrated no potential for general nor cholestatic hepatotoxicity as the levels of both LDH and ATP in **PIPE-791**-treated SCHH were comparable to those of solvent control, regardless of whether excess bile acids were added (Table 11).

The in vitro and in vivo pharmacology of **PIPE-791**, including its efficacy in various preclinical disease models of multiple

https://doi.org/10.1021/acs.jmedchem.6c01049
J. Med. Chem. 2026, 69, 15888−15927

Table 11. LDH Leakage and ATP Content Following 24 h Exposure of SCHH to Test Articles

compound	testing concentration (μM)	standard media		media with 250 μM bile acid mixture	
		LDH content (% of control)[a]	ATP content (% of control)[b]	LDH content (% of control)[a]	ATP content (% of control)[b]
imatinib	50	280	4.3	299	1.9
troglitazone	75	101	78.0	219	3.4
PIPE-791	1	124	81.9	107	85.5
	3	107	99.8	92.8	111
	10	106	77.3	103	79.8
	30	109	106	87.8	110

[a]LDH, lactate dehydrogenase. [b]ATP, adenosine triphosphate.

Table 12. In Vitro Potency and Selectivity Profile of PIPE-791

	PIPE-791
LPAR1 radioligand competitive binding assay: K_i (nM)[a]	0.752
LPAR1 binding kinetics with [^{3}H]-PIPE-791: K_d (nM)/K_{off} (min^{-1})/K_{on} (M^{-1} min^{-1})/$t_{1/2}$ (min)	0.341/0.00133/3.91 × 10^6/519
functional LPAR1 Ca^{2+} mobilization assay IC_{50} (nM): 30 min preincubation/3 h preincubation/24 h preincubation[a]	91.8/45.2/9.9
fold selectivity versus LPAR1 in transiently transfected HEK293T cells: LPAR2/LPAR3/LPAR4/LPAR5/LPAR6	58*x*/50*x*/76*x*/14*x*/101*x*
Eurofins SAFETYscan E/IC_{50} − 78 assays	PDE3A IC_{50} = 9.0 μM[b]
	CNR1 EC_{50} = 15.1 μM[c]
manual patch clamp hERG[d] IC_{50} (μM) @ 34 °C	>30

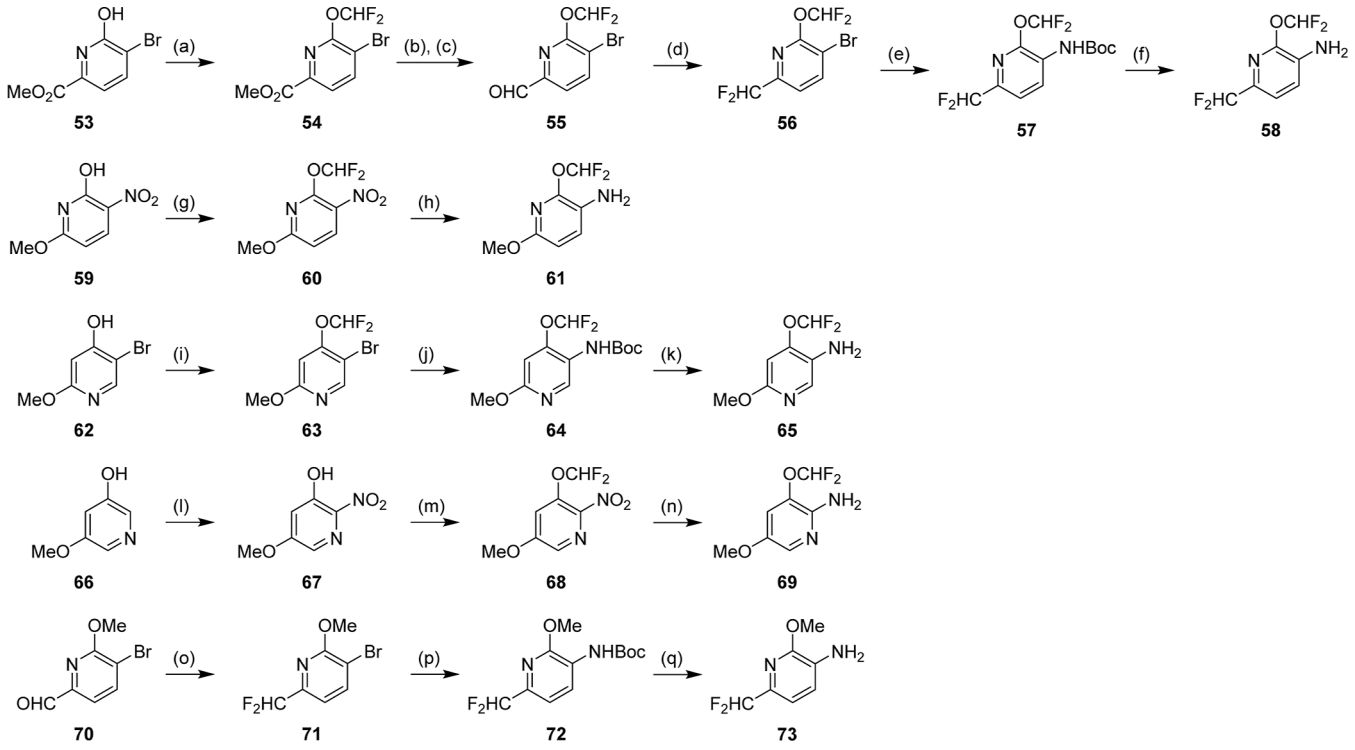
[a]For number of replicates and standard error of the mean, see the Supporting Information. [b]PDE3A, phosphodiesterase 3A. Plasma protein binding. [c]CNR1, type 1 cannabinoid receptor. [d]hERG, human ether-à-go-go-related gene.

sclerosis,[57] lung fibrosis,[58] chronic peripheral neuropathy,[59] and ocular hypertensive glaucoma,[60] had been previously published. For completeness, only the most salient in vitro potency and selectivity profile of **PIPE-791** is presented here (Table 12). In a competitive membrane filter binding assay, **PIPE-791** was found to potently bind membranes prepared from cells overexpressing human LPAR1 with a calculated K_i of 0.752 nM. Using a forward kinetics method and tritiated **PIPE-791** as the radioligand, **PIPE-791** was found to exhibit slow binding (K_{on} = 3.91 × 10^6 M^{-1} min^{-1}) and dissociation (K_{off} = 0.00133 min^{-1}) kinetics to LPAR1, with a calculated half-life of 519 min. This explained why, in a functional calcium mobilization assay, the LPAR1 IC_{50} of **PIPE-791** improved from 91.8 nM to 9.9 nM as the incubation time increased from 30 min to 24 h. To determine the functional selectivity of **PIPE-791** against other LPA receptor isoforms, we relied on HEK293T cells that were transiently transfected with human LPAR1−6 plasmids. After establishing their respective 18:1 LPA EC_{80}, the transfected cells were preincubated with increasing concentrations of **PIPE-791** for 3 h before the LPA-induced Ca^{2+} mobilization was quantified. In so doing, we were able to make the potency comparison using the same background cell type, the same overexpression method, and the same functional end point. In this paradigm, **PIPE-791** had a LPAR1 functional IC_{50} of 8.0 nM, and was greater than 10-fold selective against the other five LPAR isoforms. It is worth noting that although **PIPE-791** was determined to be 14-fold selective against LPAR5 in this assay, when cell lines stably transfected with either LPAR1 or LPAR5 were used instead (Eurofins DiscoverX Calcium No Wash^{PLUS} assays), the selectivity window of **PIPE-791** increased to >220-fold. **PIPE-791** was also tested against a panel of 78 assays using the Eurofins SAFETYscan E/IC_{50} ELECT service and found to only inhibit phosphodiesterase 3A (PDE3A) with an IC_{50} of 9.0 μM as well as to partially agonize the type 1 cannabinoid receptor (CNR1) with an EC_{50} of 15.1 μM (see Supporting Information). Importantly, no measurable blockade of the hERG channel was observed with **PIPE-791** at a top testing concentration of 30 μM using the manual patch clamp assay. **PIPE-791** was considered to be negative for mutagenicity in a bacterial reverse mutation (Ames) assay as treatment with **PIPE-791**, both with and without metabolic activation, did not significantly increase the number of revertant colonies in the *S. typhimurium* strains TA98, TA100, TA1535, and TA1537, as well as in the *E. coli* strain WP2 *uvRA*, beyond what was observed with vehicle control. Finally, when **PIPE-791** (50 μM) was incubated at 37 °C with human liver microsomes (1 mg/mL) in the presence of NADPH (1 mM) and glutathione (GSH, 5 mM) for 60 min, no GSH-trapped reactive metabolite peaks were detected by LC−MS/MS using either a constant neutral loss scan of 129 Da or a negative precursor scan of 272 Da.

Sprague−Dawley rats and Göttingen minipigs were the preclinical species selected to evaluate the potential toxicities of **PIPE-791** as all the human metabolites observed in vitro were covered by a combination of these two species (Figure 5). We acknowledge that Cynomolgus monkeys could also have been an appropriate nonrodent species for the preclinical safety testing of **PIPE-791**, however their limited availability in 2021 and 2022 at the height of the Covid-19 pandemic precluded their use. Gratifyingly, in GLP toxicity studies, administration of **PIPE-791** by once daily oral gavage to both Sprague−Dawley rats and Göttingen minipigs at dose levels of 30, 100, and 1000 mg/kg/day for 28 consecutive days did not result in test article-related mortality or adverse findings. Additionally, treatment with **PIPE-791** did not lead to induction of micronuclei in polychromatic erythrocytes of the rat bone marrow which further confirmed its lack of genotoxic potential in vivo. Most importantly, even at a high dose of 1000 mg/kg/day, no signals associated with hepatobiliary toxicity[23,28] (as adjudicated by histopathology and standard clinical chemistry panel) nor neurotoxicity[27] (as adjudicated by clinical observations and histopathology) that scuttled the development of earlier LPAR1 antagonists were observed with **PIPE-791**, a CNS-penetrant LPAR1 antagonist. Based on the above and a comprehensive IND-enabling preclinical data package, **PIPE-791** was approved

https://doi.org/10.1021/acs.jmedchem.6c01049
J. Med. Chem. 2026, 69, 15888−15927

Scheme 2. Preparation Of Non-Commercial Aminopyridines 58, 61, 65, 69, and 73[a]



[a]Reagent and conditions: (a) Cs_2CO_3 (3 equiv), $ClCF_2CO_2Na$ (1.2 equiv), DMF, 80 °C, 1 h, 45%. (b) $NaBH_4$ (25 equiv), MeOH, RT, 2 h, quantitative. (c) Dess-Martin periodinane (1.5 equiv), DCM, RT, 1 h, 42%. (d) BAST (1.5 equiv), DCM, 0 °C to RT, 1 h, 61%. (e) KO^{t}Bu (3 equiv), BrettPhos Pd G3 (0.2 equiv), $BocNH_2$ (10 equiv), 1,4-dioxane, 90 °C, 1 h, 55%. (f) TFA (150 equiv), DCM, RT, 1 h, 88%. (g) NaH (2.8 equiv), MeCN, RT, 10 min; then $FSO_2CF_2CO_2H$ (1.8 equiv), 16 h; then $FSO_2CF_2CO_2H$ (1.8 equiv), 48 h 75%. (h) 10% (w/w) dry Pd/C (0.08 equiv), H_2 (balloon), MeOH, RT, 90 min, quantitative. (i) Cs_2CO_3 (3 equiv), $ClCF_2CO_2Na$ (1.5 equiv), DMF, 100 °C, 70 min, 47%. (j) Cs_2CO_3 (3 equiv), BrettPhos Pd G3 (0.1 equiv), $BocNH_2$ (50 equiv), 1,4-dioxane, 90 °C, 2 h, 87%. (k) 4 M HCl in 1,4-dioxane (10 equiv), DCM, RT, 2 h, 62%. (l) NBu_4NO_3 (1.6 equiv), TFAA (1.6 equiv), DCM, 0 °C to RT, 2.5 h, 31%. (m) Cs_2CO_3 (3 equiv), $ClCF_2CO_2Na$ (1.5 equiv), DMF, 80 °C, 30 min, 32%. (n) 10% (w/w) dry Pd/C (0.2 equiv), H_2 (balloon), MeOH, RT, 60 min, 97%. (o) BAST (2.5 equiv), DCM, 0 °C to RT, 16 h, 85%. (p) KO^{t}Bu (3 equiv), BrettPhos Pd G3 (0.2 equiv), $BocNH_2$ (50 equiv), 1,4-dioxane, 90 °C, 2 h, 87%. (q) TFA (150 equiv), DCM, RT, 1 h, 91%.

by the FDA to enter Phase 1 clinical development in 2023, and its associated human PK and pharmacological properties will be communicated in due course.

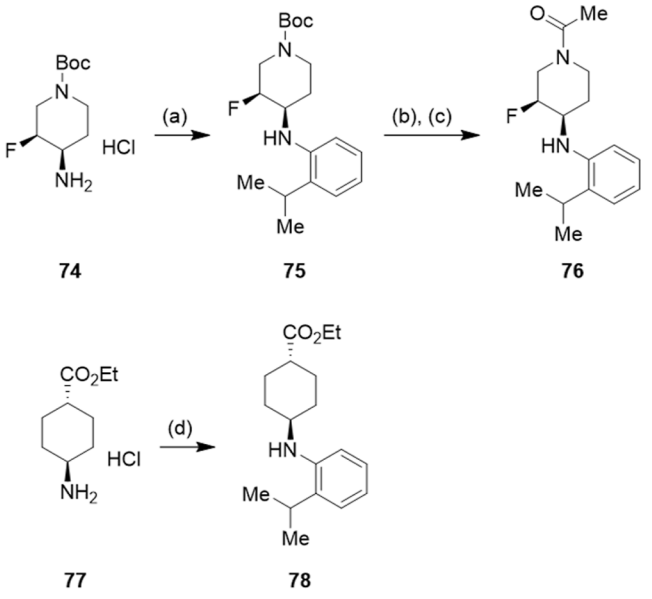
SYNTHESIS

Preparation of noncommercial, western aminopyridines used for the synthesis of compounds described in Table 2 is summarized in Scheme 2. To install the difluoromethoxy group present in aminopyridines **58**, **65**, and **69**, the appropriate hydroxy-bromo-pyridine (**53** and **62**) or hydroxy-nitro-pyridine (**67**) precursors were first deprotonated with Cs_2CO_3 and then quenched with sodium chlorodifluoroacetate (32% to 47% isolated yield).[61] While this reaction condition surprisingly failed to achieve the desired *O*-difluoromethylation of hydroxy-nitro-pyridine **59**, the requisite difluoromethoxy-nitro-pyridine **60** could however be obtained in 75% yield when NaH and 2,2-difluoro-2-(fluorosulfonyl)acetic acid were used instead.[62] The difluoromethyl group present in aminopyridines **58** and **73** was readily established by treating the corresponding aldehydes **55** and **70** with bis(2-methoxyethyl)aminosulfur trifluoride (BAST), with reaction yields ranging from 61% to 85%.[63] Pd-catalyzed hydrogenation of nitropyridines **60** and **68** (97% to 100% yield) or a two-step sequence involving an initial Buchwald amination of bromopyridines **56**, **63**, and **71** with excess *tert*-butyl carbamate followed by acid-mediated removal of the Boc protecting group (48% to 79% yield over two steps),[64] completed the synthesis of the targeted aminopyridines.

As was shown in Scheme 1, eastern aniline **16** could be readily accessed via two alternative but equally facile synthetic routes. The approach that was chosen, Buchwald−Hartwig coupling or reductive amination, was ultimately dependent on the availability of the requisite starting materials and whether it was more advantageous to deploy a reaction that was stereospecific or stereodivergent (refer to EXPERIMENTAL SECTION to see which approach was taken for a given compound). As an illustration (Scheme 3), for the preparation of aniline **76**, which was the precursor for the synthesis of compound **39** (Table 4), the enantiopure *tert*-butyl (3*S*,4*R*)-4-amino-3-fluoropiperidine-1-carboxylate (**74**) and its enantiomer (used for the preparation of compound **40**, Table 4) were both commercially available as their corresponding hydrochloride salts. Therefore, amine **74** was heated with commercially available 1-iodo-2-isopropylbenzene and potassium *tert*-butoxide in the presence of catalytic quantities of tris(dibenzylidineacetone)dipalladium(0) and XantPhos to afford aniline **75** in 78% yield as a single stereoisomer. TFA-mediated cleavage of the Boc protecting group in **75** followed by acylation with triethylamine as the base afforded acetamide **76** in 78% overall yield. With a bite angle between 111° and 112°, the bidentate diphosphine ligand XantPhos was found to be the optimal ligand for the Buchwald−Hartwig coupling of all

https://doi.org/10.1021/acs.jmedchem.6c01049
J. Med. Chem. 2026, 69, 15888−15927

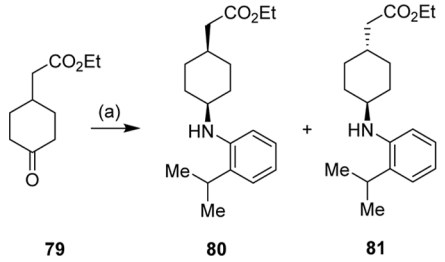
Scheme 3. Preparation of Anilines 76 and 78[a]



[a]Reagent and conditions: (a) 1-iodo-2-isopropylbenzene (1.1 equiv), $Pd_2(dba)_3$ (0.2 equiv), XantPhos (0.3 equiv), KO^{t}Bu (3 equiv), 1,4-dioxane, 100 °C, 48 h, 78%. (b) TFA (150 equiv), DCM, RT, 2 h, quantitative. (c) TEA (2.5 equiv), AcCl (1.5 equiv), DCM, RT, 1 h, 78%. (d) 1-iodo-2-isopropylbenzene (1.4 equiv), $Pd_2(dba)_3$ (0.1 equiv), CPhos (0.2 equiv), Cs_2CO_3 (4 equiv), 1,4-dioxane, 90 °C, 48 h, 67%.

substituted 4-aminopiperidines exemplified in Table 4.[65] However, minimal conversion was observed when this and other bidentate ligands were used to effect the Buchwald–Hartwig coupling of *trans*-ethyl 4-aminocyclohexane-1-carboxylate (**77**). We suspected that the ethyl ester may be occupying one of the available coordination sites of the palladium complex and hindering subsequent oxidative addition into the sterically congested 1-iodo-2-isopropylbenzene. Gratifyingly, the desired coupling to afford aniline **78** could be realized in 67% yield when the electron-rich, monodentate CPhos was used as the ligand. Additionally, Cs_2CO_3 was chosen as a mild, nonalkoxide base to ensure that there was no epimerization at the ester-bearing carbon. In situations where the concurrent preparation of a mixture stereoisomeric products was more advantageous (Scheme 4), reductive amination proved to be the superior approach. In this instance, starting with commercially available ketone **79**, an initial Schiff base condensation with 2-isopropylaniline followed by reduction with excess sodium triacetoxyborohydride furnished both *cis*-aniline **80** (used to prepare compound **49**, Table 5) and *trans*-aniline **81** (used to prepare compound **48**, Table 5) in 48% and 22% yield, respectively.

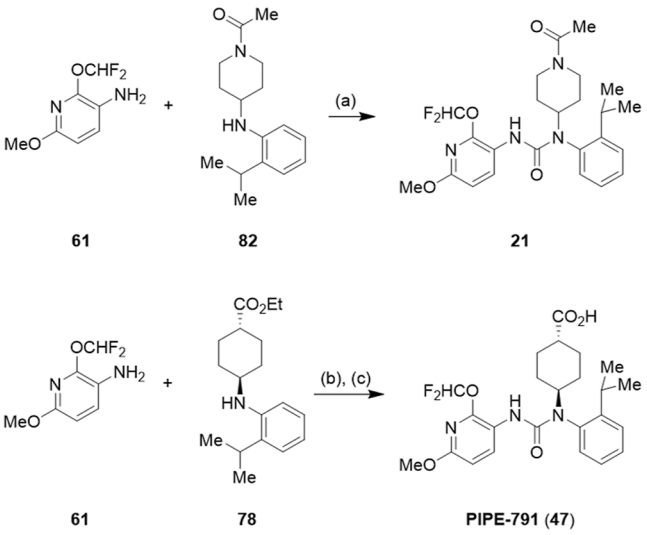
Scheme 4. Preparation of Anilines 80 and 81[a]



[a]Reagent and conditions: (a) 2-isopropylaniline (1 equiv), $NaB(OAc)_3H$ (1.2 equiv), DCM, RT, 10 min, 48% of **80** and 22% of **81**.

Union of western aminopyridine with eastern aniline to deliver the targeted urea product was successfully achieved under several conditions, two of which are shown in Scheme 5.

Scheme 5. Preparation of Compound 21 and PIPE-791 (47)[a]



[a]Reagent and conditions: (a) pyridine (3 equiv), phosgene (15% w/w solution in toluene, 1.5 equiv), DCM, RT, 30 min, then **82** (1 equiv), pyridine (3 equiv), activated 4 Å molecular sieves, DCM, RT, 16 h, 38%. (b) CDI (2 equiv), MeCN, 60 °C, 48 h, 94%. (c) LiOH (1 M aqueous solution, 4 equiv), MeOH, THF, RT, 18 h, 80%.

For small scale reactions and for less nucleophilic western aminopyridines, it was best to first react the aminopyridine with excess phosgene in the presence of pyridine until all the starting material was consumed. The volatiles, including unreacted phosgene, were then thoroughly removed from the reaction mixture. The carbamic chloride thus obtained was reconstituted in DCM and added to a pyridine solution of the appropriate eastern aniline coupling partner and freshly activated 4 Å molecular sieves. As a representative example, aminopyridine **61** could be unified with aniline **82** to give urea **21** in 38% isolated yield using this approach. For larger scale deliveries, neither phosgene nor heating with triphosgene were deemed to be viable given the associated safety risks. 1,1′-Carbonyldiimidazole (CDI), however, proved to be an appropriate C═O source for the synthesis of **PIPE-791** from aminopyridine **61** and aniline **78**. Combining these components together in MeCN and heating at 60 °C for 48 h afforded multigram quantities (>10 g) of ester **85**. Direct monitoring of the reaction mixture by LCMS revealed that aminopyridine **61** was first converted by CDI to acyl imidazole **83** and urea **84** with minimal participation from aniline **78** (Figure 6). Following extended heating, intermediates **83** and **84** were converted to ester **85** but symmetrical urea **86** was not observed as the reaction progressed. We were unable to achieve significant formation of ester **85** when we heated isolated urea **84** with aniline **78** in MeCN. However, when the same transformation was carried out in the presence of 1 equiv of imidazole, **84** could be converted into ester **85** with the concomitant release of aminopyridine **61**. Additionally, acyl imidazole **83** was also observed in the crude reaction mixture. This suggested that urea **84** can be converted

https://doi.org/10.1021/acs.jmedchem.6c01049
J. Med. Chem. 2026, 69, 15888−15927

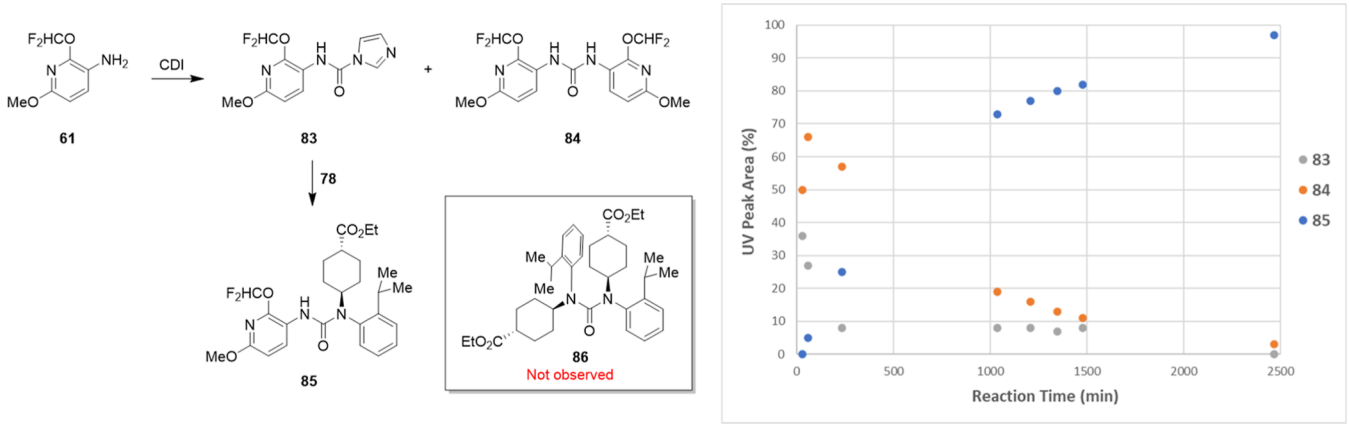
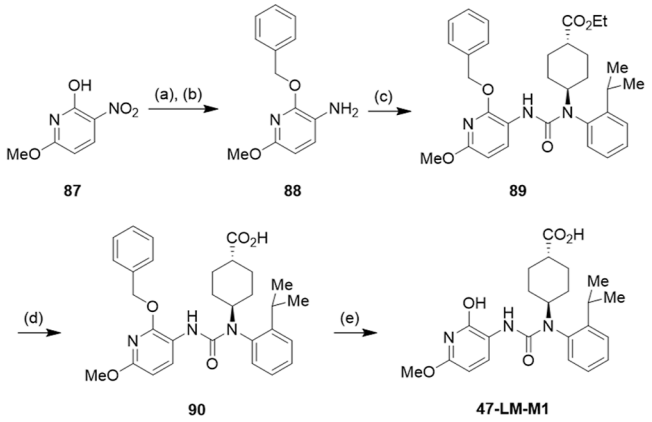


Figure 6. Reaction monitoring of CDI-mediated condensation of aminopyridine **61** and aniline **78**.

into acyl imidazole **83** and be productively funneled into ester **85**. Finally, the saponification of ester **85** into **PIPE-791** was accomplished using aqueous LiOH in 80% yield.

The synthesis of metabolite **47-LM-M1** is depicted in Scheme 6. From commercially available 6-methoxy-3-nitropyridin-2-ol

Scheme 6. Preparation of Metabolite 47-LM-M1[a]



[a]Reagent and conditions: (a) BnBr (1.2 equiv), Ag_2CO_3 (1.2 equiv), toluene, 130 °C, 1 h. (b) Fe (5 equiv), NH_4Cl (5 equiv), EtOH, H_2O, 80 °C, 12 h, 43%. (c) Pyridine (3 equiv), phosgene (15% w/w solution in toluene, 1.5 equiv), DCM, RT, 30 min, then **78** (1 equiv), pyridine (3 equiv), activated 4 Å molecular sieves, DCM, RT, 16 h, 44%. (d) LiOH (1 M aqueous solution, 5 equiv), MeOH, THF, 60 °C, 1 h. 67%. (e) 10% (w/w) dry Pd/C (0.04 equiv), H_2 (balloon), MeOH, RT, 18 h, 14%.

(**87**), protection of the free phenol as a benzyl ether followed by iron-mediated reduction of the nitro group afforded aminopyridine **88** in 43% yield. After the activation of **88** by phosgene and pyridine, the resulting carbamic chloride was then quenched with aniline **78** to deliver urea **89** in 44% yield. Sequential removal of the protecting groups in **89**; an initial hydrolysis of the ethyl ester followed by hydrogenolysis of the benzyl ether, furnished **47-LM-M1** as a white solid. Metabolite **47-LM-M3**, also known as **47-Hep-M6**, was prepared using a similar sequence (Scheme 7). In this instance, the requisite aminopyridine **92** used for the formation of urea **93** was itself synthesized in three steps from commercially available 6-chloro-3-nitropyridin-2-ol (**91**). Specifically, S_NAr displacement of chlorine in **91** with benzyl alcohol was then followed by difluoromethylation of the free phenol and completed with nitro reduction. Finally, by reversing the deprotection sequence from what was previously used for **47-LM-M1**, metabolite **47-LM-M3**/**47-Hep-M6** was synthesized from **93** with a significantly higher overall yield (57% vs 9.4% yield).

Synthesis of metabolite **47-LM-M2**, also known as **47-Hep-M4**, necessitated the preparation of eastern aniline **99** (Scheme 8), which was itself assembled in four steps from 2′-iodoacetophenone (**95**). Wittig olefination of the carbonyl group in **95** under standard conditions followed by an anti-Markovnikov hydroboration-oxidation sequence on the resulting alkene **96** delivered primary alcohol **97**. The free hydroxyl group was then protected as a TBS ether to give **98**. If left unprotected, the alcohol in **97** was found to readily undergo undesired cyclization onto the aryl iodide to give 3-methyl-2,3-dihydrobenzofuran. The Buchwald−Hartwig coupling of iodide **98** with commercially available *trans*-methyl 4-aminocyclohexane-1-carboxylate hydrochloride was prone to stalling out with either XantPhos or CPhos as ligand. Although higher conversion could be achieved with the use of a stronger base such as potassium *tert*-butoxide, its use was also accompanied by undesired epimerization. Focused screening revealed tri-*tert*-butylphosphonium tetrafluoroborate as the best ligand for this substrate. Under these optimized conditions, the requisite aniline **99** was isolated as a single stereoisomer in 50% yield. Phosgene-promoted urea formation with aminopyridine **61** proceeded without incidence to afford **100** in 51% yield. Sequential removal of the TBS group with excess TBAF followed by saponification provided metabolite **47-LM-M2**/**47-Hep-M4**.

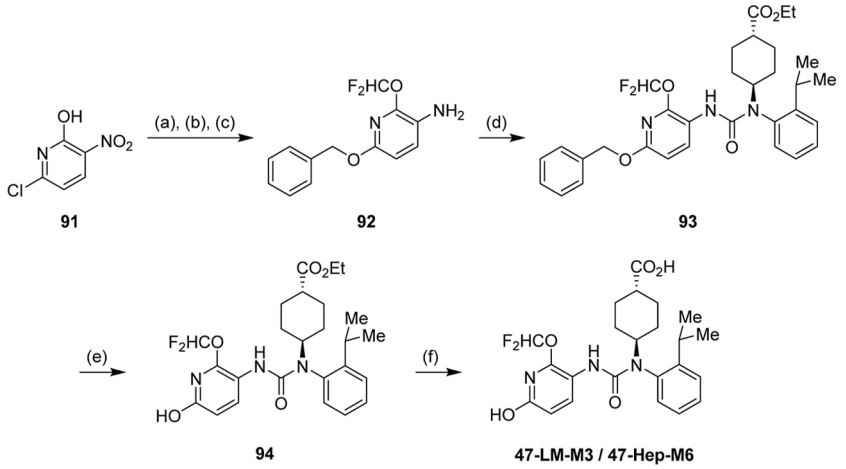
We found that the acyl glucuronide metabolite **47-Hep-M8** was best prepared in two steps from **PIPE-791** (Scheme 9).[66] HATU-mediated acylation of allyl D-glucuronate (**101**) with **PIPE-791** in MeCN took place selectively at the anomeric carbon to deliver ester **102** almost exclusively as the β-anomer (ratio of β-to-α anomer >95:5). Mild deprotection of the allyl ester in **102** with morpholine and polymer-supported Pd-$(PPh_3)_4$ in THF facilitated the isolation of metabolite **47-Hep-M8** with minimal manipulation.

CONCLUSIONS

At the outset of our search for a CNS-penetrant LPAR1 antagonist, we deliberately pivoted toward chemical scaffolds that were absent of carboxylic acid functional groups or isosteres. We had subscribed to the dogma that, being ionized and charged at physiological pH, a carboxylic acid-bearing compound would encounter difficulties penetrating the hydrophobic, lipid-based

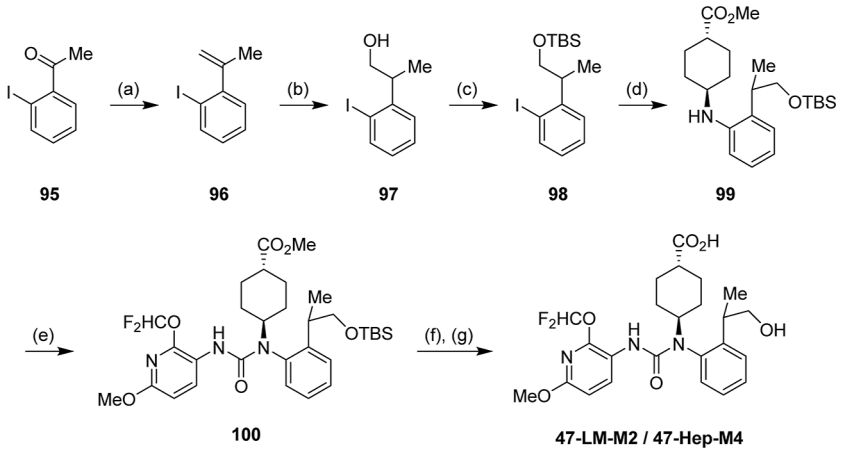
https://doi.org/10.1021/acs.jmedchem.6c01049
J. Med. Chem. 2026, 69, 15888−15927

Scheme 7. Preparation of Metabolite 47-LM-M3/47-Hep-M6[a]



[a]Reagent and conditions: (a) BnOH (1.1 equiv), KOH (3 equiv), 18-crown-6 (0.03 equiv), toluene, 80 °C, 16 h, 64%. (b) NaH (2.4 equiv), MeCN, RT, 10 min; then $FSO_2CF_2CO_2H$ (1.8 equiv), 16 h; then $FSO_2CF_2CO_2H$ (1.8 equiv), 64%. (c) Fe (10 equiv), NH_4Cl (10 equiv), EtOH, H_2O, 90 °C, 1 h, 57%. (d) Pyridine (3 equiv), triphosgene (0.4 equiv), DCM, RT, 30 min, then **78** (1 equiv), RT, 16 h, 99%. (e) 10% (w/w) dry Pd/C (0.2 equiv), H_2 (balloon), MeOH, RT, 18 h. 78%. (f) LiOH (1 M aqueous solution, 5 equiv), MeOH, RT, 5 h, 73%.

Scheme 8. Preparation of Metabolite 47-LM-M2/47-Hep-M4[a]



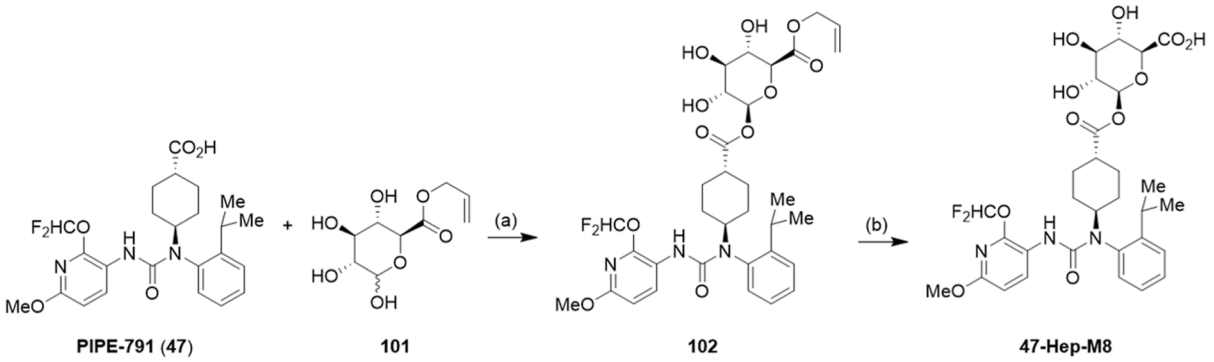
[a]Reagent and conditions: (a) Ph_3PMeBr (1.2 equiv), KO^{t}Bu (1.2 equiv), THF, 0 °C to RT, 16 h, 42%. (b) BH_3 (1.0 M solution in THF, 1.1 equiv), THF, 0 °C, 90 min; then 1 N aq. NaOH (3.5 equiv), 0 °C, 90 min; then 30% (w/w) aq. H_2O_2 (7 equiv), 0 °C to RT, 1 h, 77%. (c) TBSCl (1.2 equiv), TEA (1.6 equiv), DMAP, (0.1 equiv), DCM, RT, 16 h, >99%. (d) *trans*-methyl 4-aminocyclohexane-1-carboxylate hydrochloride (1.1 equiv), $Pd(OAc)_2$ (0.06 equiv), P^{t}Bu$_3$·HBF_4 (0.12 equiv), Cs_2CO_3 (4 equiv), 1,4-dioxane, 95 °C, 18 h, 50%. (e) **61** (1.1 equiv), pyridine (3 equiv), phosgene (15% w/w solution in toluene, 1.5 equiv), DCM, RT, 30 min, then **99** (1 equiv), pyridine (3 equiv), activated 4 Å molecular sieves, DCM, RT, 16 h, 51%. (f) TBAF (1.0 M solution in THF, 1.2 equiv), THF, RT, 2 h, 87%. (f) LiOH (1 M aqueous solution, 9 equiv), MeOH, 60 °C, 2 h, 92%.

outer membranes of the endothelial cells that make up the BBB, which repelled charged ions.[67] Additionally, given the affinity of carboxylic acids for binding to both Site I and Sudlow Site II pockets of serum albumin,[68] it was expected that the high protein-binding and low volume of distribution typically associated with carboxylic acid-containing drugs would keep them from effectively penetrating into the brain. In fact, to deliver carboxylic acid-containing drugs into the CNS, strategies to mask carboxylic acids as prodrugs[69] or to engage endogenous uptake transporters located along the BBB such as the monocarboxylate transport system[70] have been extensively reviewed in the literature. Furthermore, even for lead optimization campaigns that were strictly focused on the antagonism of LPAR1 in the periphery, concerns surrounding the susceptibility of lipophilic carboxylic acids to engage bile acid transporters, difficulties associated with predicting the human PK for compounds that undergo enterohepatic recirculation accurately, and perceived liabilities around the formation of potentially reactive acyl glucuronide metabolites, had similarly dissuaded other accomplished drug discovery teams from pursuing an LPAR1 antagonist possessing a carboxylic acid headgroup.[27,35,71]

When we were unable to overcome the high first-pass metabolism and low oral bioavailability of our chemical lead **15** strictly through the blockade of its metabolic soft spots without substantial loss in intrinsic potency against LPAR1, it was the installation of polarity in the form of a carboxylic acid headgroup that ultimately got the team out of this quagmire. Contrary to our initial expectations, addition of a carboxylic acid was not accompanied by an increase in plasma protein binding. The

https://doi.org/10.1021/acs.jmedchem.6c01049
J. Med. Chem. 2026, 69, 15888−15927

Scheme 9. Preparation of Metabolite 47-Hep-M8[a]



[a]Reagent and conditions: (a) HATU (1 equiv), NMM (2 equiv), MeCN, RT, 16 h, 50%. (b) $Pd(PPh_3)_4$ (0.5 equiv), morpholine (1 equiv), THF, RT, 16 h, 41%.

plasma free fraction of **PIPE-791** was in fact improved when compared to its matched molecular pairs containing instead an acetamide (**21**), a methyl sulfonamide (**45**) or a methyl sulfone (**46**). Importantly, the presence of a carboxylate anion did not result in a catastrophic loss in CNS penetration. While we did detect the formation of **47-Hep-M8** (the acyl glucuronide metabolite of **PIPE-791**) both in vitro and in vivo, we were able to rationally evaluate its associated risk by proactively synthesizing an authentic standard so that its circulating levels and its reactivity can be quantified. We also believed that the blunted peak-to-trough ratio and extended half-life observed in the preclinical PK profiles of **PIPE-791**—likely a consequence of enterohepatic recirculation of **47-Hep-M8** and **PIPE-791**—would translate to an increased therapeutic index as efficacy is often AUC- and/or C_{trough}-driven, while unwanted toxicity and DDI are conservatively assumed to be C_{max}-driven. Additionally, this therapeutic index can be further expanded by the slow off-rate kinetics of **PIPE-791**, a key feature that initially attracted us to this urea-bearing scaffold, where sustained target inhibition and longer duration of action would allow for lower and less frequent dosing. Indeed, **PIPE-791** was found to be fully efficacious using low, daily QD dosing in multiple preclinical disease models, but was well tolerated in GLP 28 day rat and minipig toxicity studies at doses up to 1000 mg/kg/day. Finally, the absence of neurotoxicity observed with **PIPE-791**, despite it being a CNS-penetrant LPAR1 antagonist, was also noteworthy.

With the successful completion of two independent Phase I clinical trials[72] involving both healthy volunteers and patients where **PIPE-791** was found to be well-tolerated at all the doses examined, we believe **PIPE-791** has the potential to be a best-in-class LPAR1 antagonist for the treatment of both CNS- and peripherally restricted disorders associated with aberrant LPA-LPAR1 signaling. We would therefore caution practicing medicinal chemists against putting too much emphasis on the perceived biases against the use of a carboxylic acid pharmacophore for CNS programs without first critically evaluating its risk-benefit ratio for the specific situation at hand.

EXPERIMENTAL SECTION

Chemistry General Methods

Unless otherwise noted, reagents and solvents were used as received from commercial suppliers. Anhydrous solvents were used for synthetic transformations sensitive to moisture and/or oxygen. Normal-phase column chromatography was carried out with CombiFlash purification systems (Teledyne ISCO) using preloaded RediSep Gold or RediSep Silver normal-phase disposable silica gel columns. Preparative reverse-phase high pressure liquid chromatography was carried out on CombiFlash E/Z Prep purification system (Teledyne ISCO) equipped with a Luna 10 μm PREP C18(2) 100 Å LC column (Phenomenex, 250 mm × 21.2 mm, AXIA Packed). Microwave-assisted reactions were carried out with Discover 2.0 microwave synthesis systems (CEM). NMR spectra were recorded on Bruker Fourier-300 MHz, Bruker Avance III-300 MHz, Bruker Avance III-400 MHz, or Bruker Avance II-500 MHz spectrometers in the specified deuterated solvent. Proton (^{1}H), Carbon (^{13}C) and Fluorine (^{19}F) NMR chemical shifts are given in parts per million (ppm) with the residual solvent signal used as reference, when available. NMR abbreviations are used as follows: s = singlet, d = doublet, dd = doublet of doublets, dt = doublet of triplets, ddd = doublet of doublets of doublets, t = triplet, td = triplet of doublets, tt = triplet of triplets, q = quartet, qd = quartet of doublets, m = multiplet, pent = pentet, sext = sextet, sept = septet, br = broad. Analytical HPLC/MS was obtained on Waters Acquity UPLC H-Class CM Core System equipped with an Acquity QDa MkII detector using Acquity UPLC BEH C18 columns (Waters, 130 Å, 1.7 μm, 2.1 mm × 50 mm) maintained at 45 °C with a 5% to 95% (v/v) gradient of MeCN and water spiked with 0.1% formic acid (total run time was 4 min, with a flow rate of 0.6 mL/min), or Shimadzu LCMS-2020 liquid chromatograph mass spectrometer using HALO C18 columns (90 Å, 2.0 μm, 3.0 mm × 30 mm) maintained at 40 °C with an initial 30% to 70% (v/v) gradient of MeCN and water spiked with 0.01% TFA over 1.2 min followed by a final 70% to 100% (v/v) gradient over 1.8 min (total run time was 3 min, with a flow rate of 1.2 mL/min). High resolution MS was obtained on Waters Acquity UPLC H-Class CM Core System equipped with a Xevo G2-XS Q TOF HRMS using Acquity UPLC BEH C18 columns (Waters, 130 Å, 1.7 μm, 2.1 mm × 50 mm) maintained at 40 °C with a 10% to 90% (v/v) gradient of MeCN and water spiked with 0.1% formic acid (total run time was 3 min, with a flow rate of 0.4 mL/min). All final compounds disclosed herein showed purity >95% (assessed by UV detection of LCMS runs).

2-(Difluoromethoxy)-6-(difluoromethyl)pyridin-3-amine (58)

(a) In a dried, round-bottom flask equipped with a magnetic stirrer was suspended Cs_2CO_3 (4.21 g, 12.9 mmol, 3 equiv) in DMF (10 mL). The reaction suspension was heated to 80 °C before a DMF solution (10 mL) of methyl 5-bromo-6-hydroxypicolinate (**53**, 1.00 g, 4.31 mmol, 1 equiv) and sodium chlorodifluoroacetate (0.79 g, 5.2 mmol, 1.2 equiv) was added dropwise over a period of 10 min. Following the completion of addition, the now orange reaction solution was heated at 80 °C for an extra 60 min before it was cooled to rt, diluted with EtOAc (50 mL), and washed sequentially with water (50 mL) and brine (50 mL). The organic layer was then dried over Na_2SO_4, filtered, and the filtrate concentrated in vacuo. Purification of the crude product thus obtained by way of column chromatography (SiO_2, 5:1 (v/v) Hex: EtOAc) afforded methyl 5-bromo-6-

https://doi.org/10.1021/acs.jmedchem.6c01049
J. Med. Chem. 2026, 69, 15888−15927

(difluoromethoxy)picolinate (**54**) as a yellow oil (0.55 g, 45% yield). LCMS: m/z = 281.9, 283.9 $[M + H]^+$.

(b) In a dried, round-bottom flask equipped with a magnetic stirrer was dissolved methyl 5-bromo-6-(difluoromethoxy)picolinate (**54**, 0.40 g, 1.4 mmol, 1 equiv) from the previous step in MeOH (15 mL). To this solution was then added $NaBH_4$ (1.35 g, 35.5 mmol, 25 equiv) portionwise over 10 min, and following a period of vigorous gas evolution, the resulting mixture was stirred at rt for 2 h. The reaction was then carefully quenched with the addition of ice water (60 mL) and extracted with EtOAc (3 × 60 mL). The combined organic extracts were then washed further with brine (2 × 100 mL), dried over $MgSO_4$, filtered, and the filtrate concentrated in vacuo. The crude (5-bromo-6-(difluoromethoxy)pyridin-2-yl)methanol thus obtained was immediately taken up in DCM (5 mL) and added Dess-Martin periodinane (0.62 g, 1.5 mmol, 1.5 equiv) in one rapid portion at rt. After 1 h of stirring at rt, the reaction was then carefully quenched with the addition of 1 M aq. NaOH (30 mL) and extracted with EtOAc (3 × 30 mL). The combined organic extracts were washed further with water (60 mL) and brine (60 mL), dried over $MgSO_4$, filtered, and the filtrate concentrated in vacuo. Purification of the crude product thus obtained by way of column chromatography (SiO_2, gradient elution: 9:1 (v/v) Hex: EtOAc → EtOAc) afforded 5-bromo-6-(difluoromethoxy)-picolinaldehyde (**55**) as an off-white solid (0.15 g, 42% yield). LCMS: m/z = 251.9, 253.9 $[M + H]^+$.

(c) In a dried, round-bottom flask equipped with a magnetic stirrer was dissolved 5-bromo-6-(difluoromethoxy)picolinaldehyde (**55**, 0.15 g, 0.59 mmol, 1 equiv) from the previous step in DCM (5 mL). To this solution was then added at 0 °C BAST (0.17 mL, 0.89 mmol, 1.5 equiv), neat and dropwise, over a period of 10 min. Following the completion of addition, the now orange reaction solution was warmed to and stirred at rt for 1 h. The reaction was then carefully quenched with saturated aq. $NaHCO_3$ (30 mL) and extracted with EtOAc (3 × 30 mL). The combined organic extracts were then washed further with water (50 mL) and brine (50 mL), dried over Na_2SO_4, filtered, and the filtrate concentrated in vacuo. Purification of the crude product thus obtained by way of column chromatography (SiO_2, gradient elution: Hex → EtOAc) afforded 3-bromo-2-(difluoromethoxy)-6-(difluoromethyl)pyridine (**56**) as a white solid (0.10 g, 61% yield). LCMS: m/z = 273.9, 275.9 $[M + H]^+$.

(d) In a thick-walled glass reaction vessel equipped with a magnetic stirrer and a Teflon screwcap was combined 3-bromo-2-(difluoromethoxy)-6-(difluoromethyl)pyridine (**56**, 80 mg, 0.29 mmol, 1 equiv) from the previous step, potassium *tert*-butoxide (98 mg, 0.87 mmol, 3 equiv), [(2-dicyclohexylphosphino-3,6-dimethoxy-2′,4′,6′-triisopropyl-1,1′-biphenyl)-2-(2′-amino-1,1′ -biphenyl)]palladium(II) methanesulfonate (53 mg, 0.058 mmol, 0.2 equiv), and *tert*-butyl carbamate (0.34 g, 2.9 mmol, 10 equiv) in 1,4-dioxane (10 mL). The resulting mixture was deoxygenated via subsurface purging with nitrogen for 10 min before the reaction vessel was tightly sealed and heated at 90 °C for 1 h. The reaction mixture was then cooled to rt, diluted with EtOAc (30 mL), and washed sequentially with water (30 mL) and brine (30 mL). The organic layer was then dried over Na_2SO_4, filtered, and the filtrate concentrated in vacuo. Purification of the crude product thus obtained by way of column chromatography (SiO_2, gradient elution: Hex → EtOAc) afforded *tert*-butyl (2-(difluoromethoxy)-6-(difluoromethyl)pyridin-3-yl)carbamate (**57**) as a white solid (50 mg, 55% yield). LCMS: m/z = 311.1 $[M + H]^+$.

(e) In a dried, round-bottom flask equipped with a magnetic stirrer was dissolved *tert*-butyl (2-(difluoromethoxy)-6-(difluoromethyl)pyridin-3-yl)carbamate (**57**, 50 mg, 0.16 mmol, 1 equiv) from the previous step in DCM (3 mL). To this solution was then added TFA (1.8 mL, 24 mmol, 150 equiv) and the resulting reaction mixture was stirred at rt for 1 h. The mixture was then rendered slightly basic (pH ∼ 8) with the addition of NH_3 (7 M solution in MeOH) and the volatiles were removed in vacuo. Purification of the crude product thus obtained by way of reverse-phase column chromatography (C_{18}, gradient elution: 9:1 (v/v) H_2O: MeCN → MeCN) afforded the title compound **58** as a light brown oil (30 mg, 88% yield). LCMS: m/z = 211.0 $[M + H]^+$.

2-(Difluoromethoxy)-6-methoxypyridin-3-amine (61)

(a) In a dried, round-bottom flask equipped with a magnetic stirrer was suspended 6-methoxy-3-nitropyridin-2-ol (**59**, 1.7 g, 10 mmol, 1 equiv) in MeCN (35 mL). To this was added NaH (60% w/w dispersion in paraffin oil, 1.1 g, 28 mmol, 2.8 equiv) in one rapid portion and the resulting mixture was stirred at rt for 10 min to afford a brownish, yellow suspension. Then, 2,2-difluoro-2-(fluorosulfonyl)acetic acid (1.86 mL, 18.0 mmol, 1.8 equiv) was added neat and dropwise over a period of 5 min, during which time a mild exotherm was observed. After 16 h of stirring, another aliquot of 2,2-difluoro-2-(fluorosulfonyl)acetic acid (1.86 mL, 18.0 mmol, 1.8 equiv) was added neat and dropwise over a period of 5 min. After another 48 h of stirring at rt, the crude reaction mixture was carefully quenched with water (35 mL) and then diluted with a 1:1 (v/v) solution of EtOAc and Hex (210 mL). The organic layer was then separated and washed sequentially with saturated aq. $NaHCO_3$ (100 mL), water (100 mL) and brine (100 mL), dried over $MgSO_4$, filtered, and the filtrate concentrated in vacuo. Purification of the crude product thus obtained by way of column chromatography (SiO_2, gradient elution: Hex → 1:1 (v/v) Hex: EtOAc) afforded 2-(difluoromethoxy)-6-methoxy-3-nitropyridine (**60**) as a yellow solid (1.65 g, 75% yield). LCMS: m/z = 221.0 $[M + H]^+$. ^1H NMR (300 MHz, $CDCl_3$) δ: 8.40 (d, J = 8.9 Hz, 1H), 7.51 (t, J = 71.4 Hz, 1H), 6.64 (d, J = 8.9 Hz, 1H), 4.02 (s, 3H).

(b) In a dried, round-bottom flask equipped with a magnetic stirrer was dissolved 2-(difluoromethoxy)-6-methoxy-3-nitropyridine (**60**, 1.65 g, 7.50 mmol, 1 equiv) from the previous step in MeOH (45 mL). The resulting yellow solution was then deoxygenated via subsurface purging with nitrogen for 10 min before palladium (10% w/w over activated carbon, dry, 0.64 g, 0.60 mmol, 0.08 equiv) was added in one rapid portion. The resulting black suspension was then subsurface purged with hydrogen for 10 min before it was stirred under a static hydrogen atmosphere (maintained with a balloon) at rt for 90 min. The reaction was subsequently diluted with EtOAc (200 mL) and filtered through a bed of DCM-wetted Celite. The insolubles were washed further with EtOAc (2 × 50 mL). Concentration of the filtrate thus obtained in vacuo afforded the title compound **61** as a reddish, brown solid (>99% yield). LCMS: m/z = 191.1 $[M + H]^+$. ^1H NMR (300 MHz, $CDCl_3$) δ: 7.40 (t, J = 73.5 Hz, 1H), 7.10 (d, J = 8.3 Hz, 1H), 6.41 (d, J = 8.3 Hz, 1H), 3.81 (s, 3H), 3.32 (br s, 2H).

4-(Difluoromethoxy)-6-methoxypyridin-3-amine (65)

(a) In a dried, round-bottom flask equipped with a magnetic stirrer was suspended Cs_2CO_3 (1.15 g, 3.53 mmol, 3 equiv) in DMF (8 mL). The reaction suspension was heated to 100 °C before a DMF solution (8 mL) of 5-bromo-2-methoxypyridin-4-ol (**62**, 0.20 g, 1.2 mmol, 1 equiv) and sodium chlorodifluoroacetate (0.27 g, 1.8 mmol, 1.5 equiv) was added dropwise over a period of 10 min. Following the completion of addition, the now orange reaction solution was heated at 100 °C for an extra 70 min before it was cooled to rt, diluted with EtOAc (200 mL), and washed sequentially with water (100 mL) and brine (100 mL). The organic layer was then dried over Na_2SO_4, filtered, and the filtrate concentrated in vacuo. Purification of the crude product thus obtained by way of column chromatography (SiO_2, 7:1 (v/v) Hex: EtOAc) afforded 5-bromo-4-(difluoromethoxy)-2-methoxypyridine (**63**) as a yellow solid (0.12 g, 47% yield). LCMS: m/z = 254.0, 256.0 $[M + H]^+$.

(b) In a thick-walled glass reaction vessel equipped with a magnetic stirrer and a Teflon screwcap was combined 5-bromo-4-

https://doi.org/10.1021/acs.jmedchem.6c01049
J. Med. Chem. 2026, 69, 15888−15927

(difluoromethoxy)-2-methoxypyridine (**63**, 0.12 g, 0.47 mmol, 1 equiv) from the previous step, Cs_2CO_3 (0.46 g, 1.4 mmol, 3 equiv), [(2-dicyclohexylphosphino-3,6-dimethoxy-2′,4′,6′- triisopropyl-1,1′-biphenyl)-2-(2′-amino-1,1′ -biphenyl)]-palladium(II) methanesulfonate (43 mg, 0.047 mmol, 0.1 equiv), and *tert*-butyl carbamate (2.75 g, 23.5 mmol, 50 equiv) in 1,4-dioxane (50 mL). The resulting yellow suspension was deoxygenated via subsurface purging with nitrogen for 10 min before the reaction vessel was tightly sealed and heated at 90 °C for 2 h. The reaction mixture was then cooled to rt, diluted with EtOAc (300 mL), and washed sequentially with water (100 mL) and brine (100 mL). The organic layer was then dried over Na_2SO_4, filtered, and the filtrate concentrated in vacuo. Purification of the crude product thus obtained by way of column chromatography (SiO_2, gradient elution: Hex → EtOAc) afforded *tert*-butyl (4-(difluoromethoxy)-6-methoxypyridin-3-yl)carbamate (**64**) as a white solid (0.12 g, 87% yield). LCMS: m/z = 291.1 $[M + H]^+$.

(c) In a dried, round-bottom flask equipped with a magnetic stirrer was dissolved *tert*-butyl (4-(difluoromethoxy)-6-methoxypyridin-3-yl)carbamate (**64**, 0.12 g, 0.43 mmol, 1 equiv) from the previous step in DCM (4 mL). To this solution was added HCl (4 M solution in 1,4-dioxane, 1.1 mL, 4.4 mmol, 10 equiv) and the resulting reaction mixture was stirred at rt for 2 h. The now white suspension was diluted with water, rendered slightly basic (pH ∼ 8) with the addition of saturated aq. $NaHCO_3$, and extracted with EtOAc (50 mL × 3). The combined organic extracts were washed further with brine (50 mL), dried over Na_2SO_4, filtered, and the filtrate concentrated in vacuo. Purification of the crude product thus obtained by way of column chromatography (SiO_2, gradient elution: Hex → EtOAc) afforded the title compound **65** as a dark solid (51 mg, 62% yield). LCMS: m/z = 191.1 $[M + H]^+$.

3-(Difluoromethoxy)-5-methoxypyridin-2-amine (69)

(a) In a dried, round-bottom flask equipped with a magnetic stirrer was combined 5-methoxypyridin-3-ol (**66**, 0.60 g, 4.8 mmol, 1 equiv) and tetrabutylammonium nitrate (2.34 g, 7.67 mmol, 1.6 equiv) in DCM (30 mL). The resulting solution was then cooled to 0 °C before TFAA (1.1 mL, 7.7 mmol, 1.6 equiv) was added neat and dropwise. The resulting mixture was stirred at 0 °C for 2 h and then at rt for an additional 30 min. The reaction was then quenched with water (100 mL) and extracted further with DCM (3 × 50 mL). The combined organic extracts were washed further with water (50 mL) and brine (50 mL), dried over Na_2SO_4, filtered, and the filtrate concentrated in vacuo. Purification of the crude product thus obtained by way of column chromatography (SiO_2, 3:1 (v/v) Hex: EtOAc) afforded 5-methoxy-2-nitropyridin-3-ol (**67**) as a yellow oil (0.25 g, 31% yield). LCMS: m/z = 171.2 $[M + H]^+$.

(b) In a dried, round-bottom flask equipped with a magnetic stirrer was suspended Cs_2CO_3 (1.37 g, 4.20 mmol, 3 equiv) in DMF (8 mL). The reaction suspension was heated to 80 °C before a DMF solution (8 mL) of 5-methoxy-2-nitropyridin-3-ol (**67**, 0.24 g, 1.4 mmol, 1 equiv) from the previous step and sodium chlorodifluoroacetate (0.32 g, 2.1 mmol, 1.5 equiv) was added dropwise over a period of 10 min. Following the completion of addition, the now orange reaction solution was heated at 80 °C for an extra 30 min before it was cooled to rt, diluted with EtOAc (200 mL), and washed sequentially with water (100 mL) and brine (100 mL). The organic layer was then dried over Na_2SO_4, filtered, and the filtrate concentrated in vacuo. Purification of the crude product thus obtained by way of column chromatography (SiO_2, 7:1 (v/v) Hex: EtOAc) afforded 3-(difluoromethoxy)-5-methoxy-2-nitropyridine (**68**) as a yellow oil (0.10 g, 32% yield). LCMS: m/z = 221.1 $[M + H]^+$.

(c) In a dried, round-bottom flask equipped with a magnetic stirrer was dissolved 3-(difluoromethoxy)-5-methoxy-2-nitropyridine (**68**, 0.44 g, 2.0 mmol, 1 equiv) from the previous step in MeOH (20 mL). The resulting yellow solution was then deoxygenated via subsurface purging with nitrogen for 10 min before palladium (10% w/w over activated carbon, dry, 0.43 g, 0.40 mmol, 0.2 equiv) was added in one rapid portion. The resulting black suspension was then subsurface purged with hydrogen for 10 min before it was stirred under a static hydrogen atmosphere at rt for 1 h. The reaction was subsequently quenched with DCM (100 mL) and filtered through a bed of DCM-wetted Celite. Concentration of the filtrate in vacuo afforded the title compound **69** as a yellow solid (0.37 g, 97% yield). LCMS: m/z = 191.1 $[M + H]^+$.

6-(Difluoromethyl)-2-methoxypyridin-3-amine (73)

(a) In a dried, round-bottom flask equipped with a magnetic stirrer was dissolved 5-bromo-6-methoxypicolinaldehyde (**70**, 0.51 g, 2.4 mmol, 1 equiv) in DCM (20 mL). To this solution was then added at 0 °C BAST (1.1 mL, 5.9 mmol, 2.5 equiv), neat and dropwise, over a period of 10 min. Following the completion of addition, the now orange reaction solution was warmed to and stirred at rt for 16 h. The reaction was then carefully quenched with ice water (100 mL) and extracted with DCM (3 × 60 mL). The combined organic extracts were then washed sequentially with saturated aq. $NaHCO_3$ (50 mL), water (50 mL), and brine (50 mL). The organic layer was then dried over Na_2SO_4, filtered, and the filtrate concentrated in vacuo. Purification of the crude product thus obtained by way of column chromatography (SiO_2, gradient elution: Hex → EtOAc) afforded 3-bromo-6-(difluoromethyl)-2-methoxypyridine (**71**) as a colorless oil (0.48 g, 85% yield). LCMS: m/z = 238.0, 240.0 $[M + H]^+$.

(b) In a thick-walled glass reaction vessel equipped with a magnetic stirrer and a Teflon screwcap was combined 3-bromo-6-(difluoromethyl)-2-methoxypyridine (**71**, 0.20 g, 0.84 mmol, 1 equiv) from the previous step, potassium *tert*-butoxide (0.28 g, 2.5 mmol, 3 equiv), [(2-dicyclohexylphosphino-3,6-dimethoxy-2′,4′,6′-triisopropyl-1,1′-biphenyl)-2-(2′-amino-1,1′ -biphenyl)]palladium(II) methanesulfonate (0.15 g, 0.17 mmol, 0.2 equiv), and *tert*-butyl carbamate (4.9 g, 42 mmol, 50 equiv) in 1,4-dioxane (20 mL). The resulting mixture was deoxygenated via subsurface purging with nitrogen for 10 min before the reaction vessel was tightly sealed and heated at 90 °C for 2 h. The reaction mixture was then cooled to rt, diluted with EtOAc (150 mL), and washed sequentially with water (75 mL) and brine (75 mL). The organic layer was then dried over Na_2SO_4, filtered, and the filtrate concentrated in vacuo. Purification of the crude product thus obtained by way of column chromatography (SiO_2, gradient elution: Hex → EtOAc) afforded *tert*-butyl (6-(difluoromethyl)-2-methoxypyridin-3-yl)carbamate (**72**) as a yellow oil (0.20 g, 87% yield). LCMS: m/z = 275.2 $[M + H]^+$.

(c) In a dried, round-bottom flask equipped with a magnetic stirrer was dissolved *tert*-butyl (6-(difluoromethyl)-2-methoxypyridin-3-yl)carbamate (**72**, 0.19 g, 0.69 mmol, 1 equiv) from the previous step in DCM (6 mL). To this solution was added TFA (7.9 mL, 100 mmol, 150 equiv) and the resulting reaction mixture was stirred at rt for 1 h. The mixture was then rendered slightly basic (pH ∼ 8) with the addition of NH_3 (7 M solution in MeOH) and the volatiles were removed in vacuo. Purification of the crude product thus obtained by way of reverse-phase column chromatography (C_{18}, gradient elution: 9:1 (v/v) H_2O: MeCN → MeCN) afforded the title compound **73** as a yellow oil (0.11 g, 91% yield). LCMS: m/z = 175.2 $[M + H]^+$.

1-(1-Acetylpiperidin-4-yl)-3-(2-(difluoromethoxy)-6-methoxypyridin-3-yl)-1-(2-isopropylphenyl)urea (21)

(a) In a thick-walled glass reaction vessel equipped with a magnetic stirrer and a Teflon screwcap was combined 1-(4-aminopiperidin-1-yl)ethan-1-one (1.42 g, 10.0 mmol, 1 equiv, Combi-Blocks, Cat. No. ST-1873), 1-iodo-2-isopropylbenzene (1.6 mL, 10 mmol, 1 equiv, Combi-Blocks, Cat. No. OR-2271), XantPhos (0.35 g, 0.60 mmol, 0.06 equiv), and sodium *tert*-pentoxide (3.3 g, 30 mmol, 3 equiv) in 1,4-dioxane (40 mL). The resulting

https://doi.org/10.1021/acs.jmedchem.6c01049
J. Med. Chem. 2026, 69, 15888−15927

yellow solution was deoxygenated via subsurface purging with nitrogen for 10 min and tris(dibenzylidineacetone)-dipalladium(0) (0.28 g, 0.30 mmol, 0.03 equiv) was then added. The reaction vessel was tightly sealed and heated at 100 °C for 10 h. The resulting dark brown suspension was cooled to rt, diluted with EtOAc (200 mL), and washed sequentially with water (2 × 100 mL) and brine (100 mL). The organic extract thus obtained was then dried over $MgSO_4$, filtered, and the filtrate concentrated in vacuo. Purification of the crude product thus obtained by way of column chromatography (SiO_2, gradient elution: Hex → EtOAc) afforded 1-(4-((2-isopropylphenyl)amino)piperidin-1-yl)ethan-1-one (**82**) as an off-white solid (2.1 g, 80% yield). LCMS: m/z = 261.2 $[M + H]^+$. ^1H NMR (300 MHz, $CDCl_3$) δ: 7.18 (d, J = 7.6 Hz, 1H), 7.11 (td, J = 7.3, 1.3 Hz, 1H), 6.87−6.66 (m, 2H), 4.51−4.43 (m, 1H), 3.85−3.77 (m, 1H), 3.61−3.52 (m, 1H), 3.21 (br t, J = 12.2 Hz, 1H), 2.92−2.79 (m, 2H), 2.19−2.04 (m, 2H), 2.11 (s, 3H), 1.72−1.57 (m, 1H), 1.51−1.37 (m, 2H), 1.25 (d, J = 6.8 Hz, 6H).

(b) In a dried, round-bottom flask equipped with a magnetic stirrer was combined 2-(difluoromethoxy)-6-methoxypyridin-3-amine (**61**, 0.38 g, 2.0 mmol, 1 equiv) and pyridine (485 μL, 6.00 mmol, 3 equiv) in anhydrous DCM (20 mL). To this was then added phosgene (15% w/w solution in toluene, 2.1 mL, 3.0 mmol, 1.5 equiv) dropwise at rt and the resulting solution was stirred at rt for 30 min. The volatiles were then removed in vacuo and the crude (2-(difluoromethoxy)-6-methoxypyridin-3-yl)-carbamic chloride thus obtained was retaken up in anhydrous DCM (10 mL). This solution was then added dropwise at rt to another DCM (10 mL) suspension of 1-(4-((2-isopropylphenyl)amino)piperidin-1-yl)ethan-1-one (**82**, 0.52 g, 2.0 mmol, 1 equiv) from the previous step, pyridine (485 μL, 6.00 mmol, 3 equiv), and freshly activated 4 Å molecular sieves (20 beads). The resulting mixture was stirred at rt for 16 h before the reaction was quenched with water (20 mL). The aqueous layer was separated and back extracted with DCM (3 × 20 mL). The combined organic extracts were dried over $MgSO_4$, filtered, and the filtrate concentrated in vacuo. Purification of the crude product thus obtained by way of reverse-phase column chromatography (C_{18}, gradient elution: 10:1 (v/v) H_2O: MeCN + 0.1% formic acid → MeCN + 0.1% formic acid) afforded the title compound **21** as a white solid (0.37 g, 38% yield). LCMS: m/z = 477.1 $[M + H]^+$. Purity (UV detection) = 100.0%. ^1H NMR (300 MHz, $CDCl_3$): δ = 8.40 (dd, J = 8.7, 2.9 Hz, 1H), 7.51−7.47 (m, 2H), 7.34−7.28 (m, 1H), 7.17 (t, J = 72.9 Hz, 1H), 7.12 (t, J = 7.7 Hz, 1H), 6.51 (d, J = 8.7 Hz, 1H), 5.96 (br s, 1H), 4.77−4.64 (m, 1H), 4.61 (tt, J = 12.8, 3.8 Hz, 1H), 3.90−3.81 (m, 1H), 3.79 (s, 3H), 3.26−3.11 (m, 2H), 2.55 (qd, J = 9.8, 2.2 Hz, 1H), 2.21−2.07 (m, 1H), 2.06 (s, 1.5H, rotamer A), 2.02 (s, 1.5H, rotamer B), 1.91−1.77 (m, 1H), 1.67−1.49 (m, 1H), 1.29−1.14 (m, 1H), 1.25 (dd, J = 7.0, 1.6 Hz, 3H), 1.16 (dd, J = 7.0, 3.2 Hz, 3H). HRMS (ESI+): m/z for $C_{24}H_{31}F_2N_4O_4$ 477.2313 $[M + H]^+$; observed 477.2310: mass error −0.6 (ppm).

1-(1-Acetylpiperidin-4-yl)-3-(2-(difluoromethoxy)-6-methylpyridin-3-yl)-1-(2-isopropylphenyl)urea (15)

The title compound **15** was prepared in a manner analogous to that described for compound **21** but using 2-(difluoromethoxy)-6-methylpyridin-3-amine[35a] in place of 2-(difluoromethoxy)-6-methoxypyridin-3-amine (**61**) in step (b). LCMS: m/z = 461.1 $[M + H]^+$. Purity (UV detection) = 100.0%. ^1H NMR (500 MHz, DMSO-d_6): δ = 8.30 (d, J = 8.5 Hz, 1H), 7.58 (d, J = 9.0 Hz, 1H), 7.50 (t, J = 8.0 Hz, 1H), 7.44 (t, J = 73.0 Hz, 1H), 7.35 (t, J = 7.5 Hz, 1H), 7.25 (d, J = 7.5 Hz, 1H), 7.04 (d, J = 8.5 Hz, 1H), 6.32 (br s, 1H), 4.46−4.39 (m, 2H), 3.87−3.81 (m, 1H), 3.12−3.07 (m, 2H), 2.57−2.53 (m, 1H), 2.31 (s, 3H), 2.04−2.00 (m, 1H), 1.94 (s, 1.5H, rotamer A), 1.91 (s, 1.5H, rotamer B), 1.76−1.74 (m, 1H), 1.56−1.32 (m, 1H), 1.22 (d, J = 7.0 Hz, 3H), 1.20−0.96 (m, 4H). HRMS (ESI+): m/z for $C_{24}H_{31}F_2N_4O_3$ 461.2364 $[M + H]^+$; observed 461.2362: mass error −0.4 (ppm).

1-(1-Acetylpiperidin-4-yl)-3-(2-(difluoromethoxy)-pyridin-3-yl)-1-(2-isopropylphenyl)urea (18)

The title compound **18** was prepared in a manner analogous to that described for compound **21** but using 2-(difluoromethoxy)pyridin-3-amine (Combi-Blocks, Cat. No. QP-4844) in place of 2-(difluoromethoxy)-6-methoxypyridin-3-amine (**61**) in step (b). LCMS: m/z = 446.8 $[M + H]^+$. Purity (UV detection) = 100%. ^1H NMR (300 MHz, DMSO-d_6): δ = 8.46 (dd, J = 7.8, 1.7 Hz, 1H), 7.80 (dd, J = 4.8, 1.7 Hz, 1H), 7.60 (dd, J = 7.8, 1.5 Hz, 1H), 7.52 (t, J = 7.1 Hz, 1H), 7.48 (t, J = 72.4 Hz, 1H), 7.37 (t, J = 7.1 Hz, 1H), 7.27 (dd, J = 7.4, 1.1 Hz, 1H), 7.22 (dd, J = 8.0, 4.8 Hz, 1H), 6.41 (br s, 1H), 4.52−4.39 (m, 2H), 3.91−3.81 (m, 1H), 3.16−3.06 (m, 2H), 2.62−2.54 (m, 1H), 2.08−1.99 (m, 1H), 1.95 (s, 1.5H, rotamer A), 1.92 (s, 1.5H, rotamer B), 1.81−1.73 (m, 1H), 1.60−1.33 (m, 1H), 1.24 (t, J = 6.3 Hz, 3H), 1.18−1.02 (m, 1H), 1.10 (d, J = 6.8 Hz, 3H).

1-(1-Acetylpiperidin-4-yl)-3-(2-(difluoromethoxy)-6-(difluoromethyl)pyridin-3-yl)-1-(2-isopropylphenyl)urea (19)

The title compound **19** was prepared in a manner analogous to that described for compound **21** but using 2-(difluoromethoxy)-6-(difluoromethyl)pyridin-3-amine (**58**) in place of 2-(difluoromethoxy)-6-methoxypyridin-3-amine (**61**) in step (b). LCMS: m/z = 497.3 $[M + H]^+$. Purity (UV detection) = 99.9%. ^1H NMR (300 MHz, DMSO-d_6): δ = 8.62 (d, J = 8.2 Hz, 1H), 7.60 (d, J = 6.6 Hz, 1H), 7.55−7.50 (m, 2H), 7.46 (t, J = 71.8 Hz, 1H), 7.37 (t, J = 7.5 Hz, 1H), 7.28 (d, J = 7.7 Hz, 1H), 6.81 (t, J = 54.8 Hz, 1H), 6.54 (br s, 1H), 4.50−4.38 (m, 2H), 3.90−3.79 (m, 1H), 3.16−3.04 (m, 2H), 2.62−2.43 (m, 1H), 2.08−1.99 (m, 1H), 1.95 (s, 1.5H, rotamer A), 1.92 (s, 1.5H, rotamer B), 1.81−1.73 (m, 1H), 1.60−1.33 (m, 1H), 1.22 (t, J = 6.3 Hz, 3H), 1.18−1.01 (m, 1H), 1.08 (d, J = 6.8 Hz, 3H).

1-(1-Acetylpiperidin-4-yl)-3-(2-(difluoromethoxy)-4-methylphenyl)-1-(2-isopropylphenyl)urea (20)

The title compound **20** was prepared in a manner analogous to that described for compound **21** but using 2-(difluoromethoxy)-4-methylaniline (Combi-Blocks, Cat. No. JA-6745) in place of 2-(difluoromethoxy)-6-methoxypyridin-3-amine (**61**) in step (b). LCMS: m/z = 460.3 $[M + H]^+$. Purity (UV detection) = 99.6%. ^1H NMR (300 MHz, DMSO-d_6): δ = 7.90 (d, J = 8.3 Hz, 1H), 7.58−7.49 (m, 2H), 7.41−7.33 (m, 2H), 6.98 (d, J = 8.4 Hz, 1H), 6.93 (s, 1H), 6.90 (t, J = 74.0 Hz, 1H), 6.63 (br s, 1H), 4.50−4.39 (m, 2H), 3.89−3.77 (m, 1H), 3.16−3.03 (m, 2H), 2.90 (s, 3H), 2.62−2.43 (m, 1H), 2.10−2.00 (m, 1H), 1.95 (s, 1.5H, rotamer A), 1.92 (s, 1.5H, rotamer B), 1.80−1.71 (m, 1H), 1.60−1.33 (m, 1H), 1.22 (t, J = 6.3 Hz, 3H), 1.18−0.99 (m, 1H), 1.08 (d, J = 6.8 Hz, 3H).

1-(1-Acetylpiperidin-4-yl)-3-(4-(difluoromethoxy)-6-methoxypyridin-3-yl)-1-(2-isopropylphenyl)urea (22)

The title compound **22** was prepared in a manner analogous to that described for compound **21** but using 4-(difluoromethoxy)-6-methoxypyridin-3-amine (**65**) in place of 2-(difluoromethoxy)-6-methoxypyridin-3-amine (**61**) in step (b). LCMS: m/z = 477.2 $[M + H]^+$. Purity (UV detection) = 97.9%. ^1H NMR (300 MHz, DMSO-d_6): δ = 8.37 (d, J = 1.8 Hz, 1H), 7.54−7.42 (m, 2H), 7.31 (t, J = 7.2 Hz, 1H), 7.25 (t, J = 72.8 Hz, 1H), 7.20 (d, J = 7.6 Hz, 1H), 6.56 (s, 1H), 6.47 (s, 1H), 4.48−4.33 (m, 2H), 3.87−3.81 (m, 1H), 3.81 (s, 3H), 3.18−3.03 (m, 2H), 2.58−2.44 (m, 1H), 2.04−1.96 (m, 1H), 1.94 (s, 1.5H, rotamer A), 1.91 (s, 1.5H, rotamer B), 1.77−1.69 (m, 1H), 1.58−1.27 (m, 1H), 1.21 (t, J = 6.3 Hz, 3H), 1.21−0.90 (m, 1H), 1.12 (d, J = 6.8 Hz, 3H).

1-(1-Acetylpiperidin-4-yl)-3-(3-(difluoromethoxy)-5-methoxypyridin-2-yl)-1-(2-isopropylphenyl)urea (23)

The title compound **23** was prepared in a manner analogous to that described for compound **21** but using 3-(difluoromethoxy)-5-methoxypyridin-2-amine (**69**) in place of 2-(difluoromethoxy)-6-methoxypyridin-3-amine (**61**) in step (b). LCMS: m/z = 477.3 $[M + H]^+$. Purity (UV detection) = 99.7%. ^1H NMR (300 MHz, DMSO-d_6): δ = 7.95 (d, J = 2.6 Hz, 1H), 7.48 (dd, J = 7.8, 1.4 Hz, 1H), 7.40 (t, J = 6.9 Hz, 1H), 7.30−7.04 (m, 4H), 7.03 (t, J = 72.3 Hz, 1H), 4.48−4.27 (m, 2H), 3.87−3.76 (m, 1H), 3.82 (s, 3H), 3.18 (sept, J = 6.6 Hz, 1H),

https://doi.org/10.1021/acs.jmedchem.6c01049
J. Med. Chem. 2026, 69, 15888−15927

3.06 (br t, J = 12.5 Hz, 1H), 2.56−2.45 (m, 1H), 2.02−1.89 (m, 1H), 1.94 (s, 1.5H, rotamer A), 1.90 (s, 1.5H, rotamer B), 1.74−1.66 (m, 1H), 1.59−1.31 (m, 1H), 1.23−0.92 (m, 7H).

1-(1-Acetylpiperidin-4-yl)-1-(2-isopropylphenyl)-3-(2-methoxy-6-methylpyridin-3-yl)urea (24)

The title compound **24** was prepared in a manner analogous to that described for compound **21** but using 2-methoxy-6-methylpyridin-3-amine (Combi-Blocks, Cat. No. PY-1976) in place of 2-(difluoromethoxy)-6-methoxypyridin-3-amine (**61**) in step (b). LCMS: m/z = 425.3 $[M + H]^+$. Purity (UV detection) = 96.9%. ^{1}H NMR (400 MHz, CD_3OD): δ = 8.17 (d, J = 8.0 Hz, 1H), 7.59 (dd, J = 7.8, 1.4 Hz, 1H), 7.54 (t, J = 7.6 Hz, 1H), 7.39 (td, J = 7.6, 1.6 Hz, 1H), 7.25 (d, J = 8.0 Hz, 1H), 6.73 (d, J = 8.0 Hz, 1H), 4.58−4.55 (m, 2H), 4.01−3.98 (m, 1H), 3.66 (s, 3H), 3.22−3.15 (m, 2H), 2.69 (br t, J = 13.0 Hz, 1H), 2.33 (s, 3H), 2.19−2.12 (m, 1H), 2.07 (s, 1.5H, rotamer A), 2.04 (s, 1.5H, rotamer B), 1.95−1.83 (m, 1H), 1.72−1.53 (m, 1H), 1.34−1.14 (m, 7H).

1-(1-Acetylpiperidin-4-yl)-1-(2-isopropylphenyl)-3-(2-methoxypyridin-3-yl)urea (25)

The title compound **25** was prepared in a manner analogous to that described for compound **21** but using 2-methoxypyridin-3-amine (Combi-Blocks, Cat. No. OR-1304) in place of 2-(difluoromethoxy)-6-methoxypyridin-3-amine (**61**) in step (b). LCMS: m/z = 410.9 $[M + H]^+$. Purity (UV detection) = 100.0%. ^{1}H NMR (300 MHz, DMSO-d_6): δ = 8.34 (dd, J = 7.8, 1.7 Hz, 1H), 7.70 (dd, J = 5.0, 1.7 Hz, 1H), 7.61 (dd, J = 8.0, 1.6 Hz, 1H), 7.54 (td, J = 7.1, 1.1 Hz, 1H), 7.38 (t, J = 7.5 Hz, 1H), 7.26 (dd, J = 7.8, 1.1 Hz, 1H), 6.93 (dd, J = 7.8, 5.0 Hz, 1H), 6.41 (br s, 1H), 4.52−4.38 (m, 2H), 3.91−3.79 (m, 1H), 3.60 (s, 3H), 3.15−3.01 (m, 2H), 2.62−2.47 (m, 1H), 2.08−1.99 (m, 1H), 1.95 (s, 1.5H, rotamer A), 1.92 (s, 1.5H, rotamer B), 1.80−1.72 (m, 1H), 1.59−1.31 (m, 1H), 1.22 (t, J = 6.4 Hz, 3H), 1.22−0.95 (m, 1H), 1.07 (d, J = 6.8 Hz, 3H).

1-(1-Acetylpiperidin-4-yl)-3-(6-(difluoromethyl)-2-methoxypyridin-3-yl)-1-(2-isopropylphenyl)urea (26)

The title compound **26** was prepared in a manner analogous to that described for compound **21** but using 6-(difluoromethyl)-2-methoxypyridin-3-amine (**73**) in place of 2-(difluoromethoxy)-6-methoxypyridin-3-amine (**61**) in step (b). LCMS: m/z = 461.3 $[M + H]^+$. Purity (UV detection) = 99.8%. ^{1}H NMR (300 MHz, DMSO-d_6): δ = 8.47 (d, J = 8.0 Hz, 1H), 7.61 (dd, J = 7.9, 1.5 Hz, 1H), 7.54 (t, J = 7.8 Hz, 1H), 7.38 (t, J = 7.4 Hz, 1H), 7.26 (t, J = 7.8 Hz, 2H), 6.76 (t, J = 55.1 Hz, 1H), 6.54 (br s, 1H), 4.51−4.37 (m, 2H), 3.90−3.79 (m, 1H), 3.63 (s, 3H), 3.15−3.02 (m, 2H), 2.58−2.52 (m, 1H), 2.07−1.98 (m, 1H), 1.95 (s, 1.5H, rotamer A), 1.92 (s, 1.5H, rotamer B), 1.79−1.72 (m, 1H), 1.59−1.32 (m, 1H), 1.21 (t, J = 6.3 Hz, 3H), 1.25−0.94 (m, 1H), 1.05 (d, J = 6.8 Hz, 3H).

1-(1-Acetylpiperidin-4-yl)-1-(2-isopropylphenyl)-3-(2-methoxy-6-(trifluoromethyl)pyridin-3-yl)urea (27)

The title compound **27** was prepared in a manner analogous to that described for compound **21** but using 2-methoxy-6-(trifluoromethyl)-pyridin-3-amine (Combi-Blocks, Cat. No. OR-1304) in place of 2-(difluoromethoxy)-6-methoxypyridin-3-amine (**61**) in step (b). LCMS: m/z = 479.1 $[M + H]^+$. Purity (UV detection) = 100.0%. ^{1}H NMR (500 MHz, DMSO-d_6): δ = 8.53 (d, J = 8.0 Hz, 1H), 7.62 (d, J = 7.5 Hz, 1H), 7.55 (t, J = 7.5 Hz, 1H), 7.47 (d, J = 8.0 Hz, 1H), 7.39 (td, J = 7.5, 1.5 Hz, 1H), 7.28 (d, J = 6.5 Hz, 1H), 6.62 (br s, 1H), 4.48−4.40 (m, 2H), 3.84 (br t, J = 15.0 Hz, 1H), 3.65 (s, 3H), 3.14−3.04 (m, 2H), 2.58−2.53 (m, 1H), 2.08−2.00 (m, 1H), 1.95 (s, 1.5H, rotamer A), 1.92 (s, 1.5H, rotamer B), 1.78−1.72 (m, 1H), 1.58−1.33 (m, 1H), 1.22 (dd, J = 10.0, 7.0 Hz, 3H), 1.24−0.96 (m, 1H), 1.05 (d, J = 7.0 Hz, 3H).

1-(1-Acetylpiperidin-4-yl)-3-(6-cyano-2-methoxypyridin-3-yl)-1-(2-isopropylphenyl)urea (28)

The title compound **28** was prepared in a manner analogous to that described for compound **21** but using 5-amino-6-methoxypicolinonitrile (Combi-Blocks, Cat. No. JF-8651) in place of 2-(difluoromethoxy)-6-methoxypyridin-3-amine (**61**) in step (b). LCMS: m/z = 435.9 $[M + H]^+$. Purity (UV detection) = 100.0%. ^{1}H NMR (300 MHz, DMSO-d_6): δ = 8.49 (d, J = 8.1 Hz, 1H), 7.63 (d, J = 8.1 Hz, 1H), 7.62 (dd, J = 7.9, 1.7 Hz, 1H), 7.56 (td, J = 7.8, 1.2 Hz, 1H), 7.40 (t, J = 7.4 Hz, 1H), 7.29 (dd, J = 7.9, 1.2 Hz, 1H), 6.69 (br s, 1H), 4.50−4.37 (m, 2H), 3.91−3.80 (m, 1H), 3.65 (s, 3H), 3.17−3.00 (m, 2H), 2.63−2.54 (m, 1H), 2.08−2.00 (m, 1H), 1.95 (s, 1.5H, rotamer A), 1.92 (s, 1.5H, rotamer B), 1.80−1.73 (m, 1H), 1.59−1.32 (m, 1H), 1.27−0.99 (m, 1H), 1.22 (t, J = 6.4 Hz, 3H), 1.05 (d, J = 6.8 Hz, 3H).

1-(1-Acetylpiperidin-4-yl)-3-(2,6-dimethoxypyridin-3-yl)-1-(2-isopropylphenyl)urea (29)

The title compound **29** was prepared in a manner analogous to that described for compound **21** but using 2,6-dimethoxypyridin-3-amine (Combi-Blocks, Cat. No. QE-2867) in place of 2-(difluoromethoxy)-6-methoxypyridin-3-amine (**61**) in step (b). LCMS: m/z = 440.9 $[M + H]^+$. Purity (UV detection) = 100.0%. ^{1}H NMR (300 MHz, DMSO-d_6): δ = 8.16 (d, J = 8.4 Hz, 1H), 7.57 (dd, J = 7.9, 1.5 Hz, 1H), 7.50 (t, J = 7.5 Hz, 1H), 7.35 (t, J = 7.5 Hz, 1H), 7.23 (d, J = 6.6 Hz, 1H), 6.33 (d, J = 8.4 Hz, 1H), 6.11 (br s, 1H), 4.48−4.37 (m, 2H), 3.89−3.78 (m, 1H), 3.76 (s, 3H), 3.65 (s, 3H), 3.14−3.05 (m, 2H), 2.61−2.53 (m, 1H), 2.06−1.97 (m, 1H), 1.95 (s, 1.5H, rotamer A), 1.92 (s, 1.5H, rotamer B), 1.78−1.70 (m, 1H), 1.61−1.29 (m, 1H), 1.22 (t, J = 6.4 Hz, 3H), 1.21−0.97 (m, 1H), 1.10 (d, J = 6.8 Hz, 3H).

1-(1-Acetylpiperidin-4-yl)-1-(2-isopropylphenyl)-3-(3-methoxypyridin-4-yl)urea (30)

The title compound **30** was prepared in a manner analogous to that described for compound **21** but using 3-methoxypyridin-4-amine (Combi-Blocks, Cat. No. QB-0217) in place of 2-(difluoromethoxy)-6-methoxypyridin-3-amine (**61**) in step (b). LCMS: m/z = 410.9 $[M + H]^+$. Purity (UV detection) = 100.0%. ^{1}H NMR (300 MHz, DMSO-d_6): δ = 8.11 (s, 1H), 8.07 (s, 2H), 7.61 (dd, J = 8.0, 1.7 Hz, 1H), 7.55 (td, J = 7.0, 1.1 Hz, 1H), 7.38 (t, J = 7.3 Hz, 1H), 7.28 (dd, J = 7.8, 1.1 Hz, 1H), 6.69 (br s, 1H), 4.52−4.38 (m, 2H), 3.91−3.80 (m, 1H), 3.58 (s, 3H), 3.17−3.01 (m, 2H), 2.62−2.54 (m, 1H), 2.10−2.00 (m, 1H), 1.95 (s, 1.5H, rotamer A), 1.92 (s, 1.5H, rotamer B), 1.81−1.73 (m, 1H), 1.59−1.31 (m, 1H), 1.22 (t, J = 6.4 Hz, 3H), 1.21−0.98 (m, 1H), 1.04 (d, J = 6.8 Hz, 3H).

Racemic 1-(1-acetylpiperidin-3-yl)-3-(2-(difluoromethoxy)-6-methoxypyridin-3-yl)-1-(2-isopropylphenyl)urea (43)

The title compound **43** was prepared in a manner analogous to that described for compound **21** but using *racemic* 1-(3-aminopiperidin-1-yl)ethan-1-one (Combi-Blocks, Cat. No. ST-9949) in place of 1-(4-aminopiperidin-1-yl)ethan-1-one in step (a). LCMS: m/z = 477.3 $[M + H]^+$. Purity (UV detection) = 99.9%. ^{1}H NMR (300 MHz, DMSO-d_6): δ = 8.17−8.07 (m, 1H), 7.81−7.26 (m, 5H), 6.63 (d, J = 8.6 Hz, 1H), 6.44−6.32 (m, 1H), 4.75−4.57 (m, 0.5H, rotamer A), 4.29−3.93 (m, 2H), 3.78 (s, 3H), 3.70 (br d, J = 12.4 Hz, 0.5H, rotamer B), 3.20−2.28 (m, 3H), 2.27−1.94 (m, 4H), 1.85−1.02 (m, 9H).

3-(2-(Difluoromethoxy)-6-methoxypyridin-3-yl)-1-(2-isopropylphenyl)-1-(1-(oxetan-3-yl)piperidin-4-yl)urea (44)

The title compound **44** was prepared in a manner analogous to that described for compound **21** but using 1-(oxetan-3-yl)piperidin-4-amine (Pharmablock, Cat. No. ST-9949) in place of 1-(4-aminopiperidin-1-yl)ethan-1-one in step (a). LCMS: m/z = 491.3 $[M + H]^+$. Purity (UV detection) = 99.3%. ^{1}H NMR (300 MHz, DMSO-d_6): δ = 8.15 (d, J = 8.6 Hz, 1H), 7.55 (dd, J = 7.9, 1.6 Hz, 1H), 7.53 (t, J = 72.5 Hz, 1H), 7.49 (td, J = 7.9, 1.2 Hz, 1H), 7.34 (td, J = 7.9, 1.7 Hz, 1H), 7.24 (dd, J = 7.8, 1.2 Hz, 1H), 6.61 (d, J = 8.6 Hz, 1H), 6.28 (br s, 1H), 4.46 (q, J = 6.2 Hz, 2H), 4.32 (q, J = 6.2 Hz, 2H), 4.23 (tt, J = 12.2, 4.2 Hz, 1H), 3.77 (s, 3H), 3.33−3.29 (m, 1H), 3.11 (sept, J = 6.8 Hz, 1H), 2.69 (br t, J = 10.5 Hz, 2H), 1.95 (br d, J = 11.6 Hz, 1H), 1.81 (br t, J = 10.5 Hz, 2H), 1.67 (br d, J = 11.2 Hz, 1H), 1.56 (qd, J = 12.0, 3.7 Hz, 1H), 1.21 (d, J = 6.8 Hz, 3H), 1.20−1.01 (m, 1H), 1.11 (d, J = 6.8 Hz, 3H). HRMS (ESI+): m/z for $C_{25}H_{33}F_2N_4O_4$ 491.2470 $[M + H]^+$; observed 491.2469: mass error −0.2 (ppm).

https://doi.org/10.1021/acs.jmedchem.6c01049
J. Med. Chem. 2026, 69, 15888−15927

1-(1-Acetylazetidin-3-yl)-3-(2-(difluoromethoxy)-6-methylpyridin-3-yl)-1-(2-isopropylphenyl)urea (14)

(a) In a thick-walled glass reaction vessel equipped with a magnetic stirrer and a Teflon screwcap was combined *tert*-butyl 3-aminoazetidine-1-carboxylate (0.69 g, 4.0 mmol, 1 equiv, Combi-Blocks, Cat. No. AM-2062), 1-iodo-2-isopropylbenzene (0.64 mL, 4.0 mmol, 1 equiv, Combi-Blocks, Cat. No. OR-2271), XPhos (0.23 g, 0.48 mmol, 0.12 equiv), and Cs_2CO_3 (10.4 g, 32.0 mmol, 8 equiv) in 1,4-dioxane (20 mL). The resulting yellow solution was deoxygenated via subsurface purging with nitrogen for 10 min and tris-(dibenzylidineacetone)dipalladium(0) (0.15 g, 0.16 mmol, 0.04 equiv) was then added. The reaction vessel was tightly sealed and heated at 100 °C for 24 h. The resulting dark brown suspension was cooled to rt, diluted with EtOAc (200 mL), and washed sequentially with water (2 × 100 mL) and brine (100 mL). The organic extract thus obtained was then dried over $MgSO_4$, filtered, and the filtrate concentrated in vacuo. Purification of the crude product thus obtained by way of column chromatography (SiO_2, gradient elution: Hex → 7:3 (v/v) Hex: EtOAc) afforded *tert*-butyl 3-((2-isopropylphenyl)-amino)azetidine-1-carboxylate as a yellow oil (0.51 g, 44% yield). LCMS: m/z = 291.2 $[M + H]^+$.

(b) In a dried, round-bottom flask equipped with a magnetic stirrer was combined 2-(difluoromethoxy)-6-methylpyridin-3-amine (0.14 g, 0.79 mmol, 1 equiv)[35a] and pyridine (192 μL, 2.38 mmol, 3 equiv) in anhydrous DCM (10 mL). To this was then added phosgene (15% w/w solution in toluene, 0.85 mL, 1.2 mmol, 1.5 equiv) dropwise at rt and the resulting solution was stirred at rt for 30 min. The volatiles were then removed in vacuo and the crude (2-(difluoromethoxy)-6-methylpyridin-3-yl)-carbamic chloride thus obtained was retaken up in anhydrous DCM (5 mL). This solution was then added dropwise at rt to another DCM (5 mL) suspension of *tert*-butyl 3-((2-isopropylphenyl)amino)azetidine-1-carboxylate (0.23 g, 0.79 mmol, 1 equiv) from the previous step, pyridine (192 μL, 2.38 mmol, 3 equiv), and freshly activated 4 Å molecular sieves (20 beads). The resulting mixture was stirred at rt for 16 h before the reaction was quenched with water (10 mL). The aqueous layer was separated and back extracted with DCM (3 × 10 mL). The combined organic extracts were dried over $MgSO_4$, filtered, and the filtrate concentrated in vacuo. Purification of the crude product thus obtained by way of column chromatography (SiO_2, gradient elution: Hex → 1:1 (v/v) Hex: EtOAc) afforded *tert*-butyl 3-(3-(2-(difluoromethoxy)-6-methylpyridin-3-yl)-1-(2-isopropylphenyl)ureido)azetidine-1-carboxylate as a colorless oil (0.28 g, 73% yield). LCMS: m/z = 491.1 $[M + H]^+$.

(c) In a round-bottom flask equipped with a magnetic stirrer was dissolved *tert*-butyl 3-(3-(2-(difluoromethoxy)-6-methylpyridin-3-yl)-1-(2-isopropylphenyl)ureido)azetidine-1-carboxylate (0.10 g, 0.20 mmol, 1 equiv) from the previous step in DCM (12 mL). To this solution was then added TFA (2 mL, 26 mmol, 130 equiv) and the resulting reaction mixture was stirred at rt for 20 min. The volatiles were then removed in vacuo via sequential azeotropic distillation with toluene and heptane. The residue thus obtained was then partitioned between EtOAc (30 mL) and saturated aq. $NaHCO_3$ (30 mL). The aqueous layer was separated and back extracted with EtOAc (2 × 30 mL). The combined organic extracts were washed further with water (30 mL) and brine (30 mL), dried over MgSO4, filtered, and the filtrate concentrated in vacuo. The crude 1-(azetidin-3-yl)-3-(2-(difluoromethoxy)-6-methylpyridin-3-yl)-1-(2-isopropylphenyl)urea thus obtained was then retaken up in DCM (4 mL) and added sequentially *N*,*N*-diisopropylethylamine (0.10 mL, 0.60 mmol, 3 equiv) and acetyl chloride (16 μL, 0.22 mmol, 1.1 equiv). After 10 min of stirring at rt, the reaction was quenched with water (20 mL) and extracted with DCM (2 × 50 mL). The combined organic extracts were washed further with brine (20 mL), dried over $MgSO_4$, filtered, and the filtrate concentrated in vacuo. Purification of the crude product thus obtained by way of reverse-phase column chromatography (C_{18}, gradient elution: 10:1 (v/v) H_2O: MeCN + 0.1% formic acid → MeCN + 0.1% formic acid) afforded the title compound **14** as a white solid (43 mg, 46% yield). LCMS: m/z = 432.8 $[M + H]^+$. Purity (UV detection) = 100.0%. ^{1}H NMR (500 MHz, DMSO-d_6): δ = 8.18 (dd, J = 8.0, 1.0 Hz, 1H), 7.59 (dd, J = 7.0, 2.0 Hz, 1H), 7.55−7.53 (m, 1H), 7.47 (t, J = 73.0 Hz, 1H), 7.41−7.37 (m, 2H), 7.06 (d, J = 8.0 Hz, 1H), 6.59 (br d, J = 6.0 Hz, 1H), 4.90−4.84 (m, 1H), 4.33 (t, J = 8.5 Hz, 1H), 4.10 (dd, J = 9.0, 6.0 Hz, 0.5H, rotamer A), 4.01−3.97 (m, 1H), 3.93 (dd, J = 9.0, 6.0 Hz, 0.5H, rotamer B), 3.70 (dd, J = 10.0, 6.0 Hz, 0.5H, rotamer A or B), 3.55 (dd, J = 10.0, 6.0 Hz, 0.5H, rotamer B or A), 3.04−2.96 (m, 1H), 2.33 (s, 3H), 1.71 (s, 1.5H, rotamer A or B), 1.69 (s, 1.5H, rotamer B or A), 1.17−1.15 (m, 6H). HRMS (ESI+): m/z for $C_{22}H_{27}F_2N_4O_3$ 433.2051 $[M + H]^+$; observed 433.2056: mass error 1.2 (ppm).

1-(2-Acetyl-2-azaspiro[3.3]-heptan-6-yl)-3-(2-(difluoromethoxy)-6-methoxypyridin-3--yl)-1-(2-isopropylphenyl)urea (31)

The title compound **31** was prepared in a manner analogous to that described for compound **14** but using *tert*-butyl 6-amino-2-azaspiro[3.3]heptane-2-carboxylate (Combi-Blocks, Cat. No. SS-0104) in place of *tert*-butyl 3-aminoazetidine-1-carboxylate in step (a) and 2-(difluoromethoxy)-6-methoxypyridin-3-amine (**61**) in place of 2-(difluoromethoxy)-6-methylpyridin-3-amine in step (b). LCMS: m/z = 489.1 $[M + H]^+$. Purity (UV detection) = 100.0%. ^{1}H NMR (500 MHz, DMSO-d_6): δ = 8.24 (d, J = 8.0 Hz, 1H), 7.58 (dd, J = 8.0, 1.5 Hz, 1H), 7.51 (t, J = 8.0 Hz, 1H), 7.45 (t, J = 72.5 Hz, 1H), 7.38 (t, J = 7.5 Hz, 1H), 7.05 (d, J = 8.0 Hz, 1H), 6.53 (d, J = 8.0 Hz, 1H), 6.38 (br d, J = 5.0 Hz, 1H), 4.67 (pent, J = 9.0 Hz, 1H), 4.16 (s, 1H), 3.91−3.85 (m, 2H), 3.61 (d, J = 10.0 Hz, 0.5H, rotamer A), 3.58 (s, 3H), 3.57 (d, J = 10.0 Hz, 0.5H, rotamer B), 2.94−2.90 (m, 1H), 2.48−2.41 (m, 1H), 2.36−2.33 (m, 1H), 2.10−2.06 (m, 1H), 1.82 (d, J = 11.0 Hz, 0.5H, rotamer A or B), 1.78 (d, J = 11.0 Hz, 0.5H, rotamer B or A), 1.70 (s, 1.5H, rotamer A or B), 1.65 (s, 1.5H, rotamer B or A), 1.19 (t, J = 7.0 Hz, 3H), 1.09 (d, J = 6.5 Hz, 3H).

3-(2-(Difluoromethoxy)-6-methoxypyridin-3-yl)-1-(2-isopropylphenyl)-1-(1-(methylsulfonyl)piperidin-4-yl)urea (45)

The title compound **45** was prepared in a manner analogous to that described for compound **14** but using *tert*-butyl 4-aminopiperidine-1-carboxylate (Combi-Blocks, Cat. No. AM-1626) in place of *tert*-butyl 3-aminoazetidine-1-carboxylate in step (a), 2-(difluoromethoxy)-6-methoxypyridin-3-amine (**61**) in place of 2-(difluoromethoxy)-6-methylpyridin-3-amine in step (b), and methanesulfonyl chloride in place of acetyl chloride in step (c). LCMS: m/z = 513.1 $[M + H]^+$. Purity (UV detection) = 100.0%. ^{1}H NMR (300 MHz, $CDCl_3$): δ = 8.38 (d, J = 8.7 Hz, 1H), 7.51−7.45 (m, 2H), 7.34−7.29 (m, 1H), 7.17 (t, J = 73.0 Hz, 1H), 7.13 (d, J = 7.6 Hz, 1H), 6.50 (d, J = 8.7 Hz, 1H), 5.97 (br s, 1H), 4.53 (tt, J = 12.2, 3.8 Hz, 1H), 3.91−3.80 (m, 2H), 3.79 (s, 3H), 3.18 (sept, J = 6.8 Hz, 1H), 2.84−2.73 (m, 2H), 2.76 (s, 3H), 2.22−2.15 (m, 1H), 1.94−1.86 (m, 1H), 1.78 (qd, J = 12.3, 4.4 Hz, 1H), 1.43 (qd, J = 12.3, 4.4 Hz, 1H), 1.25 (d, J = 6.8 Hz, 3H), 1.15 (d, J = 6.8 Hz, 3H). HRMS (ESI+): m/z for $C_{23}H_{31}F_2N_4O_5S$ 513.1983 $[M + H]^+$; observed 513.1977: mass error −1.2 (ppm).

1-((3*S*,4*R*)-1-Acetyl-3-fluoropiperidin-4-yl)-3-(2-(difluoromethoxy)-6-methoxypyridin-3-yl)-1-(2-isopropylphenyl)-urea (39)

(a) In a thick-walled glass reaction vessel equipped with a magnetic stirrer and a Teflon screwcap was combined *tert*-butyl (3*S*,4*R*)-4-amino-3-fluoropiperidine-1-carboxylate hydrochloride (**74**, 0.12 g, 0.46 mmol, 1 equiv, Pharmablock, Cat. No. PBZS0024), 1-iodo-2-isopropylbenzene (81 μL, 0.51 mmol, 1.1 equiv, Combi-Blocks, Cat. No. OR-2271), XantPhos (80 mg, 0.14 mmol, 0.3 equiv), and potassium *tert*-butoxide (0.15 g, 1.4 mmol, 3 equiv) in 1,4-dioxane (10 mL). The resulting yellow solution was deoxygenated via subsurface purging with nitrogen

https://doi.org/10.1021/acs.jmedchem.6c01049
J. Med. Chem. 2026, 69, 15888−15927

for 10 min and tris(dibenzylidineacetone)dipalladium(0) (93 mg, 0.09 mmol, 0.2 equiv) was then added. The reaction vessel was tightly sealed and heated at 100 °C for 48 h. The resulting dark brown suspension was cooled to rt, diluted with EtOAc (100 mL), and washed sequentially with water (2 × 50 mL) and brine (50 mL). The organic extract thus obtained was then dried over $MgSO_4$, filtered, and the filtrate concentrated in vacuo. Purification of the crude product thus obtained by way of column chromatography (SiO_2, gradient elution: Hex → EtOAc) afforded *tert*-butyl (3*S*,4*R*)-3-fluoro-4-((2-isopropylphenyl)amino)piperidine-1-carboxylate (**75**) as a colorless oil (0.12 g, 78% yield). LCMS: m/z = 337.3 $[M + H]^+$.

(b) In a round-bottom flask equipped with a magnetic stirrer was dissolved *tert*-butyl (3*S*,4*R*)-3-fluoro-4-((2-isopropylphenyl)-amino)piperidine-1-carboxylate (**75**, 0.12 g, 0.36 mmol, 1 equiv) from the previous step in DCM (6 mL). To this solution was added TFA (4.0 mL, 54 mmol, 150 equiv, Sigma-Aldrich) and the resulting reaction mixture was stirred at rt for 2 h. The volatiles were then removed in vacuo via sequential azeotropic distillation with toluene and heptane. The residue thus obtained was then partitioned between EtOAc (50 mL) and saturated aq. $NaHCO_3$ (50 mL). The aqueous layer was separated and back extracted with EtOAc (2 × 50 mL). The combined organic extracts were washed further with water (50 mL) and brine (50 mL), dried over MgSO4, filtered, and the filtrate concentrated in vacuo. The crude (3*S*,4*R*)-3-fluoro-*N*-(2-isopropylphenyl)-piperidin-4-amine thus obtained was then retaken up in DCM (5 mL) and added sequentially triethylamine (125 μL, 0.900 mmol, 2.5 equiv) and acetyl chloride (38 μL, 0.54 mmol, 1.5 equiv). After 1 h of stirring at rt, the reaction was quenched with water (20 mL) and extracted with DCM (50 mL). The combined organic extracts were washed further with brine (20 mL), dried over $MgSO_4$, filtered, and the filtrate concentrated in vacuo. Purification of the crude product thus obtained by way of column chromatography (SiO_2, gradient elution: Hex → 1:1 (v/v) Hex: EtOAc) afforded 1-((3*S*,4*R*)-3-fluoro-4-((2-isopropylphenyl)amino)piperidin-1-yl)ethan-1-one (**76**) as a colorless oil (78 mg, 78% yield). LCMS: m/z = 279.3 $[M + H]^+$.

(c) In a dried, round-bottom flask equipped with a magnetic stirrer was combined 2-(difluoromethoxy)-6-methoxypyridin-3-amine (**61**, 33 mg, 0.17 mmol, 1.2 equiv) and pyridine (35 μL, 0.43 mmol, 3 equiv) in anhydrous DCE (4 mL). To this was then added triphosgene (17 mg, 0.056 mmol, 0.4 equiv) in one rapid portion at rt and the resulting solution was stirred at rt for 30 min. 1-((3*S*,4*R*)-3-fluoro-4-((2-isopropylphenyl)amino)-piperidin-1-yl)ethan-1-one (**76**, 40 mg, 0.14 mmol, 1 equiv) from the previous step was then added in one rapid portion and a reflux condenser was attached. The resulting mixture was heated at 50 °C for 7 days before the reaction was quenched with water (10 mL). The aqueous layer was separated and back extracted with DCM (3 × 30 mL). The combined organic extracts were dried over $MgSO_4$, filtered, and the filtrate concentrated in vacuo. Purification of the crude product thus obtained by way of reverse-phase column chromatography (C_{18}, gradient elution: 10:1 (v/v) H_2O: MeCN + 0.1% formic acid → MeCN + 0.1% formic acid) afforded the title compound **39** as a white solid (23 mg, 33% yield). LCMS: m/z = 495.2 $[M + H]^+$. Purity (UV detection) = 96.9%. ^{1}H NMR (300 MHz, DMSO-d_6): δ = 8.17 (dd, J = 8.6, 5.8 Hz, 0.26H, rotamer A), 8.17 (dd, J = 8.6, 4.9 Hz, 0.74H, rotamer B), 7.55 (t, J = 72.5 Hz, 0.74H, rotamer B), 7.54 (t, J = 72.5 Hz, 0.26H, rotamer A), 7.53−7.43 (m, 2H), 7.37−7.19 (m, 2H), 6.64 (d, J = 8.6 Hz, 0.26H, rotamer A), 6.63 (d, J = 8.6 Hz, 0.74H, rotamer B), 6.47 (d, J = 7.9 Hz, 0.74H, rotamer B), 6.32 (d, J = 7.0 Hz, 0.26H, rotamer A), 5.34−5.04 (m, 1H), 4.85−4.33 (m, 2H), 4.16−3.79 (m, 1H), 3.79 (s, 2.2H, rotamer B), 3.78 (s, 0.8H, rotamer A), 3.53−3.16 (m, 1H), 3.07−2.57 (m, 2H), 1.97−1.90 (m, 3H), 1.83−1.34 (m, 1H), 1.31−1.02 (m, 7H).

1-(3-Acetyl-3-azabicyclo[3.1.1]-heptan-6-yl)-3-(2-(difluoromethoxy)-6-methoxypyridin-3--yl)-1-(2-isopropylphenyl)urea (32)

The title compound **32** was prepared in a manner analogous to that described for compound **39** but using *tert*-butyl 6-amino-3-azabicyclo[3.1.1]heptane-3-carboxylate (Pharmablock, Cat. No. PBZX1043) in place of *tert*-butyl (3*S*,4*R*)-4-amino-3-fluoropiperidine-1-carboxylate hydrochloride (**74**) in step (a). LCMS: m/z = 489.3 $[M + H]^+$. Purity (UV detection) = 95.1%. ^{1}H NMR (300 MHz, DMSO-d_6): δ = 8.07 (dd, J = 8.6, 3.0 Hz, 1H), 7.57 (t, J = 72.6 Hz, 1H), 7.55−7.46 (m, 3H), 7.37 (d, J = 7.8 Hz, 1H), 6.64−6.61 (m, 2H), 3.84−3.51 (m, 4H), 3.79 (s, 3H), 3.41−3.35 (m, 1H), 2.90 (sept, J = 6.5 Hz, 1H), 2.73−2.58 (m, 1H), 2.43−2.32 (m, 1H), 2.01 (s, 1.5H, rotamer A), 1.98 (s, 1.5H, rotamer B), 1.91−1.78 (m, 1H), 1.32−1.23 (m, 1H), 1.16 (t, J = 7.5 Hz, 6H).

1-((1*R*,5*S*,8*s*)-3-Acetyl-3-azabicyclo[3.2.1]-octan-8-yl)-3-(2-(difluoromethoxy)-6-methoxypyridin-3-yl)-1-(2-isopropylphenyl)urea (33)

The title compound **33** was prepared in a manner analogous to that described for compound **39** but using *tert*-butyl (1*R*,5*S*,8*s*)-8-amino-3-azabicyclo[3.2.1]octane-3-carboxylate (Pharmablock, Cat. No. PBU2596) in place of *tert*-butyl (3*S*,4*R*)-4-amino-3-fluoropiperidine-1-carboxylate hydrochloride (**74**) in step (a). LCMS: m/z = 503.3 $[M + H]^+$. Purity (UV detection) = 98.5%. ^{1}H NMR (300 MHz, DMSO-d_6): δ = 8.15 (dd, J = 8.6, 3.5 Hz, 1H), 7.54−7.45 (m, 2H), 7.51 (t, J = 72.5 Hz, 1H), 7.35−7.33 (m, 2H), 6.62 (d, J = 8.6 Hz, 1H), 6.34 (br s, 1H), 4.21−4.03 (m, 2H), 3.77 (s, 3H), 3.69−3.52 (m, 1H), 3.35−3.20 (m, 1H), 2.99−2.88 (m, 1H), 2.81−2.65 (m, 2H), 2.00 (s, 1.5H, rotamer A), 1.93 (s, 1.5H, rotamer B), 1.88−1.76 (m, 1H), 1.67 (br s, 1H), 1.52−1.19 (m, 3H), 1.26 (dd, J = 6.1, 1.1 Hz, 3H), 1.07 (d, J = 6.5 Hz, 3H).

1-((1*R*,5*S*,8*r*)-3-Acetyl-3-azabicyclo[3.2.1]-octan-8-yl)-3-(2-(difluoromethoxy)-6-methoxypyridin-3-yl)-1-(2-isopropylphenyl)urea (34)

The title compound **34** was prepared in a manner analogous to that described for compound **39** but using *tert*-butyl (1*R*,5*S*,8*r*)-8-amino-3-azabicyclo[3.2.1]octane-3-carboxylate (Pharmablock, Cat. No. PBU4146) in place of *tert*-butyl (3*S*,4*R*)-4-amino-3-fluoropiperidine-1-carboxylate hydrochloride (**74**) in step (a). LCMS: m/z = 503.3 $[M + H]^+$. Purity (UV detection) = 99.9%. ^{1}H NMR (300 MHz, DMSO-d_6): δ = 8.12 (d, J = 8.6 Hz, 1H), 7.55−7.44 (m, 3H), 7.53 (t, J = 72.5 Hz, 1H), 7.38−7.31 (m, 1H), 6.62 (d, J = 8.6 Hz, 1H), 6.52 (br d, J = 1.7 Hz, 1H), 3.96 (q, J = 3.8 Hz,1H), 3.77 (s, 3H), 3.75 (dd, J = 11.4, 3.5 Hz, 0.5H, rotamer A), 3.59 (dd, J = 13.3, 2.6 Hz, 0.5H, rotamer B), 3.24−3.03 (m, 2H), 2.80 (br s, 0.5H, rotamer A or B), 2.69 (br d, J = 12.1 Hz, 0.5H, rotamer A or B), 2.68 (br s, 0.5H, rotamer B or A), 2.60 (br d, J = 13.9 Hz, 0.5H, rotamer B or A), 2.25 (br s, 0.5H, rotamer A or B), 2.11 (br s, 0.5H, rotamer B or A), 1.94 (s, 1.5H, rotamer A or B), 1.89 (s, 1.5H, rotamer B or A), 1.81−1.68 (m, 2H), 1.55−1.25 (m, 3H), 1.21 (dd, J = 9.1, 6.9 Hz, 3H), 1.10 (dd, J = 6.7, 2.4 Hz, 3H).

1-((1*R*,3*r*,5*S*)-8-Acetyl-8-azabicyclo[3.2.1]-octan-3-yl)-3-(2-(difluoromethoxy)-6-methoxypyridin-3-yl)-1-(2-isopropylphenyl)urea (35)

The title compound **35** was prepared in a manner analogous to that described for compound **39** but using *tert*-butyl (1*R*,3*r*,5*S*)-3-amino-8-azabicyclo[3.2.1]octane-8-carboxylate (Pharmablock, Cat. No. PB00083) in place of *tert*-butyl (3*S*,4*R*)-4-amino-3-fluoropiperidine-1-carboxylate hydrochloride (**74**) in step (a). LCMS: m/z = 503.3 $[M + H]^+$. Purity (UV detection) = 99.7%. ^{1}H NMR (300 MHz, DMSO-d_6): δ = 8.09 (dd, J = 8.4, 6.6 Hz, 1H), 7.55−7.44 (m, 2H), 7.53 (t, J = 73.4 Hz, 1H), 7.33 (t, J = 7.3 Hz, 1H), 7.23 (d, J = 7.9 Hz, 1H), 6.60 (d, J = 8.5 Hz, 1H), 6.26 (br d, J = 9.0 Hz, 1H), 4.46 (q, J = 8.4 Hz,1H), 4.22 (q, J = 8.0 Hz,1H), 3.84−3.62 (m, 1H), 3.77 (s, 3H), 3.14−3.02 (m, 1H), 2.60−2.29 (m, 2H), 2.01−1.33 (m, 9H), 1.21−1.12 (m, 6H).

https://doi.org/10.1021/acs.jmedchem.6c01049
J. Med. Chem. 2026, 69, 15888−15927

1-((1*R*,3*s*,5*S*)-8-Acetyl-8-azabicyclo[3.2.1]-octan-3-yl)-3-(2-(difluoromethoxy)-6-methoxypyridin-3-yl)-1-(2-isopropylphenyl)urea (36)

The title compound **36** was prepared in a manner analogous to that described for compound **39** but using *tert*-butyl (1*R*,3*s*,5*S*)-3-amino-8-azabicyclo[3.2.1]octane-8-carboxylate (Pharmablock, Cat. No. PB00084) in place of *tert*-butyl (3*S*,4*R*)-4-amino-3-fluoropiperidine-1-carboxylate hydrochloride (**74**) in step (a). LCMS: m/z = 503.3 [M + H]$^+$. Purity (UV detection) = 98.4%. ^{1}H NMR (300 MHz, DMSO-d_6): δ = 8.15 (d, J = 8.6 Hz, 1H), 7.55 (dd, J = 7.9, 1.4 Hz, 1H), 7.52 (t, J = 72.5 Hz, 1H), 7.47 (t, J = 7.0 Hz, 1H), 7.32 (t, J = 7.5 Hz, 1H), 7.18 (t, J = 7.0 Hz, 1H), 6.61 (d, J = 8.6 Hz, 1H), 6.22 (br s, 1H), 4.74 (sept, J = 6.7 Hz,1H), 4.48−4.39 (m,1H), 4.22 (br s, 1H), 3.76 (s, 3H), 3.15−3.02 (m, 1H), 2.02−1.58 (m, 7H), 1.88 (s, 1.5H, rotamer A), 1.82 (s, 1.5H, rotamer B), 1.41−1.29 (m, 1H), 1.19 (dd, J = 6.7, 4.3 Hz, 3H), 1.11 (dd, J = 6.7, 2.1 Hz, 3H).

1-(2-Acetyl-2-azabicyclo[2.2.1]-heptan-5-yl)-3-(2-(difluoromethoxy)-6-methoxypyridin-3--yl)-1-(2-isopropylphenyl)urea (37)

The title compound **37** was prepared in a manner analogous to that described for compound **39** but using *tert*-butyl 5-amino-2-azabicyclo[2.2.1]heptane-2-carboxylate (Ambeed, Cat. No. A861765) in place of *tert*-butyl (3*S*,4*R*)-4-amino-3-fluoropiperidine-1-carboxylate hydrochloride (**74**) in step (a). LCMS: m/z = 489.3 [M + H]$^+$. Purity (UV detection): 2:1 mixture of diastereomers, combined purity = 99.0%. ^{1}H NMR (300 MHz, $CDCl_3$): δ = 8.37−8.27 (m, 1H), 7.50−6.92 (m, 5H), 6.50 (dd, J = 8.7, 2.3 Hz, 1H), 6.06−5.98 (m, 1H), 4.65−2.80 (m, 6H), 3.79 (s, 3H), 2.52−1.09 (m, 13H).

Racemic 1-((3*S*,4*S*)-1-acetyl-3-fluoropiperidin-4-yl)-3-(2-(difluoromethoxy)-6-methoxypyridin-3-yl)-1-(2-isopropylphenyl)-urea (38)

The title compound **38** was prepared in a manner analogous to that described for compound **39** but using *racemic tert*-butyl (3*S*,4*S*)-4-amino-3-fluoropiperidine-1-carboxylate (Pharmablock, Cat. No. PBZS1009) in place of *tert*-butyl (3*S*,4*R*)-4-amino-3-fluoropiperidine-1-carboxylate hydrochloride (**74**) in step (a). LCMS: m/z = 495.3 [M + H]$^+$. Purity (UV detection) = 95.1%. ^{1}H NMR (300 MHz, DMSO-d_6): δ = 8.07 (dd, J = 8.6, 5.9 Hz, 1H), 7.59−7.25 (m, 4H), 7.54 (t, J = 72.5 Hz, 1H), 6.62 (dd, J = 8.6, 2.0 Hz, 1H), 6.44 (br s, 1H), 4.82−4.51 (m, 2H), 4.36−3.74 (m, 2H), 3.77 (s, 3H), 3.26−3.07 (m, 2H), 2.76−2.53 (m, 1H), 2.07−1.90 (m, 4H), 1.49−1.10 (m, 7H).

1-((3*R*,4*S*)-1-Acetyl-3-fluoropiperidin-4-yl)-3-(2-(difluoromethoxy)-6-methoxypyridin-3-yl)-1-(2-isopropylphenyl)-urea (40)

The title compound **40** was prepared in a manner analogous to that described for compound **39** but using *tert*-butyl (3*R*,4*S*)-4-amino-3-fluoropiperidine-1-carboxylate hydrochloride (Pharmablock, Cat. No. PB07759) in place of *tert*-butyl (3*S*,4*R*)-4-amino-3-fluoropiperidine-1-carboxylate hydrochloride (**74**) in step (a). LCMS: m/z = 495.3 [M + H]$^+$. Purity (UV detection) = 99.2%. ^{1}H NMR (300 MHz, DMSO-d_6): δ = 8.17 (dd, J = 8.6, 5.8 Hz, 0.26H, rotamer A), 8.17 (dd, J = 8.6, 4.9 Hz, 0.74H, rotamer B), 7.55 (t, J = 72.5 Hz, 0.74H, rotamer B), 7.54 (t, J = 72.5 Hz, 0.26H, rotamer A), 7.53−7.43 (m, 2H), 7.37−7.19 (m, 2H), 6.64 (d, J = 8.6 Hz, 0.26H, rotamer A), 6.63 (d, J = 8.6 Hz, 0.74H, rotamer B), 6.47 (d, J = 7.9 Hz, 0.74H, rotamer B), 6.32 (d, J = 7.0 Hz, 0.26H, rotamer A), 5.34−5.04 (m, 1H), 4.85−4.33 (m, 2H), 4.16−3.79 (m, 1H), 3.79 (s, 2.2H, rotamer B), 3.78 (s, 0.8H, rotamer A), 3.53−3.16 (m, 1H), 3.07−2.57 (m, 2H), 1.97−1.90 (m, 3H), 1.83−1.34 (m, 1H), 1.31−1.02 (m, 7H).

(1*r*,4*r*)-4-(3-(2-(Difluoromethoxy)-6-methoxypyridin-3-yl)-1-(2-isopropylphenyl)ureido)cyclohexane-1-carboxylic acid (PIPE-791, 47)

(a) In a thick-walled glass reaction vessel equipped with a magnetic stirrer and a Teflon screwcap was combined *trans*-ethyl 4-aminocyclohexanecarboxylate hydrochloride (**77**, 3.12 g, 15.0 mmol, 1 equiv, ChemScene, Cat. No. CS-0043141), 1-iodo-2-isopropylbenzene (3.4 mL, 21 mmol, 1.4 equiv, Combi-Blocks, Cat. No. OR-2271), tris(dibenzylidineacetone)dipalladium(0) (1.38 g, 1.51 mmol, 0.1 equiv), CPhos (1.31 g, 3.00 mmol, 0.2 equiv), and Cs_2CO_3 (19.5 g, 60.0 mmol, 4 equiv) in 1,4-dioxane (100 mL). The resulting purple suspension was then deoxygenated via subsurface purging with nitrogen for 10 min before the reaction vessel was tightly sealed and heated at 90 °C for 48 h. The resulting orange, brown suspension was cooled to rt, diluted with MTBE (400 mL), and washed sequentially with water (250 mL) and brine (250 mL). The organic extract thus obtained was then dried over $MgSO_4$, treated with activated charcoal (50 g), filtered through a bed of Celite, and the filtrate concentrated in vacuo. Purification of the crude product thus obtained by way of column chromatography (SiO_2, gradient elution: Hex → 4:1 (v/v) Hex: EtOAc) afforded ethyl (1*r*,4*r*)-4-((2-isopropylphenyl)amino)cyclohexane-1-carboxylate (**78**) as a golden yellow oil (2.91 g, 67% yield). LCMS: m/z = 289.8 [M + H]$^+$. ^{1}H NMR (300 MHz, $CDCl_3$): δ = 7.15 (dd, J = 7.6, 1.5 Hz, 1H), 7.10 (td, J = 7.5, 1.6 Hz, 1H), 6.72 (td, J = 7.5, 1.1 Hz, 1H), 6.67 (d, J = 8.1 Hz, 1H), 4.15 (q, J = 7.1 Hz, 2H), 3.51 (br s, 1H), 3.32 (tt, J = 11.0, 3.7 Hz, 1H), 2.84 (sept, J = 6.8 Hz, 1H), 2.32 (tt, J = 12.1, 3.7 Hz, 1H), 2.28−2.21 (m, 2H), 2.15−2.04 (m, 2H), 1.62 (qd, J = 13.2, 3.3 Hz, 2H), 1.28 (t, J = 7.1 Hz, 3H), 1.26 (d, J = 6.8 Hz, 6H), 1.20 (qd, J = 13.2, 3.3 Hz, 2H).

(b) In a dried, round-bottom flask equipped with a magnetic stirrer and a reflux condenser was dissolved 2-(difluoromethoxy)-6-methoxypyridin-3-amine (**61**, 15.2 g, 80.0 mmol, 1.2 equiv) and ethyl (1*r*,4*r*)-4-((2-isopropylphenyl)amino)cyclohexane-1-carboxylate (**78**, 19.3 g, 66.7 mmol, 1 equiv) from the previous step in anhydrous MeCN (450 mL). The resulting solution was subsurface purged with nitrogen for 15 min before CDI (21.6 g, 133 mmol, 2 equiv) was added portionwise over 5 min. Following the completion of addition, the resulting reaction mixture was heated at 60 °C for 48 h. Upon cooling to rt, the volatiles were removed in vacuo. The residual viscous oil was then partitioned between MTBE (1.8 L) and 1 M aqueous HCl (1.2 L). The aqueous layer was separated and back extracted with MTBE (2 × 1.2 L). The combined organic extracts were washed sequentially with saturated aqueous $NaHCO_3$ (1.2 L), water (1.2 L) and brine (1.2 L), treated with activated charcoal (100 g), dried over $MgSO_4$, filtered through a bed of Celite, and the filtrate concentrated in vacuo. Purification of the crude product thus obtained by way of column chromatography (SiO_2, gradient elution: Hex → 1:1 (v/v) Hex: EtOAc) afforded ethyl (1*r*,4*r*)-4-(3-(2-(difluoromethoxy)-6-methoxypyridin-3-yl)-1-(2-isopropylphenyl)ureido)cyclohexane-1-carboxylate (**85**) as an off-white solid (31.6 g, 94% yield). LCMS: m/z = 505.8 [M + H]$^+$. ^{1}H NMR (300 MHz, $CDCl_3$): δ = 8.42 (d, J = 8.7 Hz, 1H), 7.51−7.43 (m, 2H), 7.30 (ddd, J = 7.9, 6.3, 2.6 Hz, 1H), 7.17 (t, J = 73.0 Hz, 1H), 7.15 (dd, J = 6.3, 1.0 Hz, 1H), 6.49 (d, J = 8.7 Hz, 1H), 5.93 (br s, 1H), 4.32 (tt, J = 11.6, 3.5 Hz, 1H), 4.15 (q, J = 7.1 Hz, 2H), 3.78 (s, 3H), 3.22 (sept, J = 6.8 Hz, 1H), 2.21−1.92 (m, 5H), 1.68−1.45 (m, 3H), 1.24 (d, J = 6.8 Hz, 3H), 1.28 (t, J = 7.1 Hz, 3H), 1.27−1.17 (m, 1H), 1.15 (d, J = 6.8 Hz, 3H).

(c) In a round-bottom flask equipped with a magnetic stirrer was dissolved ethyl (1*r*,4*r*)-4-(3-(2-(difluoromethoxy)-6-methoxypyridin-3-yl)-1-(2-isopropylphenyl)ureido)cyclohexane-1-carboxylate (**85**, 31.6 g, 62.5 mmol, 1 equiv) from the previous step in a 1:1 (v/v) solution of THF and MeOH (750 mL). To this colorless solution was added LiOH (1 M solution in water, 250 mL, 250 mmol, 4 equiv) and the resulting mixture was stirred at rt for 18 h. The reaction mixture was then carefully quenched with HCl (1 M solution in water, 250 mL, 250 mmol, 4 equiv) at 0 °C and the volatiles were removed in vacuo. The resulting suspension was back extracted with EtOAc (3 × 800 mL). The combined organic extracts were washed sequentially with water (1 L) and brine (1 L), dried over $MgSO_4$, treated with activated charcoal (50 g), and filtered through a bed of Celite. Concentration of the filtrate thus obtained in vacuo afforded a

https://doi.org/10.1021/acs.jmedchem.6c01049
J. Med. Chem. 2026, 69, 15888−15927

yellow solid that was then taken up in isopropanol (800 mL). After heating to 60 °C, heptane (800 mL) was added dropwise over 30 min under vigorous stirring. The resulting suspension was then slowly cooled to rt over 6 h and stirred at rt for an additional 16 h. The solid thus obtained was filtered, washed further with ice cold 1:1 (v/v) solution of isopropanol and heptane (3 × 200 mL), and dried in a vacuum oven at 35 °C until constant weight. **PIPE-791** was isolated as a white crystalline solid (23.9 g, 80% yield). LCMS: m/z = 477.8 [M + H]$^+$. Purity (UV detection) = 100.0%. ^{1}H NMR (300 MHz, DMSO-d_6): δ = 12.04 (s, 1H), 8.17 (d, J = 8.6 Hz, 1H), 7.54 (dd, J = 7.3, 1.6 Hz, 1H), 7.52 (t, J = 72.6 Hz, 1H), 7.46 (td, J = 7.3, 1.2 Hz, 1H), 7.32 (td, J = 7.8, 1.7 Hz, 1H), 7.22 (dd, J = 7.8, 1.7 Hz, 1H), 6.61 (d, J = 8.6 Hz, 1H), 6.24 (br s, 1H), 4.21−4.11 (m, 1H), 3.76 (s, 3H), 3.12 (sept, J = 6.8 Hz, 1H), 2.05−1.78 (m, 5H), 1.47−1.33 (m, 3H), 1.21 (d, J = 6.8 Hz, 3H), 1.11 (d, J = 6.8 Hz, 3H), 1.03 (qd, J = 12.5, 3.1 Hz, 1H). ^{13}C NMR (75 MHz, DMSO-d_6): δ = 176.74, 157.42, 154.01, 148.78, 146.87, 135.12 (2C), 131.03, 129.83, 128.08, 127.49, 116.60, 115.15 (t, J_{C-F} = 254.3 Hz), 105.40, 55.65, 54.15, 41.94, 31.19, 29.82, 28.62. 28.56, 27.68, 24.61, 24.61, 24.03. ^{19}F NMR (100 MHz, DMSO-d_6): δ = −86.96 (dd, J = 72.6, 13.5 Hz). HRMS (ESI+): m/z for $C_{24}H_{30}F_2N_3O_5$, 478.2154 [M + H]$^+$; observed 478.2154: mass error 0.0 (ppm).

2-((1*r*,4*r*)-4-(3-(2-(Difluoromethoxy)-6-methoxypyridin-3-yl)-1-(2-isopropylphenyl)ureido)cyclohexyl)acetic acid (48) and 2-((1*s*,4*s*)-4-(3-(2-(difluoromethoxy)-6-methoxypyridin-3-yl)-1-(2-isopropylphenyl)ureido)cyclohexyl)acetic acid (49)

(a) In a dried, round-bottom flask equipped with a magnetic stirrer was combined 2-isopropylaniline (625 mg, 4.62 mmol, 1 equiv, Combi-Blocks, Cat. No. QW-3911) and ethyl 2-(4-oxocyclohexyl)acetate (**79**, 852 mg, 4.62 mmol, 1 equiv, Combi-Blocks, Cat. No. QC-2675) in DCM (3 mL). To this mixture was added sodium triacetoxyborohydride (1.16 g, 5.55 mmol, 1.2 equiv) in one rapid portion, and the resulting suspension was allowed to stir at rt for 10 min. The volatiles were then removed in vacuo and the crude product thus obtained was purified further by way of column chromatography (SiO_2, gradient elution: Hex → 10:1 (v/v) Hex: EtOAc) to afford ethyl 2-((1*s*,4*s*)-4-((2-isopropylphenyl)amino)cyclohexyl)acetate (**80**, faster eluting peak, 0.68 g, 48% yield) and ethyl 2-((1*r*,4*r*)-4-((2-isopropylphenyl)amino)cyclohexyl)acetate (**81**, slower eluting peak, 0.31 g, 22% yield). Compound **80**: LCMS: m/z = 304.2 [M + H]$^+$. ^{1}H NMR (300 MHz, DMSO-d_6): δ = 7.04 (dd, J = 7.9, 1.6 Hz, 1H), 6.97 (td, J = 7.7, 1.6 Hz, 1H), 6.58−6.54 (m, 2H), 4.27 (br s, 1H), 4.06 (q, J = 7.1 Hz, 2H), 3.47 (br s, 1H), 3.04 (sept, J = 6.8 Hz, 1H), 2.31 (d, J = 7.3 Hz, 2H), 1.74−1.49 (m, 7H), 1.44−1.33 (m, 2H), 1.18 (t, J = 7.1 Hz, 3H), 1.17 (d, J = 6.8 Hz, 6H). Compound **81**: LCMS: m/z = 304.1 [M + H]$^+$. ^{1}H NMR (300 MHz, DMSO-d_6): δ = 7.02 (dd, J = 7.5, 1.5 Hz, 1H), 6.96 (td, J = 7.7, 1.6 Hz, 1H), 6.58−6.52 (m, 2H), 4.31 (d, J = 8.2 Hz, 1H), 4.06 (q, J = 7.1 Hz, 2H), 3.26−3.13 (m, 1H), 3.00 (sept, J = 6.8 Hz, 1H), 2.21 (d, J = 6.6 Hz, 2H), 1.98 (br d, J = 12.6 Hz, 2H), 1.78−1.62 (m, 3H), 1.31−1.05 (m, 4H), 1.19 (t, J = 7.1 Hz, 3H), 1.13 (d, J = 6.8 Hz, 6H).

(b) In a dried, round-bottom flask equipped with a magnetic stirrer was combined 2-(difluoromethoxy)-6-methoxypyridin-3-amine (**61**, 44 mg, 0.23 mmol, 1 equiv) and pyridine (56 μL, 0.69 mmol, 3 equiv) in anhydrous DCM (3 mL). To this was then added phosgene (15% w/w solution in toluene, 0.250 mL, 0.35 mmol, 1.5 equiv) dropwise at rt and the resulting solution was stirred at rt for 30 min. The volatiles were then removed in vacuo and the crude (2-(difluoromethoxy)-6-methoxypyridin-3-yl)-carbamic chloride thus obtained was retaken up in anhydrous DCM (4 mL). This solution was then added dropwise at rt to another DCM (3 mL) suspension of ethyl 2-((1*r*,4*r*)-4-((2-isopropylphenyl)amino)cyclohexyl)acetate (**81**, 70 mg, 0.23 mmol, 1 equiv) from the previous step (slower eluting peak), pyridine (56 μL, 0.69 mmol, 3 equiv), and freshly activated 4 Å molecular sieves (10 beads). The resulting mixture was stirred at rt for 16 h before the reaction was quenched with water (10 mL). The aqueous layer was separated and back extracted with DCM (2 × 10 mL). The combined organic extracts were dried over $MgSO_4$, filtered, and the filtrate concentrated in vacuo. Purification of the crude product thus obtained by way of column chromatography (SiO_2, gradient elution: Hex → 5:1 (v/v) Hex: EtOAc) afforded ethyl 2-((1*r*,4*r*)-4-(3-(2-(difluoromethoxy)-6-methoxypyridin-3-yl)-1-(2-isopropylphenyl)ureido)-cyclohexyl)acetate as a white solid (80 mg, 67% yield). LCMS: m/z = 520.1 [M + H]. Similarly, ethyl 2-((1*s*,4*s*)-4-((2-isopropylphenyl)amino)cyclohexyl)acetate (**80**, 81 mg, 0.27 mmol, 1 equiv) from the previous step (faster eluting peak) was converted to ethyl 2-((1*s*,4*s*)-4-(3-(2-(difluoromethoxy)-6-methoxypyridin-3-yl)-1-(2-isopropylphenyl)ureido)-cyclohexyl)acetate (90 mg, 65% yield). LCMS: m/z = 520.1 [M + H].

(c) In a round-bottom flask equipped with a magnetic stirrer was dissolved ethyl 2-((1*r*,4*r*)-4-(3-(2-(difluoromethoxy)-6-methoxypyridin-3-yl)-1-(2-isopropylphenyl)ureido)cyclohexyl)-acetate (75 mg, 0.14 mmol, 1 equiv) from the previous step in MeOH (3 mL). To this colorless solution was added LiOH (1 M solution in water, 0.72 mL, 0.72 mmol, 5 equiv) and the resulting mixture was heated at 60 °C for 1 h. The reaction mixture was then cooled to rt and carefully quenched with HCl (1 M solution in water, 0.72 mL, 0.72 mmol, 5 equiv) at 0 °C. The volatiles were removed in vacuo and the resulting suspension was back extracted with EtOAc (2 × 15 mL). The combined organic extracts were washed sequentially with water (10 mL) and brine (10 mL), dried over Na_2SO_4, and filtered. Concentration of the filtrate thus obtained in vacuo afforded the title compound **48** as a white crystalline solid (37 mg, 52% yield). LCMS: m/z = 492.0 [M + H]$^+$. Purity (UV detection) = 100.0%. ^{1}H NMR (300 MHz, DMSO-d_6): δ = 11.99 (s, 1H), 8.19 (d, J = 8.6 Hz, 1H), 7.55 (dd, J = 8.0, 1.7 Hz, 1H), 7.53 (t, J = 72.5 Hz, 1H), 7.48 (td, J = 7.4, 1.4 Hz, 1H), 7.33 (td, J = 7.9, 1.7 Hz, 1H), 7.23 (dd, J = 7.9, 1.1 Hz, 1H), 6.62 (d, J = 8.6 Hz, 1H), 6.22 (br s, 1H), 4.22−4.12 (m, 1H), 3.77 (s, 3H), 3.13 (sept, J = 6.8 Hz, 1H), 2.10−1.97 (m, 3H), 1.78−1.69 (m, 3H), 1.50−1.31 (m, 2H), 1.26−0.97 (m, 3H), 1.21 (d, J = 6.8 Hz, 3H), 1.12 (d, J = 6.8 Hz, 3H). HRMS (ESI+): m/z for $C_{25}H_{32}F_2N_3O_5$, 492.2310 [M + H]$^+$; observed 492.2310: mass error 0.0 (ppm). Similarly, ethyl 2-((1*s*,4*s*)-4-(3-(2-(difluoromethoxy)-6-methoxypyridin-3-yl)-1-(2-isopropylphenyl)ureido)cyclohexyl)acetate (80 mg, 0.15 mmol, 1 equiv) from the previous step was saponified into title compound **49** (40 mg, 53% yield). LCMS: m/z = 492.0 [M + H]$^+$. Purity (UV detection) = 100.0%. ^{1}H NMR (300 MHz, DMSO-d_6): δ = 11.99 (s, 1H), 8.18 (d, J = 8.6 Hz, 1H), 7.55 (dd, J = 8.0, 1.7 Hz, 1H), 7.53 (t, J = 72.5 Hz, 1H), 7.48 (td, J = 7.5, 1.3 Hz, 1H), 7.37 (td, J = 7.8, 1.7 Hz, 1H), 7.26 (dd, J = 7.8, 1.3 Hz, 1H), 6.62 (d, J = 8.6 Hz, 1H), 6.22 (br s, 1H), 4.12−4.02 (m, 1H), 3.77 (s, 3H), 3.14 (sept, J = 6.8 Hz, 1H), 2.15−2.04 (m, 2H), 1.83−1.76 (m, 1H), 1.63−1.52 (m, 6H), 1.26−1.18 (m, 2H), 1.21 (d, J = 6.8 Hz, 3H), 1.13 (d, J = 6.8 Hz, 3H). HRMS (ESI+): m/z for $C_{25}H_{32}F_2N_3O_5$, 492.2310 [M + H]$^+$; observed 492.2304: mass error −1.2 (ppm).

Racemic 3-(2-(difluoromethoxy)-6-methoxypyridin-3-yl)-1-(2-isopropylphenyl)-1-((7*S*,8a*S*)-3-oxooctahydroindolizin-7-yl)urea (41) and *Racemic* 3-(2-(difluoromethoxy)-6-methoxypyridin-3-yl)-1-(2-isopropylphenyl)-1-((7*S*,8a*R*)-3-oxooctahydroindolizin-7-yl)-urea (42)

The title compounds **41** and **42** were prepared in a manner analogous to that described for compounds **48** and **49** but using hexahydroindolizine-3,7-dione (J&W PharmLab, Cat. No. 10R0473) in place of ethyl

https://doi.org/10.1021/acs.jmedchem.6c01049
J. Med. Chem. 2026, 69, 15888−15927

2-(4-oxocyclohexyl)acetate (**79**) in step (a) and omitting step (c). Compound **41**: LCMS: m/z = 489.0 $[M + H]^+$. Purity (UV detection) = 98.1%. ^{1}H NMR (300 MHz, $CDCl_3$): δ = 8.36 (d, J = 8.7 Hz, 0.4H, rotamer A), 8.31 (d, J = 8.7 Hz, 0.6H, rotamer B), 7.52−7.48 (m, 2H), 7.37−7.28 (m, 2H), 7.18 (t, J = 73.0 Hz, 0.6H, rotamer B), 7.17 (t, J = 73.0 Hz, 0.4H, rotamer A), 6.50 (d, J = 8.7 Hz, 1H), 6.01 (br s, 1H), 4.53−4.45 (m, 0.4H, rotamer A), 4.36−4.30 (m, 0.6H, rotamer B), 4.12−4.00 (m, 1H), 3.88−3.72 (m, 1H), 3.79 (s, 3H), 3.55−3.42 (m, 0.6H, rotamer B), 3.41−3.31 (m, 0.4H, rotamer A), 3.24−2.48 (m, 3H), 2.41−2.21 (m, 3H), 2.10−1.56 (m, 2H), 1.47−1.23 (m, 4H), 1.14 (d, J = 6.8 Hz, 3H). Compound **42**: LCMS: m/z = 489.1 $[M + H]^+$. Purity (UV detection) = 95.1%. ^{1}H NMR (300 MHz, $CDCl_3$): δ = 8.38 (dd, J = 8.6, 2.2 Hz, 1H), 7.50−7.44 (m, 2H), 7.35−7.26 (m, 1H), 7.16 (t, J = 73.0 Hz, 1H), 7.13−7.09 (m, 1H), 6.50 (d, J = 8.6 Hz, 1H), 5.95 (br s, 1H), 4.65−4.53 (m, 1H), 4.21−4.11 (m, 2H), 3.78 (s, 3H), 3.68−3.56 (m, 1H), 3.24−3.14 (m, 1H), 2.85−2.72 (m, 2H), 2.40−2.72 (m, 3H), 1.99−1.51 (m, 2H), 1.29−1.12 (m, 7H).

3-(2-(Difluoromethoxy)-6-methoxypyridin-3-yl)-1-(2-isopropylphenyl)-1-((1*s*,4*s*)-4-(methylsulfonyl)cyclohexyl)urea (46)

The title compound **46** was prepared in a manner analogous to that described for compounds **48** and **49** but using 4-(methylsulfonyl)-cyclohexan-1-one (Combi-Blocks, Cat. No. QW-3911) in place of ethyl 2-(4-oxocyclohexyl)acetate (**79**) in step (a) and omitting step (c). The title compound was the first eluting peak obtained following normal-phase column chromatography (SiO_2, gradient elution: 1:1 (v/v) Hex: EtOAc → EtOAc). LCMS: m/z = 512.1 $[M + H]^+$. Purity (UV detection) = 100.0%. ^{1}H NMR (300 MHz, DMSO-d_6): δ = 8.15 (d, J = 8.6 Hz, 1H), 7.56 (dd, J = 8.6, 1.6 Hz, 1H), 7.54 (t, J = 72.5 Hz, 1H), 7.48 (td, J = 7.1, 1.3 Hz, 1H), 7.34 (td, J = 7.8, 1.7 Hz, 1H), 7.24 (dd, J = 7.8, 1.3 Hz, 1H), 6.63 (d, J = 8.6 Hz, 1H), 6.32 (br s, 1H), 4.27−4.17 (m, 1H), 3.78 (s, 3H), 3.13 (sept, J = 6.8 Hz, 1H), 2.99−2.90 (m, 1H), 2.88 (s, 3H), 2.59−2.50 (m, 1H), 2.19−2.05 (m, 3H), 1.96−1.88 (m, 1H), 1.62−1.43 (m, 3H), 1.23 (d, J = 6.8 Hz, 3H), 1.13 (d, J = 6.8 Hz, 3H). HRMS (ESI+): m/z for $C_{24}H_{32}F_2N_3O_5S$, 512.2031 $[M + H]^+$; observed 512.2029: mass error −0.4 (ppm).

(1*r*,4*r*)-4-(3-(2-(Difluoromethoxy)-6-methoxypyridin-3-yl)-1-(2-isopropylphenyl)-ureido)-1-methylcyclohexane-1-carboxylic acid (50)

(a) In a thick-walled glass reaction vessel equipped with a magnetic stirrer and a Teflon screwcap was combined ethyl (1*r*,4*r*)-4-amino-1-methylcyclohexane-1-carboxylate hydrochloride (0.26 g, 1.4 mmol, 1 equiv, Combi-Blocks, Cat. No. JZ-3081), 1-iodo-2-isopropylbenzene (0.67 mL, 4.2 mmol, 3 equiv, Combi-Blocks, Cat. No. OR-2271), tris(dibenzylidineacetone)-dipalladium(0) (0.15 g, 0.14 mmol, 0.1 equiv), CPhos (0.12 g, 0.28 mmol, 0.2 equiv), and Cs_2CO_3 (1.83 g, 5.61 mmol, 4 equiv) in 1,4-dioxane (12 mL). The resulting purple suspension was then deoxygenated via subsurface purging with nitrogen for 10 min before the reaction vessel was tightly sealed and heated at 90 °C for 72 h. The resulting orange, brown suspension was cooled to rt, diluted with EtOAc (50 mL), and washed sequentially with water (50 mL) and brine (50 mL). The organic extract thus obtained was then dried over Na_2SO_4, filtered, and the filtrate concentrated in vacuo. Purification of the crude product thus obtained by way of column chromatography (SiO_2, gradient elution: Hex → 9:1 (v/v) Hex: EtOAc) afforded ethyl (1*r*,4*r*)-4-((2-isopropylphenyl)amino)-1-methylcyclohexane-1-carboxylate as a yellow oil (0.25 g, 59% yield). LCMS: m/z = 304.2 $[M + H]^+$.

(b) In a dried, round-bottom flask equipped with a magnetic stirrer was combined 2-(difluoromethoxy)-6-methoxypyridin-3-amine (**61**, 145 mg, 0.760 mmol, 1 equiv) and pyridine (184 μL, 2.27 mmol, 3 equiv) in anhydrous DCM (6 mL). To this was then added triphosgene (90 mg, 0.30 mmol, 0.4 equiv) in one rapid portion at rt and the resulting solution was stirred at rt for 1 h. Ethyl (1*r*,4*r*)-4-((2-isopropylphenyl)amino)-1-methylcyclohexane-1-carboxylate (0.23 g, 0.76 mmol, 1 equiv) from the previous step was then added in one rapid portion. The resulting mixture was stirred at rt for 48 h before the reaction was quenched with water (30 mL). The aqueous layer was separated and back extracted with DCM (3 × 30 mL). The combined organic extracts were dried over Na_2SO_4, filtered, and the filtrate concentrated in vacuo. Purification of the crude product thus obtained by way of column chromatography (SiO_2, gradient elution: Hex → 9:1 (v/v) Hex: EtOAc) afforded ethyl (1*r*,4*r*)-4-(3-(2-(difluoromethoxy)-6-methoxypyridin-3-yl)-1-(2-isopropylphenyl)ureido)-1-methylcyclohexane-1-carboxylate as a yellow oil (0.21 g, 52% yield). LCMS: m/z = 520.6 $[M + H]^+$.

(c) In a round-bottom flask equipped with a magnetic stirrer was dissolved ethyl (1*r*,4*r*)-4-(3-(2-(difluoromethoxy)-6-methoxypyridin-3-yl)-1-(2-isopropylphenyl)ureido)-1-methylcyclohexane-1-carboxylate (156 mg, 0.300 mmol, 1 equiv) from the previous step in a 1:1 (v/v) solution of THF and MeOH (9 mL). To this colorless solution was added LiOH (1 M solution in water, 0.90 mL, 0.90 mmol, 3 equiv) and the resulting mixture was heated at 50 °C for 5 days. The reaction mixture was then cooled to rt and carefully quenched with HCl (1 M solution in water, 0.90 mL, 0.90 mmol, 3 equiv) at 0 °C. The volatiles were removed in vacuo. Purification of the crude product thus obtained by way of reverse-phase column chromatography (C_{18}, gradient elution: 95:5 (v/v) H_2O: MeCN + 0.1% formic acid → 5:95 (v/v) H_2O: MeCN + 0.1% formic acid) afforded the title compound **50** as a white solid (70 mg, 47% yield). LCMS: m/z = 492.3 $[M + H]^+$. Purity (UV detection) = 99.7%. ^{1}H NMR (300 MHz, CD_3OD): δ = 8.11 (d, J = 8.7 Hz, 1H), 7.58 (dd, J = 7.8, 1.5 Hz, 1H), 7.52 (td, J = 7.5, 1.2 Hz, 1H), 7.40 (td, J = 7.5, 1.8 Hz, 1H), 7.38 (t, J = 72.9 Hz, 1H), 7.31 (dd, J = 7.8, 1.2 Hz, 1H), 6.56 (d, J = 8.7 Hz, 1H), 4.25−4.16 (m, 1H), 3.84 (s, 3H), 3.26 (sept, J = 6.8 Hz, 1H), 2.08−1.94 (m, 1H), 1.88−1.71 (m, 6H), 1.36 (qd, J = 12.6, 3.6 Hz, 1H), 1.31 (d, J = 6.8 Hz, 3H), 1.23 (d, J = 6.8 Hz, 3H), 1.11 (s, 3H). HRMS (ESI+): m/z for $C_{25}H_{32}F_2N_3O_5$, 492.2310 $[M + H]^+$; observed 492.2306: mass error −0.8 (ppm).

(1*S*,4*R*,6*R*)-4-(3-(2-(Difluoromethoxy)-6-methoxypyridin-3-yl)-1-(2-isopropylphenyl)ureido)bicyclo[4.1.0]-heptane-1-carboxylic acid (51)

The title compound **51** was prepared in a manner analogous to that described for compound **50** but using methyl (1*S*,4*R*,6*R*)-4-aminobicyclo[4.1.0]heptane-1-carboxylate (PharmaBlock, Cat. No. PCS3491) in place of ethyl (1*r*,4*r*)-4-amino-1-methylcyclohexane-1-carboxylate hydrochloride in step (a). LCMS: m/z = 490.3 $[M + H]^+$. Purity (UV detection) = 99.8%. ^{1}H NMR (300 MHz, DMSO-d_6): δ = 12.09 (br s, 1H), 8.14 (d, J = 8.6 Hz, 1H), 7.55−7.51 (m, 1H), 7.52 (t, J = 72.7 Hz, 1H), 7.45 (t, J = 7.3 Hz, 1H), 7.31 (t, J = 7.6 Hz, 1H), 7.19 (t, J = 6.7 Hz, 1H), 6.60 (d, J = 8.6 Hz, 1H), 6.25 (br s, 1H), 4.03−3.91 (m, 1H), 3.76 (s, 3H), 3.08 (sept, J = 6.8 Hz, 1H), 2.31−1.77 (m, 3H), 1.61−1.42 (m, 2H), 1.31−0.81 (m, 9H), 0.57−0.50 (m, 1H). HRMS (ESI+): m/z for $C_{25}H_{30}F_2N_3O_5$, 490.2154 $[M + H]^+$; observed 490.2157: mass error 0.6 (ppm).

(1*R*,4*S*,6*S*)-4-(3-(2-(Difluoromethoxy)-6-methoxypyridin-3-yl)-1-(2-isopropylphenyl)ureido)bicyclo[4.1.0]-heptane-1-carboxylic acid (52)

The title compound **52** was prepared in a manner analogous to that described for compound **50** but using methyl (1*R*,4*S*,6*S*)-4-aminobicyclo[4.1.0]heptane-1-carboxylate (*PharmaBlock*, Cat. No. PCS3479) in place of ethyl (1*r*,4*r*)-4-amino-1-methylcyclohexane-1-carboxylate hydrochloride in step (a). LCMS: m/z = 490.3 $[M + H]^+$. Purity (UV detection) = 99.9%. ^{1}H NMR (300 MHz, DMSO-d_6): δ = 12.07 (br s, 1H), 8.13 (d, J = 8.7 Hz, 1H), 7.55−7.53 (m, 1H), 7.53 (t, J = 72.6 Hz, 1H), 7.45 (t, J = 7.6 Hz, 1H), 7.31 (td, J = 7.8, 1.5 Hz, 1H), 7.19 (t, J = 6.8 Hz, 1H), 6.61 (d, J = 8.7 Hz, 1H), 6.26 (br s, 1H), 4.05−3.90 (m, 1H), 3.76 (s, 3H), 3.08 (sept, J = 6.5 Hz, 1H), 2.31−1.76 (m, 3H), 1.61−1.42 (m, 2H), 1.31−0.81 (m, 9H), 0.56−0.50 (m, 1H). HRMS (ESI+): m/z for $C_{25}H_{30}F_2N_3O_5$, 490.2154 $[M + H]^+$; observed 490.2157: mass error 0.6 (ppm).

https://doi.org/10.1021/acs.jmedchem.6c01049
J. Med. Chem. 2026, 69, 15888−15927

(1*r*,4*r*)-4-(3-(2-Hydroxy-6-methoxypyridin-3-yl)-1-(2-isopropylphenyl)ureido)cyclohexane-1-carboxylic acid (47-LM-M1)

(a) In a microwavable glass reaction vessel equipped with a magnetic stirrer was suspended 6-methoxy-3-nitropyridin-2-ol (**87**, 220 mg, 1.29 mmol, 1 equiv, Combi-Blocks, Cat. No. HA-9240), Ag_2CO_3 (264 mg, 1.55 mmol, 1.2 equiv), and benzyl bromide (184 μL, 1.55 mmol, 1.2 equiv) in toluene (13 mL). The vessel was then tightly sealed before it was heated at 130 °C in a microwave reactor for 1 h. After cooling to rt, the reaction suspension was filtered through a bed of Celite and the insolubles were washed further with EtOAc (2 × 15 mL). The filtrate thus obtained was washed sequentially with water (15 mL) and brine (15 mL), dried over $MgSO_4$, and filtered. Concentration of the filtrate in vacuo afforded crude 2-(benzyloxy)-6-methoxy-3-nitropyridine as a brown oil. LCMS: m/z = 260.9 $[M + H]^+$.

(b) In a dried, round-bottom flask equipped with a magnetic stirrer was combined 2-(benzyloxy)-6-methoxy-3-nitropyridine (300 mg, 1.15 mmol, 1 equiv) from the previous step and NH_4Cl (0.31 g, 5.8 mmol, 5 equiv) in a 2:1 (v/v) solution of EtOH and water (30 mL). To this solution was added iron powder (0.32 g, 5.8 mmol, 5 equiv) in one rapid portion and the resulting gray suspension was heated at 80 °C under a nitrogen atmosphere for 12 h. The reaction suspension was then cooled to rt, filtered through a bed of Celite, and the insolubles washed with DCM (2 × 30 mL). The filtrate thus obtained was then diluted with water (50 mL) and extracted with DCM (2 × 50 mL). The combined organic extracts were washed further with water (50 mL) and brine (50 mL), dried over Na_2SO_4, filtered, and the filtrate concentrated in vacuo. Purification of the crude product thus obtained by way of column chromatography (SiO_2, gradient elution: Hex → EtOAc) afforded 2-(benzyloxy)-6-methoxypyridin-3-amine (**88**) as a thick, brown oil (115 mg, 43% yield over two steps). LCMS: m/z = 231.0 $[M + H]^+$. ^1H NMR (300 MHz, $CDCl_3$): δ = 7.45−7.42 (m, 2H), 7.36−7.25 (m, 3H), 6.93 (d, J = 8.1 Hz, 1H), 6.15 (d, J = 8.1 Hz, 1H), 5.39 (s, 2H), 3.80 (s, 3H), 3.30 (br s, 2H).

(c) In a dried, round-bottom flask equipped with a magnetic stirrer was combined 2-(benzyloxy)-6-methoxypyridin-3-amine (**88**, 115 mg, 0.499 mmol, 1 equiv) from the previous step and pyridine (0.12 mL, 1.5 mmol, 3 equiv) in anhydrous DCM (3 mL). To this was then added phosgene (15% w/w solution in toluene, 0.53 mL, 0.75 mmol, 1.5 equiv) dropwise at rt and the resulting solution was stirred at rt for 30 min. The volatiles were then removed in vacuo and the crude (2-(benzyloxy)-6-methoxypyridin-3-yl)carbamic chloride thus obtained was retaken up in anhydrous DCM (4 mL). This solution was then added dropwise at rt to another DCM (3 mL) suspension of ethyl (1*r*,4*r*)-4-((2-isopropylphenyl)amino)cyclohexane-1-carboxylate (**78**, 145 mg, 0.499 mmol, 1 equiv), pyridine (0.121 mL, 1.5 mmol, 3 equiv), and freshly activated 4 Å molecular sieves (15 beads). The resulting mixture was stirred at rt for 16 h before the reaction was quenched with water (10 mL). The aqueous layer was separated and back extracted with DCM (2 × 10 mL). The combined organic extracts were dried over $MgSO_4$, filtered, and the filtrate concentrated in vacuo. Purification of the crude product thus obtained by way of column chromatography (SiO_2, gradient elution: Hex → 5:1 (v/v) Hex: EtOAc) afforded ethyl (1*r*,4*r*)-4-(3-(2-(benzyloxy)-6-methoxypyridin-3-yl)-1-(2-isopropylphenyl)ureido)cyclohexane-1-carboxylate (**89**) as a white solid (120 mg, 44% yield). LCMS: m/z = 545.8 $[M + H]^+$.

(d) In a round-bottom flask equipped with a magnetic stirrer was dissolved ethyl (1*r*,4*r*)-4-(3-(2-(benzyloxy)-6-methoxypyridin-3-yl)-1-(2-isopropylphenyl)ureido)cyclohexane-1-carboxylate (**89**, 110 mg, 0.202 mmol, 1 equiv) from the previous step in a 1:1 (v/v) solution of THF and MeOH (2 mL). To this colorless solution was added LiOH (1 M solution in water, 1.0 mL, 1.0 mmol, 5 equiv) and the resulting mixture was heated at 60 °C for 1 h. The reaction mixture was then cooled to rt and carefully quenched with HCl (1 M solution in water, 1.0 mL, 1.0 mmol, 5 equiv) at 0 °C. The volatiles were removed in vacuo and the resulting suspension was back extracted with EtOAc (2 × 15 mL). The combined organic extracts were washed sequentially with water (10 mL) and brine (10 mL), dried over Na_2SO_4, and filtered. Concentration of the filtrate thus obtained in vacuo afforded (1*r*,4*r*)-4-(3-(2-(benzyloxy)-6-methoxypyridin-3-yl)-1-(2-isopropylphenyl)ureido)cyclohexane-1-carboxylic acid (**90**) as a white solid (70 mg, 67% yield). LCMS: m/z = 517.9 $[M + H]^+$.

(e) In a dried, round-bottom flask equipped with a magnetic stirrer was dissolved (1*r*,4*r*)-4-(3-(2-(benzyloxy)-6-methoxypyridin-3-yl)-1-(2-isopropylphenyl)ureido)cyclohexane-1-carboxylic acid (**90**, 70 mg, 0.14 mmol, 1 equiv) from the previous step in MeOH (2 mL). The resulting yellow solution was then deoxygenated via subsurface purging with nitrogen for 10 min before palladium (10% w/w over activated carbon, dry, 5.6 mg, 0.0053 mmol, 0.04 equiv) was added in one rapid portion. The resulting black suspension was then subsurface purged with hydrogen for 10 min before it was stirred under a static hydrogen atmosphere (maintained with a balloon) at rt for 18 h. The reaction was subsequently diluted with EtOAc (10 mL) and filtered through a bed of DCM-wetted Celite. The insolubles were washed further with EtOAc (3 × 10 mL) and the filtrate was concentrated in vacuo. Purification of the crude product thus obtained by way of column chromatography (SiO_2, gradient elution: 5:1 (v/v) Hex: EtOAc → EtOAc) afforded the title compound **47-LM-M1** as an off-white solid (8.0 mg,14% yield). LCMS: m/z = 428.7 $[M + H]^+$. Purity (UV detection) = 98.7%. ^1H NMR (300 MHz, DMSO-d_6): δ = 12.01 (br s, 2H), 8.07 (d, J = 8.2 Hz, 1H), 7.54 (dd, J = 7.9, 1.7 Hz, 1H), 7.47 (td, J = 7.5, 1.2 Hz, 1H), 7.33 (td, J = 7.8, 1.7 Hz, 1H), 7.21 (dd, J = 7.8, 1.2 Hz, 1H), 6.54 (br s, 1H), 5.69 (br s, 1H), 4.25−4.15 (m, 1H), 3.71 (s, 3H), 3.04 (sept, J = 6.8 Hz, 1H), 2.07−1.87 (m, 4H), 1.81−1.73 (m, 1H), 1.48−1.34 (m, 3H), 1.20 (d, J = 6.8 Hz, 3H), 1.06 (d, J = 6.8 Hz, 3H), 1.04−0.92 (m, 1H).

(1r,4r)-4-(3-(2-(Difluoromethoxy)-6-hydroxypyridin-3-yl)-1-(2-isopropylphenyl)ureido)cyclohexane-1-carboxylic acid (47-LM-M3/47-Hep-M6)

(a) In a dried, round-bottom flask equipped with a magnetic stirrer was combined 6-chloro-3-nitropyridin-2-ol (**91**, 500 mg, 2.87 mmol, 1 equiv, Combi-Blocks, Cat. No. PY-1594), benzyl alcohol (328 μL, 3.15 mmol, 1.1 equiv), freshly powdered KOH (480 mg, 8.60 mmol, 3 equiv), and 18-crown-6 (20 mg, 0.076 mmol, 0.03 equiv) in toluene (15 mL). The resulting suspension was heated at 80 °C for 2 h. The reaction was then quenched with the addition of 1 M aq. HCl until a pH of ∼ 4 and extracted with EtOAc (3 × 30 mL). The combined organic extracts were washed further with water (50 mL) and brine (50 mL), dried over Na_2SO_4, filtered, and the filtrate concentrated in vacuo. Purification of the crude product thus obtained by way of column chromatography (SiO_2, 2:1 (v/v) Hex: EtOAc) afforded 6-(benzyloxy)-3-nitropyridin-2-ol as a yellow oil (450 mg, 64% yield). LCMS: m/z = 247.2 $[M + H]^+$.

(b) In a dried, round-bottom flask equipped with a magnetic stirrer was suspended 6-(benzyloxy)-3-nitropyridin-2-ol (430 mg, 1.75 mmol, 1 equiv) from the previous step in MeCN (8 mL). To this was then added NaH (60% w/w dispersion in paraffin oil, 0.20 g, 5.0 mmol, 2.8 equiv) in one rapid portion and the resulting mixture was stirred at rt for 10 min to afford a brownish, yellow suspension. Then, 2,2-difluoro-2-(fluorosulfonyl)acetic acid (325 μL, 3.15 mmol, 1.8 equiv) was added neat and dropwise over a period of 5 min, during which time a mild exotherm was observed. After 16 h of stirring, another aliquot of 2,2-difluoro-2-(fluorosulfonyl)acetic acid (325 μL, 3.15 mmol, 1.8 equiv) was

https://doi.org/10.1021/acs.jmedchem.6c01049
J. Med. Chem. 2026, 69, 15888−15927

added neat and dropwise over a period of 5 min. After another 48 h of stirring at rt, the crude reaction mixture was carefully quenched with water (10 mL) and then diluted with a 1:1 (v/v) solution of EtOAc and Hex (50 mL). The organic layer was then separated and washed sequentially with saturated aq. $NaHCO_3$ (25 mL), water (25 mL) and brine (25 mL), dried over $MgSO_4$, filtered, and the filtrate concentrated in vacuo. Purification of the crude product thus obtained by way of column chromatography (SiO_2, gradient elution: Hex → 1:1 (v/v) Hex: EtOAc) afforded 6-(benzyloxy)-2-(difluoromethoxy)-3-nitropyridine as a yellow oil (330 mg, 64% yield). LCMS: m/z = 297.2 $[M + H]^+$.

(c) In a dried, round-bottom flask equipped with a magnetic stirrer was combined 6-(benzyloxy)-2-(difluoromethoxy)-3-nitropyridine (265 mg, 0.895 mmol, 1 equiv) from the previous step and NH_4Cl (479 mg, 8.95 mmol, 10 equiv) in a 1:1 (v/v) solution of EtOH and water (4 mL). To this solution was then added iron powder (500 mg, 8.95 mmol, 10 equiv) in one rapid portion and the resulting gray suspension was heated at 90 °C under a nitrogen atmosphere for 1 h. The reaction suspension was then cooled to rt, filtered through a bed of Celite, and the insolubles washed with EtOAc (2 × 20 mL). The filtrate thus obtained was then diluted with water (20 mL) and extracted further with EtOAc (2 × 20 mL). The combined organic extracts were washed further with water (20 mL) and brine (20 mL), dried over Na_2SO_4, filtered, and the filtrate concentrated in vacuo. Purification of the crude product thus obtained by way of column chromatography (SiO_2, gradient elution: Hex → EtOAc) afforded 6-(benzyloxy)-2-(difluoromethoxy)pyridin-3-amine (**92**) as a yellow oil (135 mg, 57% yield). LCMS: m/z = 267.2 $[M + H]^+$.

(d) In a dried, round-bottom flask equipped with a magnetic stirrer was combined 6-(benzyloxy)-2-(difluoromethoxy)pyridin-3-amine (**92**, 130 mg, 0.488 mmol, 1 equiv) from the previous step and pyridine (118 μL, 1.46 mmol, 3 equiv) in anhydrous DCM (6 mL). To this was then added triphosgene (58 mg, 0.20 mmol, 0.4 equiv) in one rapid portion at rt and the resulting solution was stirred at rt for 30 min. Ethyl (1*r*,4*r*)-4-((2-isopropylphenyl)amino)cyclohexane-1-carboxylate (**78**, 141 mg, 0.488 mmol, 1 equiv) was then added in one rapid portion and the resulting mixture was stirred at rt for an additional 16 h. The reaction was then quenched with water (10 mL) and back extracted with DCM (3 × 20 mL). The combined organic extracts were dried over $MgSO_4$, filtered, and the filtrate concentrated in vacuo. Purification of the crude product thus obtained by way of column chromatography (SiO_2, gradient elution: Hex → 1:1 (v/v) Hex: EtOAc) afforded ethyl (1*r*,4*r*)-4-(3-(6-(benzyloxy)-2-(difluoromethoxy)pyridin-3-yl)-1-(2-isopropylphenyl)ureido)cyclohexane-1-carboxylate (**93**) as a yellow oil (280 mg, 99% yield). LCMS: m/z = 582.6 $[M + H]^+$.

(e) In a dried, round-bottom flask equipped with a magnetic stirrer was dissolved ethyl (1*r*,4*r*)-4-(3-(6-(benzyloxy)-2-(difluoromethoxy)pyridin-3-yl)-1-(2-isopropylphenyl)ureido)-cyclohexane-1-carboxylate (**93**, 270 mg, 0.465 mmol, 1 equiv) from the previous step in MeOH (6 mL). The resulting yellow solution was then deoxygenated via subsurface purging with nitrogen for 10 min before palladium (10% w/w over activated carbon, dry, 0.10 g, 0.094 mmol, 0.2 equiv) was added in one rapid portion. The resulting black suspension was then subsurface purged with hydrogen for 10 min before it was stirred under a static hydrogen atmosphere (maintained with a balloon) at rt for 18 h. The reaction was subsequently diluted with EtOAc (30 mL) and filtered through a bed of DCM-wetted Celite. The insolubles were washed further with EtOAc (3 × 30 mL). Concentration of the filtrate thus obtained in vacuo afforded ethyl (1*r*,4*r*)-4-(3-(2-(difluoromethoxy)-6-hydroxypyridin-3-yl)-1-(2-isopropylphenyl)ureido)cyclohexane-1-carboxylate (**94**) as an off-white solid (180 mg, 78% yield). LCMS: m/z = 492.5 $[M + H]^+$.

(f) In a round-bottom flask equipped with a magnetic stirrer was dissolved ethyl (1*r*,4*r*)-4-(3-(2-(difluoromethoxy)-6-hydroxypyridin-3-yl)-1-(2-isopropylphenyl)ureido)cyclohexane-1-carboxylate (**94**, 100 mg, 0.203 mmol, 1 equiv) from the previous step in MeOH (9 mL). To this colorless solution was added LiOH (1 M solution in water, 1.0 mL, 1.0 mmol, 5 equiv) and the resulting mixture was stirred at rt for 5 h. The reaction mixture was then carefully quenched with HCl (1 M solution in water, 1.0 mL, 1.0 mmol, 5 equiv) at 0 °C before the volatiles were removed in vacuo. Purification of the crude product thus obtained by way of reverse-phase column chromatography (C_{18}, gradient elution: 95:5 (v/v) H_2O: MeCN → 5:95 (v/v) H_2O: MeCN) afforded the title compound **47-LM-M3/47-Hep-M6** as a white solid (69 mg, 73% yield). LCMS: m/z = 464.5 $[M + H]^+$. Purity (UV detection) = 100.0%. ^1H NMR (300 MHz, DMSO-d_6): δ = 12.04 (br s, 1H), 10.77 (br s, 1H), 8.06 (d, J = 8.5 Hz, 1H), 7.53 (dd, J = 7.8, 1.3 Hz, 1H), 7.45 (t, J = 7.5 Hz, 1H), 7.33 (t, J = 72.8 Hz, 1H), 7.31 (td, J = 7.5, 1.5 Hz, 1H), 7.20 (d, J = 7.8 Hz, 1H), 6.41 (d, J = 8.5 Hz, 1H), 6.15 (br s, 1H), 4.19−4.09 (m, 1H), 3.12 (sept, J = 6.8 Hz, 1H), 2.08−1.75 (m, 5H), 1.47−1.32 (m, 3H), 1.21 (d, J = 6.8 Hz, 3H), 1.11 (d, J = 6.8 Hz, 3H), 1.02 (qd, J = 12.5, 2.9 Hz, 1H).

(1*r*,4*r*)-4-(3-(2-(Difluoromethoxy)-6-methoxypyridin-3-yl)-1-(2-(1-hydroxypropan-2-yl)phenyl)ureido)-cyclohexane-1-carboxylic acid (47-LM-M2/47-Hep-M4)

(a) In a dried, round-bottom flask equipped with a magnetic stirrer was combined, at 0 °C, methyltriphenylphosphonium bromide (4.35 g, 12.2 mmol, 1.2 equiv) and potassium *tert*-butoxide (1.37 g, 12.2 mmol, 1.2 equiv) in anhydrous THF (16 mL). The resulting bright yellow suspension was stirred at 0 °C for 30 min after which time 2′-iodoacetophenone (**95**, 2.5 g, 10 mmol, 1 equiv) was added as a solution in THF (8 mL) dropwise over a period of 5 min. The resulting suspension was then allowed to warm slowly to rt over 16 h. The insolubles were removed via vacuum filtration and washed further with diethyl ether (2 × 50 mL). The filtrate thus obtained was concentrated in vacuo. The resulting residue was then purified by way of column chromatography (SiO_2, Hex) to afford 1-iodo-2-(prop-1-en-2-yl)benzene (**96**) as a colorless oil (1.05 g, 42% yield). LCMS: product did not ionize on MS. ^1H NMR (300 MHz, $CDCl_3$): δ = 7.83 (dd, J = 7.9, 0.9 Hz, 1H), 7.30 (td, J = 7.5, 1.2 Hz, 1H), 7.17 (dd, J = 7.5, 1.8 Hz, 1H), 6.94 (td, J = 7.9, 1.8 Hz, 1H), 5.23−5.21 (m, 1H), 4.90−4.88 (m, 1H), 2.07−2.06 (m, 3H).

(b) In a dried, round-bottom flask equipped with a magnetic stirrer was dissolved 1-iodo-2-(prop-1-en-2-yl)benzene (**96**, 1.0 g, 4.1 mmol, 1 equiv) from the previous step in anhydrous THF (20 mL). To this solution was then added, at 0 °C, BH_3 (1 M solution in THF, 4.5 mL, 4.5 mmol, 1.1 equiv) dropwise over a period of 5 min. The resulting solution was stirred at 0 °C for 90 min before the reaction was quenched with the sequential and dropwise addition of NaOH (2.5 M solution in water, 5.7 mL, 14 mmol, 3.5 equiv) and H_2O_2 (30% w/w solution in water, 2.9 mL, 29 mmol, 7 equiv). After the completion of addition, the cooling bath was removed, and the biphasic solution was stirred vigorously at rt for 1 h. The reaction mixture was then diluted with water (50 mL) and extracted with EtOAc (3 × 30 mL). The combined organic extracts were washed further with water (30 mL) and brine (30 mL), dried over $MgSO_4$, filtered, and the filtrate concentrated in vacuo. Purification of the crude product thus obtained by way of column chromatography (SiO_2, gradient elution: Hex → 2:3 (v/v) Hex: EtOAc) afforded 2-(2-iodophenyl)propan-1-ol (**97**) as a colorless oil (830 mg, 77% yield). LCMS: m/z = 245.0 $[M-OH]^+$. ^1H NMR (300 MHz, $CDCl_3$): δ = 7.86 (dd, J = 7.8, 1.2 Hz, 1H), 7.33 (td, J = 7.3, 1.0 Hz, 1H), 7.22 (dd, J = 7.8, 1.8 Hz, 1H), 6.92 (ddd, J = 7.9, 7.3, 1.8 Hz, 1H), 3.82−3.65 (m, 2H), 3.34 (sext, J = 6.7 Hz, 1H), 1.37 (br s, 1H), 1.27 (d, J = 6.7 Hz, 3H).

(c) In a dried, round-bottom flask equipped with a magnetic stirrer was combined 2-(2-iodophenyl)propan-1-ol (**97**, 0.47 g, 1.8 mmol, 1 equiv) from the previous step, TBSCl (0.32 g, 2.2

https://doi.org/10.1021/acs.jmedchem.6c01049
J. Med. Chem. 2026, 69, 15888−15927

mmol, 1.2 equiv), triethylamine (0.40 mL, 2.9 mmol, 1.6 equiv), and DMAP (22 mg, 0.18 mmol, 0.1 equiv) in DCM (8 mL). The resulting mixture was stirred at rt for 16 h and then quenched with the addition of water (20 mL). The aqueous layer was separated and back extracted with DCM (2 × 20 mL). The combined organic extracts were washed further with water (20 mL) and brine (20 mL), dried over $MgSO_4$, and filtered. Concentration of the filtrate in vacuo furnished *tert*-butyl(2-(2-iodophenyl)propoxy)dimethylsilane (**98**) as a colorless oil (0.68 g, >99% yield). LCMS: product did not ionize on MS. ^{1}H NMR (300 MHz, $CDCl_3$): δ = 7.82 (dd, J = 7.9, 1.2 Hz, 1H), 7.28 (td, J = 7.5, 1.2 Hz, 1H), 7.20 (dd, J = 7.8, 1.8 Hz, 1H), 6.87 (ddd, J = 7.9, 7.3, 1.8 Hz, 1H), 3.72 (dd, J = 9.9, 5.3 Hz, 1H), 3.54 (dd, J = 9.9, 7.1 Hz, 1H), 3.30−3.19 (m, 1H), 1.26 (d, J = 6.9 Hz, 3H), 0.84 (s, 9H), 0.09 (s, 3H), −0.04 (s, 3H).

(d) In a thick-walled glass reaction vessel equipped with a magnetic stirrer and a Teflon screwcap was combined *tert*-butyl(2-(2-iodophenyl)propoxy)dimethylsilane (**98**, 390 mg, 1.04 mmol, 1 equiv) from the previous step, *trans*-methyl 4-aminocyclohexanecarboxylate hydrochloride (220 mg, 1.14 mmol, 1.1 equiv), palladium(II) acetate (14 mg, 0.062 mmol, 0.06 equiv), tri-*tert*-butylphosphonium tetrafluoroborate (36 mg, 0.12 mmol, 0.12 equiv), and Cs_2CO_3 (1.35 g, 4.16 mmol, 4 equiv) in 1,4-dioxane (10 mL). The resulting yellow suspension was then deoxygenated via subsurface purging with nitrogen for 10 min before the reaction vessel was tightly sealed and heated at 95 °C for 18 h. The resulting brown suspension was cooled to rt, diluted with MTBE (100 mL), and washed sequentially with water (50 mL) and brine (50 mL). The organic extract thus obtained was then dried over $MgSO_4$, treated with charcoal (0.5 g), filtered through a bed of Celite, and the filtrate concentrated in vacuo. Purification of the crude product thus obtained by way of column chromatography (SiO_2, gradient elution: Hex → 1:1 (v/v) Hex: EtOAc) afforded methyl (1*r*,4*r*)-4-((2-(1-((*tert*-butyldimethylsilyl)oxy)propan-2-yl)phenyl)amino)-cyclohexane-1-carboxylate (**99**) as a golden yellow oil (210 mg, 50% yield). LCMS: m/z = 406.3 $[M + H]^+$. ^{1}H NMR (300 MHz, $CDCl_3$): δ = 7.13−7.05 (m, 2H), 6.71 (dd, J = 7.4, 1.0 Hz, 1H), 6.66 (d, J = 8.7 Hz, 1H), 3.83 (br s, 1H), 3.69 (s, 3H), 3.62 (dq, J = 9.7, 7.3 Hz, 2H), 3.26 (tt, J = 11.0, 3.7 Hz, 1H), 2.92 (sext, J = 6.7 Hz, 1H), 2.33 (tt, J = 12.1, 3.7 Hz, 1H), 2.27−2.17 (m, 2H), 2.12−2.02 (m, 2H), 1.68−1.48 (m, 3H), 1.28 (d, J = 6.7 Hz, 3H), 1.24−1.10 (m, 1H), 0.86 (s, 9H), 0.01 (s, 6H).

(e) In a dried, round-bottom flask equipped with a magnetic stirrer was combined 2-(difluoromethoxy)-6-methoxypyridin-3-amine (**61**, 79 mg, 0.42 mmol, 1.1 equiv) and pyridine (0.15 mL, 1.9 mmol, 3 equiv) in anhydrous DCM (6 mL). To this was then added phosgene (15% w/w solution in toluene, 0.41 mL, 0.57 mmol, 1.5 equiv) dropwise at rt and the resulting solution was stirred at rt for 30 min. The volatiles were then removed in vacuo and the crude (2-(difluoromethoxy)-6-methoxypyridin-3-yl)-carbamic chloride thus obtained was retaken up in anhydrous DCM (6 mL). This solution was then added dropwise at rt to another DCM (6 mL) suspension of methyl (1*r*,4*r*)-4-((2-(1-((*tert*-butyldimethylsilyl)oxy)propan-2-yl)phenyl)amino)-cyclohexane-1-carboxylate (**99**, 153 mg, 0.377 mmol, 1 equiv) from the previous step, pyridine (0.15 mL, 1.9 mmol, 3 equiv), and freshly activated 4 Å molecular sieves (25 beads). The resulting mixture was stirred at rt for 16 h before the reaction was quenched with water (20 mL). The aqueous layer was separated and back extracted with DCM (2 × 20 mL). The combined organic extracts were dried over $MgSO_4$, filtered, and the filtrate concentrated in vacuo. Purification of the crude product thus obtained by way of column chromatography (SiO_2, gradient elution: Hex → 4:1 (v/v) Hex: EtOAc) afforded methyl (1*r*,4*r*)-4-(1-(2-(1-((*tert*-butyldimethylsilyl)oxy)propan-2-yl)phenyl)-3-(2-(difluoromethoxy)-6-methoxypyridin-3-yl)ureido)-cyclohexane-1-carboxylate (**100**) as a colorless oil (120 mg, 51% yield). LCMS: m/z = 622.3 $[M + H]^+$. ^{1}H NMR (300 MHz, $CDCl_3$): δ = 8.41 (d, J = 8.7 Hz, 0.5H, rotamer A), 8.34 (d, J = 8.7 Hz, 0.5H, rotamer B), 7.47−7.43 (m, 2H), 7.36−7.29 (m, 1H), 7.19 (d, J = 7.9 Hz, 1H), 7.16 (t, J = 73.0 Hz, 1H), 6.49 (d, J = 8.7 Hz, 1H), 5.95 (br s, 0.5H, rotamer A or B), 5.90 (br s, 0.5H, rotamer B or A), 4.34−4.15 (m, 1H), 3.78 (s, 1.5H, rotamer A or B), 3.77 (s, 1.5H, rotamer B or A), 3.73−3.46 (m, 2H), 3.64 (s, 1.5H, rotamer A or B), 3.63 (s, 1.5H, rotamer B or A), 3.33−3.21 (m, 1H), 2.25−1.93 (m, 5H), 1.67−1.49 (m, 3H), 1.36−1.19 (m, 1H), 1.29 (d, J = 6.8 Hz, 1.5H, rotamer A or B), 1.14 (d, J = 6.8 Hz, 1.5H, rotamer B or A), 0.85 (s, 4.5H, rotamer A or B), 0.76 (s, 4.5H, rotamer B or A), 0.01 (s, 1.5H, rotamer A or B), −0.02 (s, 1.5H, rotamer B or A), −0.17 (s, 3H).

(f) In a glass round-bottom flask equipped with a magnetic stirrer was dissolved methyl (1*r*,4*r*)-4-(1-(2-(1-((*tert*-butyldimethylsilyl)oxy)propan-2-yl)phenyl)-3-(2-(difluoromethoxy)-6-methoxypyridin-3-yl)ureido)cyclohexane-1-carboxylate (**100**, 156 mg, 0.251 mmol, 1 equiv) from the previous step in THF (10 mL). To this solution was then added TBAF (1 M solution in THF, 0.30 mL, 0.30 mmol, 1.2 equiv) dropwise over a period of 1 min, and the resulting mixture was stirred at rt for 2 h. The volatiles were then removed in vacuo and the resulting residue was directly subjected to purification by way of column chromatography (SiO_2, gradient elution: Hex → 1:1 (v/v) Hex: EtOAc) to afford methyl (1*r*,4*r*)-4-(3-(2-(difluoromethoxy)-6-methoxypyridin-3-yl)-1-(2-(1-hydroxypropan-2-yl)phenyl)-ureido)cyclohexane-1-carboxylate as a white solid (110 mg, 87% yield). LCMS: m/z = 508.2 $[M + H]^+$. ^{1}H NMR ($CDCl_3$): δ = 8.42 (d, J = 8.7 Hz, 0.33H, rotamer A), 8.27 (d, J = 8.7 Hz, 0.67H, rotamer B), 7.48−7.44 (m, 2H), 7.38−7.21 (m, 2H), 7.19 (t, J = 72.0 Hz, 0.67H, rotamer B), 7.17 (t, J = 72.0 Hz, 0.33H, rotamer A), 6.49 (d, J = 8.7 Hz, 0.33H, rotamer A), 6.48 (d, J = 8.7 Hz, 0.67H, rotamer B), 6.26 (br s, 0.67H, rotamer B), 5.89 (br s, 0.33H, rotamer A), 4.28−4.15 (m, 1H), 3.78 (s, 2H, rotamer B), 3.78−3.66 (m, 5H), 3.64 (s, 1H, rotamer A), 3.43−3.29 (m, 1H), 2.25−1.95 (m, 5H), 1.64−1.31 (m, 5H), 1.26 (d, J = 6.8 Hz, 2H, rotamer B), 1.17 (d, J = 6.8 Hz, 1H, rotamer A).

(g) In a glass round-bottom flask equipped with a magnetic stirrer was dissolved methyl (1*r*,4*r*)-4-(3-(2-(difluoromethoxy)-6-methoxypyridin-3-yl)-1-(2-(1-hydroxypropan-2-yl)phenyl)-ureido)cyclohexane-1-carboxylate (110 mg, 0.22 mmol, 1 equiv) from the previous step in MeOH (10 mL). To this colorless solution was then added LiOH (1 M solution in water, 1.95 mL, 1.95 mmol, 9 equiv) and the resulting mixture was heated at 60 °C for 2 h. Upon cooling to rt, the reaction mixture was carefully quenched with HCl (1 M solution in water, 1.95 mL, 1.95 mmol, 9 equiv) and the volatiles were removed in vacuo. The resulting suspension was back extracted with EtOAc (3 × 20 mL). The combined organic extracts were washed sequentially with water (10 mL) and brine (10 mL), dried over $MgSO_4$, and filtered. Concentration of the filtrate in vacuo afforded the title compound **47-LM-M2/47-Hep-M4** as a white solid (100 mg, 92% yield). LCMS: m/z = 494.0 $[M + H]^+$. Purity (UV detection) = 100.0%. ^{1}H NMR ($CDCl_3$): δ = 8.41 (d, J = 8.7 Hz, 0.36H, rotamer A), 8.25 (d, J = 8.7 Hz, 0.64H, rotamer B), 7.51−7.40 (m, 2H), 7.38−7.21 (m, 2H), 7.19 (t, J = 73.1 Hz, 0.64H, rotamer B), 7.17 (t, J = 73.1 Hz, 0.36H, rotamer A), 6.50 (d, J = 8.7 Hz, 0.36H, rotamer A), 6.48 (d, J = 8.7 Hz, 0.64H, rotamer B), 6.26 (br s, 0.64H, rotamer B), 5.90 (br s, 0.36H, rotamer A), 4.30−4.16 (m, 1H), 3.79−3.63 (m, 5H), 3.43−3.29 (m, 1H), 2.22−1.96 (m, 5H), 1.65−1.23 (m, 5H), 1.27 (d, J = 6.9 Hz, 1.9H, rotamer B), 1.17 (d, J = 6.9 Hz, 1.1H, rotamer A).

(2*S*,3*S*,4*S*,5*R*,6*S*)-6-(((1*r*,4*S*)-4-(3-(2-(Difluoromethoxy)-6-methoxypyridin-3-yl)-1-(2-isopropylphenyl)ureido)-cyclohexane-1-carbonyl)-oxy)-3,4,5-trihydroxytetrahydro-2H-pyran-2-carboxylic acid (47-Hep-M8)

(a) In a round-bottom flask equipped with a magnetic stirrer was combined **PIPE-791** (369 mg, 0.773 mmol, 1 equiv), allyl D-glucuronate (**101**, 181 mg, 0.773 mmol, 1 equiv, Combi-Blocks,

https://doi.org/10.1021/acs.jmedchem.6c01049
J. Med. Chem. 2026, 69, 15888−15927

Cat. No. QC-4243), and HATU (293 mg, 0.773 mmol, 1 equiv) in MeCN (20 mL). To this suspension was added *N*-methylmorpholine (170 μL, 1.5 mmol, 2 equiv) and the reaction mixture was stirred at rt for 16 h. The volatiles were removed in vacuo, and the resulting residue was partitioned between MTBE (50 mL) and water (50 mL). The aqueous layer was separated and back extracted with MTBE (3 × 30 mL). The combined organic extracts were washed sequentially with water (50 mL) and brine (50 mL), dried over $MgSO_4$, filtered, and the filtrate concentrated in vacuo. Purification of the crude product thus obtained by way of column chromatography (SiO_2, gradient elution: 9:1 (v/v) Hex: EtOAc → EtOAc → 10:1 (v/v) EtOAc: MeOH) afforded allyl (2*S*,3*S*,4*S*,5*R*,6*S*)-6-(((1*r*,4*S*)-4-(3-(2-(difluoromethoxy)-6-methoxypyridin-3-yl)-1-(2-isopropylphenyl)ureido)cyclohexane-1-carbonyl)oxy)-3,4,5-trihydroxytetrahydro-2H-pyran-2-carboxylate (**102**) as a viscous oil (265 mg, 50% yield). LCMS: m/z = 716.1 $[M + Na]^+$. ^1H NMR (300 MHz, $CDCl_3$): δ = 8.37 (dd, J = 8.7, 1.5 Hz, 1H), 7.48−7.41 (m, 2H), 7.30−7.25 (m, 1H), 7.15 (t, J = 73.0 Hz, 1H), 7.12 (d, J = 7.8 Hz, 1H), 6.47 (d, J = 8.7 Hz, 1H), 5.94−5.80 (m, 1H), 5.91 (br s, 1H), 5.54 (d, J = 7.7 Hz, 1H), 5.30 (d, J = 17.2 Hz, 1H), 5.21 (d, J = 10.4 Hz, 1H), 4.75−4.56 (m, 1H), 4.64 (d, J = 5.5 Hz, 2H), 4.33−4.17 (m, 2H), 4.14−3.99 (m, 1H), 3.98 (d, J = 9.5 Hz, 1H), 3.76 (s, 3H), 3.72 (d, J = 9.5 Hz, 1H), 3.63 (t, J = 8.7 Hz, 1H), 3.54 (t, J = 8.4 Hz, 1H), 3.19 (sept, J = 6.8 Hz, 1H), 2.24−1.89 (m, 5H), 1.67−1.40 (m, 3H), 1.21 (d, J = 6.8 Hz, 3H), 1.13 (d, J = 6.8 Hz, 3H), 1.18−1.05 (m, 1H).

(b) In a round-bottom flask equipped with a magnetic stirrer was suspended tetrakis(triphenylphosphine)palladium(0), polymer-bound (0.06 mmol/g loading, 2.4 g, 0.14 mmol, 0.5 equiv, Sigma-Aldrich, Cat. No. 10987) in 20 mL of THF. The resulting suspension was stirred under an inert atmosphere for 16 h. The supernatant was removed by a syringe and to the residual solid was then added a THF solution (10 mL) of morpholine (25 μL, 0.29 mmol, 1 equiv) and allyl (2*S*,3*S*,4*S*,5*R*,6*S*)-6-(((1*r*,4*S*)-4-(3-(2-(difluoromethoxy)-6-methoxypyridin-3-yl)-1-(2-isopropylphenyl)ureido)cyclohexane-1-carbonyl)oxy)-3,4,5-trihydroxytetrahydro-2H-pyran-2-carboxylate (**102**, 0.20 g, 0.29 mmol, 1 equiv) from the previous step. After an additional 16 h of stirring at rt, the reaction suspension was filtered and the insolubles were washed further with THF (2 × 10 mL). The filtrate thus obtained was concentrated in vacuo. Purification of the crude product thus obtained by way of column chromatography (SiO_2, gradient elution: DCM → 9:1 (v/v) DCM: MeOH → 3:7 (v/v) DCM: MeOH) afforded the title compound as a white solid (78 mg, 41% yield). LCMS: m/z = 654.2 $[M + H]^+$. Purity (UV detection) = 100.0%. ^1H NMR (300 MHz, DMSO-d_6): δ = 8.18 (d, J = 8.6 Hz, 1H), 7.54 (d, J = 7.8 Hz, 1H), 7.53 (t, J = 72.3 Hz, 1H), 7.47 (t, J = 7.5 Hz, 1H), 7.33 (td, J = 7.5, 1.5 Hz, 1H), 7.23 (d, J = 7.8 Hz, 1H), 6.62 (d, J = 8.6 Hz, 1H), 6.25 (br s, 1H), 5.25 (d, J = 7.9 Hz, 1H), 5.16 (br t, J = 4.2 Hz, 1H), 5.03 (br s, 1H), 4.23−4.09 (m, 1H), 3.77 (s, 3H), 3.28−3.02 (m, 6H), 2.20−1.81 (m, 5H), 1.54−1.38 (m, 3H), 1.22 (d, J = 6.8 Hz, 3H), 1.11 (d, J = 6.8 Hz, 3H), 1.08−0.97 (m, 1H).

Human LPAR1 Recombinant Membrane Binding Assay

Competition binding of the test article to human LPAR1 membranes at final testing concentrations of 100 pM to 10 μM against tritiated 1-(4′-(4-(((benzyloxy)carbonyl)amino)-3-methylisoxazol-5-yl)-(1,1′-biphenyl)-4 yl)cyclopropane-1-carboxylic acid (Vitrax, 57.8 Ci/mmol, provided as a 1 mCi/mL stock solution in ethanol, human LPAR1 K_d = 0.2 nM),[73] was determined. For the preparation of the requisite membrane, human LPAR1 overexpressing B103 cells (J. Chun Lab, UCSD) were suspended in an aqueous hypotonic buffer (0.24 M sucrose, 0.2 mM EDTA) over ice and centrifuged (30 min at 41,415*g*, 4 °C). The membrane pellet thus obtained was separated from the supernatant, qualified with Bio-Rad DC Protein Assay (Bio-Rad, Cat. No. 5000111), suspended in a storage buffer (20 mM HEPES, pH = 7.4), and stored at −80 °C until use. Prior to the start of the assay, the radioligand was diluted in a ligand dilution buffer (50 mM HEPES, 100 mM NaCl, 0.5% Tween-20, pH = 7.4) to a concentration of 5 nM. Additionally, freshly thawed membrane pellet was diluted in an assay buffer (50 mM HEPES, 100 mM NaCl, 2 mM EDTA, pH = 7.4) to a concentration of 9.4 mg/L. To each well of a 96-well assay plate (Thermo Fisher Scientific, Cat. No. 278752) was added the test article in DMSO (3 μL, at 100× of final testing concentration), the radioligand in ligand dilution buffer (30 μL), and the membrane pellet in assay buffer (267 μL). The assay plate was shaken (300 rpm) at rt for 2 h before the assay was terminated by vacuum filtration through a preconditioned filter plate (PerkinElmer, UniFilter-96 Gf/b, White 96-well Barex Microplate with Gf/b filter of 1 μm pore size, Cat. No. 6005177) on a Brandel Harvester. The filter plate was then washed three times with 2 mL ice cold assay buffer and dried at rt. To each well of the dried filter plate was applied 50 μL of BetaPlate Scint Cocktail (PerkinElmer, Cat. No. 1205-440) before the plate was sealed and incubated for 20 min at rt. The plate thus obtained was read on a PerkinElmer TopCount instrument for 1 min (using ^3H-microplate Unifilter, Program 3) to determine the radioactive counts per minute (cpm). Data were analyzed as background subtracted percent of positive control, where positive control was defined as cpm obtained in competition binding with 1 μM of cold 1-(4′-(4-(((benzyloxy)-carbonyl)amino)-3-methylisoxazol-5-yl)-(1,1′-biphenyl)-4 yl)-cyclopropane-1-carboxylic acid) and background was defined as cpm obtained in competition binding with 0.1% DMSO. Dose response curves and IC_{50} values were generated using Prism (GraphPad). The study was performed at Contineum Therapeutics (San Diego, CA, USA).

Human LPAR1 Ca^{2+} Mobilization Assay, 30 min Pre-Incubation

Ability of the test article to antagonize LPA-induced calcium mobilization in B103 cells stably overexpressing human LPAR1 (J. Chun Lab, UCSD) after 30 min preincubation at final testing concentrations of 100 pM to 10 μM was determined. The requisite B103 cells were suspended in DMEM containing 10% FBS, 1% Penicillin−Streptomycin, and 0.1% Geneticin, hence known as *Growth Media*, at a concentration of 500 viable cells per μL. 100 μL of this cellular suspension was then added into each well of a Costar 96-well black clear bottom plate (Corning, Cat. No. 3603) to give a density of 5 × 10^4 cells per well. The plate thus prepared was incubated at 37 °C under a 5% CO_2 atmosphere in an incubator for 23 h. The *Growth Media* was removed and 50 μL of Fluo-4 NW calcium assay dye (Invitrogen, Cat. No. F36206), prepared according to manufacturer's recommendations in Ca^{2+} and Mg^{2+} free HBSS containing 0.1% BSA, hence known as *Assay Buffer*, was then added to the cells. After 30 min of incubation at 37 °C under a 5% CO_2 atmosphere in an incubator, the plate was equilibrated and kept at rt for an additional 30 min before 25 μL of a solution of the test article (at 3× of final testing concentration) in a 332:1 (v/v) mixture of *Assay Buffer* and DMSO was added, to give a final DMSO concentration of 0.1%. The plate was held at rt for 30 min before 25 μL of a 12 μM solution of 18:1 LPA (Avanti, Cat. No. 857130C) in *Assay Buffer* was added. The calcium flux was measured simultaneously with LPA addition using a Molecular Devices FlexStation 3 instrument. Data were analyzed as background subtracted percent of positive control, where positive control was defined as the assay response in the absence of any test article and background was defined as the assay response in the absence of any 18:1 LPA. Dose response curves and IC_{50} values were generated using Prism (GraphPad). The study was performed at Contineum Therapeutics (San Diego, CA, USA).

Human LPAR1 Ca^{2+} Mobilization Assay, 24 h Pre-Incubation

Ability of the test article to antagonize LPA-induced calcium mobilization in B103 cells stably overexpressing human LPAR1 (J. Chun Lab, UCSD) after 24 h preincubation at final testing concentrations of 100 pM to 10 μM was determined. The requisite B103 cells were suspended in *Growth Media* (*vide supra*) at a concentration of 556 viable cells per μL. 90 μL of this cellular suspension was then added into each well of a Costar 96-well black clear

https://doi.org/10.1021/acs.jmedchem.6c01049
J. Med. Chem. 2026, 69, 15888−15927

bottom plate (Corning, Cat. No. 3603) that already contained 10 μL of a solution of the test article (at 10× of final testing concentration) in a 99:1 (v/v) mixture of *Growth Media* and DMSO, to give a density of 5×10^4 cells per well. The plate thus prepared was incubated at 37 °C under a 5% CO_2 atmosphere in an incubator for 23 h. The *Growth Media* was removed and 50 μL of Fluo-4 NW calcium assay dye (Invitrogen, Cat. No. F36206), prepared according to manufacturer's recommendations in *Assay Buffer* (*vide supra*), was then added to the cells. 25 μL of a solution of the test article (at 3× of final testing concentration) in a 332:1 (v/v) mixture of *Assay Buffer* and DMSO was also added, to give a final DMSO concentration of 0.1%. The resulting plate was returned to the incubator and incubated at 37 °C under a 5% CO_2 atmosphere for 30 min. The plate was then equilibrated and kept at rt for an additional 30 min before 25 μL of a 12 μM solution of 18:1 LPA (Avanti, Cat. No. 857130C) in *Assay Buffer* was added. The calcium flux was measured simultaneously with LPA addition using a Molecular Devices FlexStation 3 instrument. Data were analyzed as background subtracted percent of positive control, where positive control was defined as the assay response in the absence of any test article and background was defined as the assay response in the absence of any 18:1 LPA. Dose response curves and IC_{50} values were generated using Prism (GraphPad). The study was performed at Contineum Therapeutics (San Diego, CA, USA).

Human LPAR1−6 Ca^{2+} Mobilization Assay in Transiently Transfected HEK293T Cells

Ability of **PIPE-791** to antagonize LPA-induced calcium mobilization in HEK293T cells transiently expressing human LPAR1−6 after 3 h preincubation at final testing concentrations of 100 pM to 10 μM was determined. Plasmids containing human LPAR1 (Origene, Cat. No. RG206066), LPAR2 (Origene, Cat. No. RG206444), LPAR3 (Origene, Cat. No. RG223706), LPAR4 (Origene, Cat. No. RG223927), LPAR5 (Origene, Cat. No. RG209907), and LPAR6 (Origene, Cat. No. RG207345) were maxiprepped at Eton Biosciences (San Diego, CA, USA). A transfection mix was prepared by adding Fugene 6 transfection mix (Promega, Cat. No. E2691) and 0.1 μg of the requisite plasmid to serum free media. HEK293T cells (ATCC, Cat. No. CRL-3216) were then added to the transfection mix and plated onto a Costar 96-well black clear bottom plate (Corning, Cat. No. 3603) at a density of 0.5×10^4 cells per well. After incubating at 37 °C under a 5% CO_2 atmosphere in an incubator for 24 h, the media was removed and 25 μL of a solution of **PIPE-791** (at 3x of final testing concentration) in a 332:1 (v/v) mixture of *Assay Buffer* (*vide supra*) and DMSO was added. The assay plate was returned to the incubator and incubated at 37 °C under a 5% CO_2 atmosphere for an additional 3 h. During the last hour of incubation, 50 μL of Fluo-4 NW calcium assay dye (Invitrogen, Cat. No. F36206), prepared according to manufacturer's recommendations in *Assay Buffer*, was then added to the cells to give a final DMSO concentration of 0.1%. The plate was then equilibrated and kept at rt for an additional 30 min before 18:1 LPA (Avanti, Cat. No. 857130C), at its previously measured EC_{80} for a given LPAR subtype (5 μM for LPAR1 and LPAR2; 10 μM for LPAR3 and LPAR4; 1 μM for LPAR5; 13 μM for LPAR6) in *Assay Buffer*, was added. The calcium flux was measured simultaneously with LPA addition using a Molecular Devices FlexStation 3 instrument. Data were analyzed as background subtracted percent of positive control, where positive control was defined as the assay response in the absence of any test article and background was defined as the assay response in the absence of any 18:1 LPA. Dose response curves and IC_{50} values were generated using Prism (GraphPad). The study was performed at Contineum Therapeutics (San Diego, CA, USA).

Plasma Protein Binding Assay

Protein binding of the test article in plasma of Sprague−Dawley rat (BioIVT), Beagle dog (BioIVT), Cynomolgus monkey (Pharmaron), Göttingen minipig (Pharmaron), and/or human (BioIVT) was assessed by the equilibrium dialysis method using a 96-well dialysis plate equipped with HTD 96B 12−14 kDa MWCO dialysis membrane strips (HTDialysis LLC, Cat. No. 1101). 120 μL of plasma spiked with test article (to give a final testing concentration of 5 μM) was dialyzed against an equal volume of 100 mM phosphate-buffered saline (pH = 7.4) as per manufacturer's instructions. The dialysis was carried out over 6 h at 37 °C on an orbital shaker (300 rpm) under a 5% CO_2 atmosphere. At the end of the dialysis, 50 μL of postdialysis samples from both the buffer (hence known as *Buffer Sample*) and plasma (hence known as *Plasma Sample*) chambers were aliquoted into separate 96-well plates for further processing. 50 μL of blank plasma was added to the aliquoted *Buffer Sample* and 50 μL of 100 mM phosphate-buffered saline (pH = 7.4) was added to the aliquoted *Plasma Sample*. The plates were shaken at 1000 rpm for 2 min before proteins were precipitated with the addition of 400 μL of MeCN containing dexamethasone as the internal standard. The plates were then vortexed at 1000 rpm for an additional 10 min and centrifuged at 4000 rpm for 30 min. For each plate, 250 μL of the supernatant was transferred to a new 96-well plate and then centrifuged once more at 4000 rpm for 30 min. 100 μL of the resulting sample was transferred to an injection plate and diluted with one volume of distilled water prior to analysis by LC−MS/MS. % Free in Plasma was calculated using the following equation

$$\left(\frac{[\text{area ratio of test article}]_{\text{BufferSample}}}{[\text{area ratio of test article}]_{\text{PlasmaSample}}}\right) \times 100\%$$

The study was performed at Pharmaron (Beijing, China).

Brain Tissue Binding Assay

Protein binding of the test article in brain homogenate of Sprague−Dawley rat (Pharmaron) and/or Beagle dog (Pharmaron) was assessed by the equilibrium dialysis method using a 96-well dialysis plate equipped with HTD 96B 12−14 kDa MWCO dialysis membrane strips (HTDialysis LLC, Cat. No. 1101). The requisite brain homogenate was prepared by homogenizing freshly removed and accurately weighed brain in water at a ratio of 1:4 by brain weight (g) to water volume (mL). 150 μL of brain homogenate thus obtained was spiked with test article (to give a final testing concentration of 1 μM) and dialyzed against an equal volume of 100 mM phosphate-buffered saline (pH = 7.4) as per manufacturer's instructions. The dialysis was carried out over 6 h at 37 °C on an orbital shaker (100 rpm) under a 5% CO_2 atmosphere. At the end of the dialysis, 50 μL of postdialysis samples from both the buffer (hence known as *Buffer Sample*) and brain homogenate (hence known as *Brain Homogenate Sample*) chambers were aliquoted into separate 96-well plates for further processing. 50 μL of naïve brain homogenate was added to the aliquoted *Buffer Sample* and 50 μL of 100 mM phosphate-buffered saline (pH = 7.4) was added to the aliquoted *Brain Homogenate Sample*. The plates were shaken at 1000 rpm for 2 min before proteins were precipitated with the addition of 400 μL of MeCN containing dexamethasone as the internal standard. The plates were then vortexed at 1000 rpm for an additional 10 min and centrifuged at 4000 rpm for 30 min. For each plate, 250 μL of the supernatant was transferred to a new 96-well plate and then centrifuged once more at 4000 rpm for 30 min. 100 μL of the resulting sample was transferred to an injection plate and diluted with one volume of distilled water prior to analysis by LC−MS/MS. % Free in Brain Homogenate was calculated using the following equation

$$\left(\frac{[\text{area ratio of test article}]_{\text{BufferSample}}}{[\text{area ratio of test article}]_{\text{BrainHomogenateSample}}}\right) \times 100\%$$

% Free in Brain was calculated using the following equation

$$\left[\frac{0.2}{(100/\%\text{Free in Brain Homogenate}) - 0.8}\right] \times 100\%$$

The study was performed at Pharmaron (Beijing, China).

Microsome Stability Assay

The in vitro metabolic stability of the test article, at a final testing concentration of 1 μM, was assessed in Sprague−Dawley (DLS, Cat. No. 452501) and human (DLS, Cat. No. 452117) microsome incubations (0.5 mg/mL) at 37 °C in the presence of NADPH cofactor (10 mM) for 0, 0.5, 15, 30, 45, and 60 min prior to quenching with four volumes of cold MeCN and centrifugation (45 min at 3,220*g*,

https://doi.org/10.1021/acs.jmedchem.6c01049
J. Med. Chem. 2026, 69, 15888−15927

4 °C). The resulting supernatant was then transferred to an injection plate and analyzed by LC−MS/MS. The disappearance constant (k) was determined by linear regression of the natural logarithm of the percentage of test article remaining vs incubation time. The in vitro half-life ($T_{1/2}$) was calculated by multiplying k with 0.693. The study was performed at Pharmaron (Beijing, China).

Metabolite Identification in Human and Rat Liver Microsome Incubations

The metabolites formed in vitro from the test article in LM incubations, at a final testing concentration of 10 μM, were identified by LC-HRMS/MS. The test article was first incubated with Sprague−Dawley rat (Xenotech, Cat. No. R10000) and human (Corning, Cat. No. 452117) microsomes (1 mg/mL) at 37 °C in the presence of NADPH cofactor (2 mM) for 0, 30, and 60 min prior to quenching with two volumes of cold MeCN and centrifugation (15 min at 16,000*g*, 4 °C). The resulting supernatant was then transferred to an injection plate and analyzed by LC−HRMS/MS. Metabolites attributable to biotransformations of the test article were identified and their corresponding structures were proposed based on a combination of high-resolution MS1 accurate mass measurement and MS/MS fragmentation pattern. Additionally, wherever possible, the identity of the proposed metabolite was confirmed by matching the retention time, the high-resolution MS1 accurate mass, and the MS/MS fragmentation pattern with an authentic standard made available through independent synthesis. Peak area analysis of the EIC for a given LM incubation was used to estimate the relative abundance of the metabolites generated (assume that all the metabolites share similar MS response factors as the test article). The study was performed at Pharmaron (Beijing, China).

Bidirectional Permeability in MDCK-MDR1 Cell Line from NIH

Bidirectional permeability of the test article across MDCKII-MDR1 (NIH) cell line monolayer, prepared and qualified according to provider's instructions, was assessed using HTS Transwell-96 well permeable supports (Corning, Cat. No. 3391). To determine the rate of test article transport in the apical-to-basolateral direction ($P_{app,A\rightarrow B}$), 125 μL of HBSS buffer (10 mM HEPES, pH = 7.4) spiked with test article (to give a final testing concentration of 1 μM) was added to the apical compartment and 235 μL of blank HBSS buffer (10 mM HEPES, pH = 7.4) was added to the basolateral compartment. The transport experiment was initiated by incubating at 37 °C without shaking for 2 h. Samples (50 μL) were taken from the apical compartment at both the start and the end of the transport period, and from the basolateral compartment at the end of the transport period. These samples were added immediately to a separate 96-well plate that contained four volumes of cold MeCN to precipitate the protein. The plate containing these quenched samples was vortexed at 1000 rpm for 5 min and then centrifuged at 3220 rpm for 30 min. 100 μL of each supernatant was transferred to an injection plate and diluted with one volume of distilled water prior to analysis by LC−MS/MS. $P_{app,A\rightarrow B}$ was calculated using the following equation

$$\{[\text{Volume}]_{\text{basolateral}} \times [\text{Test article concentration}]_{\text{basolateralatt=2h}}\} / \{\text{Surface area of membrane} \times \text{Duration of transport period} \times [\text{Test article concentration}]_{\text{apicalatt=0h}}\}$$

To determine the rate of test article transport in the basolateral-to-apical direction ($P_{app,B\rightarrow A}$), 285 μL of HBSS buffer (10 mM HEPES, pH = 7.4) spiked with test article (to give a final testing concentration of 1 μM) was added to the basolateral compartment and 75 μL of blank HBSS buffer (10 mM HEPES, pH = 7.4) was added to the apical compartment. The transport experiment was initiated by incubating at 37 °C without shaking for 2 h. Samples (50 μL) were taken from the basolateral compartment at both the start and the end of the transport period, and from the apical compartment at the end of the transport period. These samples were processed as above prior to analysis by LC−MS/MS. $P_{app,B\rightarrow A}$ was calculated using the following equation

$$\{[\text{Volume}]_{\text{apical}} \times [\text{Test article concentration}]_{\text{apicalatt=2h}}\} / \{\text{Surface area of membrane} \times \text{Duration of transport period} \times [\text{Test article concentration}]_{\text{basolateralatt=0h}}\}$$

The efflux ratio was calculated as a ratio of $P_{app,B\rightarrow A}$ over $P_{app,A\rightarrow B}$. The study was performed at Pharmaron (Beijing, China).

CYP1A2, CYP2C9, CYP2C19, CYP2D6 and CYP3A4$_{mid}$ Marker Substrate Cocktail Inhibition Assay

Ability of the test article to inhibit CYP1A2-mediated *O*-deethylation of phenacetin, CYP2C9-mediated 4′-hydroxylation of diclofenac, 2C19-mediated 4′-hydroxylation of *S*-mephenytoin, CYP2D6-mediated 1′-hydroxylation of bufuralol, and CYP3A4-mediated 1′-hydroxylation of midazolam at testing concentrations of 100 pM to 30 μM was determined. To each well of a 96-well assay plate was dispensed 176 μL of phosphate-buffered saline (pH = 7.4), 1 μL of the CYP marker substrate cocktail (stock solution of 6 mM phenacetin, 2 mM diclofenac, 7 mM *S*-mephenytoin, 1 mM bufuralol, and 0.6 mM midazolam in a 3:1:1 (v/v/v) mixture of MeCN, DMSO, and water), 2 μL of a 20 mg/mL solution of human liver microsome (Corning, Cat. No. 452117) in phosphate-buffered saline (pH = 7.4), and 1 μL of a solution of the test article (at 200× of final testing concentration) in a 3:2 (v/v) mixture of DMSO and MeCN. The assay plate was warmed to 37 °C and the reactions were initiated with the addition of 20 μL of a 10 mM solution of NADPH in phosphate-buffered saline (pH = 7.4). After 5 min of incubation at 37 °C, the reactions were quenched with the addition of 200 μL of cold MeCN containing 30 nM verapamil and 3% formic acid. The quenched assay plate was then centrifuged at 4000 rpm for 90 min at 4 °C to ensure complete protein precipitation. 200 μL of the supernatant thus obtained was transferred to an injection plate and analyzed by LC−MS/MS. The extent of CYP activity inhibited by the test article for each isoform was quantified as the percentage decrease in the amount of marker metabolite formed when compared to vehicle control. IC_{50} was generated by fitting the dose concentration responses (% CYP activity inhibition) of the test article to a sigmoid curve using Prism (GraphPad). The study was performed at Pharmaron (Beijing, China).

hERG Inhibition Assay

Ability of the test article to block hERG channel current at testing concentrations of 370 nM to 30 μM was determined using a manual patch-clamp system at 34 °C. HEK293 cell line stably transfected with hERG gene (Invitrogen, Cat. No. K1239) was induced with 1 μg/mL of doxycycline for 48 h and then plated onto the coverslip of a 3.5 cm cell culture dish (Nunc, Cat. No. 150460) at a density of 5×10^4 cells. The coverslip was then transferred to an Olympus IX71 microscope stage that was warmed to 34 °C. Suitable cells were located and manually patched with a glass micropipette through which an electrode connected to a HEKA EPC10 amplifier could be inserted. The hERG current was selectively elicited by first depolarizing the cell at +30 mV for 4.8 s. The voltage was then taken back to −50 mV for 5.2 s and the resulting deactivating tail current was monitored to determine the hERG current amplitude and stability. If the patch-clamped cell was deemed to be stable, vehicle control was applied to establish a baseline (set as 0% inhibition). After steady state was reached, increasing levels of the test article were applied sequentially and the resulting dose-dependent changes in hERG current, if any, were measured over 5 min intervals. At the end of the study, dofetilide (450 nM) was applied as an internal control for full hERG blockade (set as 100% inhibition). The % current inhibition at a given dose of test article was calculated using the following equation

$$\left(1 - \frac{[\text{Peak tail current}]_{\text{test article}} - [\text{Peak tail current}]_{\text{dofetilide}}}{[\text{Peak tail current}]_{\text{vehicle control}} - [\text{Peak tail current}]_{\text{dofetilide}}}\right) \times 100\%$$

IC_{50} was generated by fitting the dose concentration responses (% current inhibition) of the test article to a sigmoid curve using Prism (GraphPad). The study was performed at Pharmaron (Beijing, China).

https://doi.org/10.1021/acs.jmedchem.6c01049
J. Med. Chem. 2026, 69, 15888−15927

Hepatocyte Stability Assay

The in vitro metabolic stability of **PIPE-791**, at a final testing concentration of 1 μM, was assessed in Beagle dog (BioIVT, Cat. No. M00205), Cynomolgus monkey (RILD, Cat. No. HP-SXH-02M), Göttingen minipig (BioIVT, Cat. No. M00615), and human (BioIVT, Cat. No. X008000) hepatocyte incubations (0.5×10^6 viable cells/mL) at 37 °C under a 5% CO_2 atmosphere for 0, 15, 30, 60, 90, and 120 min on an orbital shaker (500 rpm) prior to quenching with cold MeCN and centrifugation (10 min at 3,220*g*, 4 °C). The resulting supernatant was then transferred to an injection plate and diluted with an equal volume of distilled water prior to analysis by LC−MS/MS. The disappearance constant (k) was determined by linear regression of the natural logarithm of the percentage of **PIPE-791** remaining vs incubation time. The in vitro half-life ($T_{1/2}$) was calculated by multiplying k with 0.693. The study was performed at Pharmaron (Beijing, China).

Metabolite Identification in Human, Monkey, Minipig, Dog, and Rat Hepatocyte Incubations

The metabolites formed in vitro from **PIPE-791** in hepatocyte incubations, at a final testing concentration of 10 μM, were identified by LC-HRMS/MS. **PIPE-791** was first incubated with Sprague−Dawley rat (BioIVT, Cat. No. M00005), Beagle dog (BioIVT, Cat. No. M00205), Cynomolgus monkey (RILD, Cat. No. HP-SXH-02M), Göttingen minipig (BioIVT, Cat. No. M00615), and human (BioIVT, Cat. No. X008000) hepatocyte incubations (1.0×10^6 viable cells/mL) at 37 °C under a 5% CO_2 atmosphere for 0, 120, and 240 min prior to quenching with two volumes of cold MeCN (containing 0.1% formic acid) and centrifugation (15 min at 16,000*g*, 4 °C). The resulting supernatant was then transferred to an injection plate and analyzed by LC-HRMS/MS. Metabolites attributable to biotransformations of **PIPE-791** were identified and their corresponding structures were proposed based on a combination of high-resolution MS1 accurate mass measurement and MS/MS fragmentation pattern. Additionally, wherever possible, the identity of the proposed metabolite was confirmed by matching the retention time, the high-resolution MS1 accurate mass, and the MS/MS fragmentation pattern with an authentic standard made available through independent synthesis. Peak area analysis of the EIC for a given hepatocyte incubation was used to estimate the relative abundance of the metabolites generated (assume that all the metabolites share similar MS response factors as **PIPE-791**). The study was performed at Pharmaron (Beijing, China).

PK Assessment in Sprague−Dawley Rats

Food fasted male Sprague−Dawley rats with jugular vein cannulas (Inotiv, n = 2 per dosing route), weighing approximately 275 to 325 g, were either administered the test article as a single oral gavage (10 mg/kg) formulated in 3 mL/kg of aqueous 1% HPMC/0.1% Tween 80 or as a single IV bolus (2 mg/kg) formulated in 1 mL/kg of aqueous 60% PEG400. After PO dosing, blood was collected predose, and at 0.25, 0.5, 1, 2, 4, 6, 8, and 24 h postdose. After IV dosing, blood was collected predose, and at 0.083, 0.25, 0.5, 1, 2, 4, 6, 8, and 24 h postdose. Blood samples were collected into K_3EDTA tubes and stored on wet ice until processed into plasma by centrifugation (10 min at 1,450*g*, 4 °C). The plasma samples thus obtained were quenched (at a 1:4 (v/v) ratio) with MeCN containing buspirone as internal standard, shaken on an orbital plate shaker (5 min at 900 rpm), and then centrifuged (10 min at 3,200*g*, 4 °C). The resulting supernatant was then transferred to an injection plate and analyzed by LC−MS/MS. Calibration standards and QC solutions of the test article were prepared in solvent and spiked into naïve Sprague−Dawley rat plasma to generate calibration curves and quality controls. The study was performed at Contineum Therapeutics (San Diego, CA, USA) and performed following the protocols evaluated and approved by the Contineum Therapeutics IACUC (Protocol # PL001-2025).

Neuro-PK Assessment in Sprague−Dawley Rats

Food fasted male Sprague−Dawley rats (Inotiv, n = 2), weighing approximately 275 to 325 g, were administered the test article as a single oral gavage (10 mg/kg) formulated in 3 mL/kg of aqueous 1% HPMC/0.1% Tween 80. After PO dosing, blood and brain tissues were collected 2 h postdose. Blood samples were collected and processed as above. Brain tissue samples were collected, immediately quick-frozen in an ice box, and kept at −80 °C until analysis. Before analysis, all thawed brain samples were weighed and homogenized with water at a ratio of 1:3 by brain weight (g) to water volume (mL). The homogenized samples thus obtained were quenched (at a 1:4 (v/v) ratio) with MeCN containing buspirone as internal standard and centrifuged (10 min at 3,200*g*, 4 °C). The resulting supernatant was then transferred to an injection plate and analyzed by LC−MS/MS. The actual brain concentration (ng/g) was the detected value determined by LC−MS/MS (ng/mL) multiplied by a dilution factor of 4. Calibration standards and quality control solutions of the test article were prepared in solvent and spiked into naïve Sprague−Dawley rat brain homogenate to generate calibration curves and quality controls. The study was performed at Contineum Therapeutics (San Diego, CA, USA) and performed following the protocols evaluated and approved by the Contineum Therapeutics IACUC (Protocol # PL002-2025).

PK Assessment in Beagle Dogs

Food fasted male Beagle dogs (Jiangsu Johnsen Bioresource, n = 3 per dosing route), weighing approximately 9 to 13 kg, were either administered **PIPE-791** as a single oral gavage (5 mg/kg) formulated in 5 mL/kg of aqueous 1% HPMC/0.1% Tween 80 or as a single IV bolus (2 mg/kg) formulated in 1 mL/kg of aqueous 60% PEG400. After PO dosing, blood was collected predose, and at 0.25, 0.5, 1, 2, 4, 8, and 24 h postdose. After IV dosing, blood was collected predose, and at 0.083, 0.25, 0.5, 1, 2, 4, 8, and 24 h postdose. Blood samples were collected into K_2EDTA tubes and stored on wet ice until processed into plasma by centrifugation (10 min at 2,000*g*, 4 °C). The plasma samples thus obtained were quenched (at a 1:4 (v/v) ratio) with MeCN containing dexamethasone as internal standard and centrifuged (30 min at 3,220*g*, 4 °C). The resulting supernatant was then transferred to an injection plate and diluted with three volumes of distilled water prior to analysis by LC−MS/MS. Calibration standards and quality control solutions of **PIPE-791** were prepared in solvent and spiked into naïve Beage dog plasma to generate calibration curves and quality controls. The study was performed at Pharmaron (Ningbo, China) and performed following the protocols evaluated and approved by the Pharmaron Ningbo IACUC (Study # PK-D-06012021).

Neuro-PK Assessment in Beagle Dogs

Food fasted male Beagle dogs (Jiangsu Johnsen Bioresource, n = 2), weighing approximately 9 to 13 kg, were administered **PIPE-791** as a single oral gavage (5 mg/kg) formulated in 5 mL/kg of aqueous 1% HPMC/0.1% Tween 80. After PO dosing, blood and brain tissues were collected 2 h postdose. Blood samples were collected and processed as above. Brain tissue samples were collected, immediately quick-frozen in an ice box, and kept at −75 °C until analysis. Before analysis, all thawed brain samples were weighed and homogenized with water at a ratio of 1:3 by brain weight (g) to water volume (mL). The homogenized samples thus obtained were quenched (at a 1:4 (v/v) ratio) with MeCN containing dexamethasone as internal standard and centrifuged (30 min at 3,220*g*, 4 °C). The resulting supernatant was then transferred to an injection plate and diluted with three volumes of distilled water prior to analysis by LC−MS/MS. The actual brain concentration (ng/g) was the detected value determined by LC−MS/MS (ng/mL) multiplied by a dilution factor of 4. Calibration standards and quality control solutions of **PIPE-791** were prepared in solvent and spiked into naïve Beage dog brain homogenate to generate calibration curves and quality controls. The study was performed at Pharmaron (Ningbo, China) and performed following the protocols evaluated and approved by the Pharmaron Ningbo IACUC (Protocol # PK-D-06012021).

PK Assessment in Cynomolgus Monkeys

Food fasted male Cynomolgus monkeys (Zhangjiang Prima Biotech, n = 3 per dosing route), weighing approximately 2 to 3 kg, were either administered **PIPE-791** as a single oral gavage (5 mg/kg) formulated in 5 mL/kg of aqueous 1% HPMC/0.1% Tween 80 or as a single IV bolus (2 mg/kg) formulated in 1 mL/kg of aqueous 60% PEG400. After PO dosing, blood was collected predose, and at 0.25, 0.5, 1, 2, 4, 8, and 24 h postdose. After IV dosing, blood was collected predose, and at 0.083,

https://doi.org/10.1021/acs.jmedchem.6c01049
J. Med. Chem. 2026, 69, 15888−15927

0.25, 0.5, 1, 2, 4, 8, and 24 h postdose. Blood samples were collected into K_2EDTA tubes and stored on wet ice until processed into plasma by centrifugation (10 min at 2,000*g*, 4 °C). The plasma samples thus obtained were quenched (at a 1:4 (v/v) ratio) with MeCN containing dexamethasone as internal standard and centrifuged (30 min at 3,220*g*, 4 °C). The resulting supernatant was then transferred to an injection plate and diluted with three volumes of distilled water prior to analysis by LC−MS/MS. Calibration standards and quality control solutions of **PIPE-791** were prepared in solvent and spiked into naïve Cynomolgus monkey plasma to generate calibration curves and quality controls. The study was performed at Pharmaron (Ningbo, China) and performed following the protocols evaluated and approved by the Pharmaron Ningbo IACUC (Protocol # PK-CM-02202021).

PK Assessment in Göttingen Minipigs

Food fasted male Göttingen minipig (Ellegard Göttingen minipig A/S), weighing approximately 19 to 24 kg, were either administered **PIPE-791** as a single oral gavage (5 mg/kg) formulated in 5 mL/kg of aqueous 1% HPMC/0.1% Tween 80 (n = 3) or as a single IV bolus (2 mg/kg) formulated in 1 mL/kg of aqueous 60% PEG400 (n = 2). After PO dosing, blood was collected predose, and at 0.25, 0.5, 1, 2, 4, 6, 8, 12, and 24 h postdose. After IV dosing, blood was collected predose, and at 0.083, 0.25, 0.5, 1, 2, 4, 6, 8, 12, and 24 h postdose. Blood samples were collected into K_2EDTA tubes and stored on wet ice until processed into plasma by centrifugation (10 min at 2,500*g*, 4 °C). The plasma samples thus obtained were quenched (at a 1:3 (v/v) ratio) with MeCN containing nifedipine as internal standard and centrifuged (5 min at 2,400*g*, 4 °C). The resulting supernatant was then transferred to an injection plate and diluted with two volumes of distilled water prior to analysis by LC−MS/MS. Calibration standards and quality control solutions of both **PIPE-791** and **47-Hep-M8** acyl glucuronide metabolite were individually prepared in solvent and spiked into naïve Göttingen minipig plasma to generate their respective calibration curves and quality controls. The study was performed at Charles River Laboratories (Edinburgh, UK) and performed following the protocols evaluated and approved by the Charles River Laboratories Edinburgh IACUC (Protocol # 189318).

Acyl Glucuronide Stability Assessment in 100 mM Potassium Phosphate Buffer (pH = 7.4)

The half-life and acyl migration rate of **47-Hep-M8** in 100 mM potassium phosphate buffer (pH = 7.4) at 37 °C was determined by LC−MS/MS. **47-Hep-M8**, at a final testing concentration of 10 μM, was spiked into 100 mM potassium phosphate buffer (pH = 7.4) and incubated for 0, 15, 30, 60, 90, 120, and 240 min prior to quenching with two volumes of cold MeCN (containing 0.1% formic acid and buspirone as internal standard) and centrifugation (15 min at 1,000*g*, 4 °C). The resulting supernatant was then transferred to an injection plate and diluted with three volumes of distilled water prior to analysis by LC−MS/MS. The degradation rate constant (k) was determined from the **47-Hep-M8** concentration versus time curve by linear regression of the semilogarithmic plot. The half-life ($T_{1/2}$) of **47-Hep-M8** was calculated by multiplying k with 0.693. The acyl migration rate was calculated using the following equation

$$\begin{aligned}&(\{[\text{total peak area of isomers of } \mathbf{47-Hep-M8}]_{t=240\text{min}}\}\\&/\{[\text{total peak area of isomers of } \mathbf{47-Hep-M8}]_{t=240\text{min}}\\&+[\text{Peak area of } \mathbf{47-Hep-M8}]_{t=240\text{min}}\}) \times 100\%\end{aligned}$$

The study was performed at Contineum Therapeutics (San Diego, CA, USA).

PXR Activation Assay

Ability of the test article to activate PXR nuclear receptor at testing concentrations of 1 and 10 μM was determined in plated cultures of DPX2 cells (Puracyp, Cat. No. DPX2-96-001). DPX2 cells were suspended in manufacturer's dosing medium (Puracyp, Cat. No. D-500-100) supplemented with 10% FBS at a density of 3.2×10^5 cells/mL. 25 μL of this cellular suspension was added into each well of a 384-well cell culture plate (Corning, Cat. No. 354660) and the resulting cell culture plate was incubated at 37 °C under a 5% CO_2 atmosphere in an incubator for 24 h. 25 nL of a DMSO solution of the test article (at 1,000× of final testing concentration) was then added, to give a final DMSO concentration of 0.1%. The cell culture plate was returned to the incubator and incubated at 37 °C under a 5% CO_2 atmosphere for an additional 48 h. The dosing medium was aspirated from each well and cell viability was confirmed using the CellTiter-Fluor Cell Viability Assay kit (Promega, Cat. No. G6081) as per manufacturer's instructions. After the cytotoxicity check was completed (the fluorescence, RFU, of each well was measured, at 400 nm excitation and 505 nm emission), 25 μL of One-Glo Luciferase Assay reagent (Vazyme, Cat. No. DD1203-03) was then added at rt and the cell culture plate was gently agitated for 5 min. The resulting luminescence (RLU) was read on an Infinite 200 PRO microplate reader. The fold-activation at a given concentration of the test article was calculated using the following equation

$$\frac{[\text{RLU}]_{\text{testarticle}}/[\text{RFU}]_{\text{testarticle}}}{[\text{RLU}]_{\text{vehicle}}/[\text{RFU}]_{\text{vehicle}}}$$

The study was performed at Pharmaron (Beijing, China).

UGT Reaction Phenotyping with Recombinant Human UGT Enzymes

The human UGT enzymes responsible for the formation of **47-Hep-M8** from **PIPE-791** was determined using LC−MS/MS. **PIPE-791**, at a final testing concentration of 10 μM, was incubated with individual recombinant human UGT (rhUGT) supersomes—1A1 (Corning, Cat. No. 456411), 1A3 (Corning, Cat. No. 456413), 1A4 (Corning, Cat. No. 456414), 1A6 (Corning, Cat. No. 456416), 1A9 (Corning, Cat. No. 456419), 2B7 (Corning, Cat. No. 456427), and 2B15 (Corning, Cat. No. 456435)—at 25 μg/mL in the presence of 1 mM of UDPGA and 1 mM $MgCl_2$ in 50 mM Tris buffer (pH = 7.5) at 37 °C for 0, 5, 10, 20, 40, and 60 min. Negative control incubations were performed with no rhUGT enzymes in the incubation samples. At the end of each incubation time point, the reactions were terminated with three volumes of ice-cold MeCN containing tolbutamide and labetalol. The mixtures were extracted and analyzed with LC−MS/MS. The study was performed at Wuxi AppTec (Cranbury, NJ, USA).

CYP Reaction Phenotyping with Recombinant Human CYP Enzymes

The human CYP enzymes responsible for the metabolism of **PIPE-791** was determined using LC−MS/MS. **PIPE-791**, at a final testing concentration of 0.3 μM, was incubated with individual recombinant human CYP (rhCYP) isozymes—1A2 (ThermoFisher, Cat. No. P2792), 2B6 (ThermoFisher, Cat. No. P3028), 2C8 (Corning, Cat. No. 456252), 2C9 (Corning, Cat. No. 456258), 2C19 (Corning, Cat. No. 456259), 2D6 (Corning, Cat. No. 456217), 3A4 (Corning, Cat. No. 456202), and 3A5 (Life technologies, Cat. No. P2512)—at 50 pmol/mL in the presence of an NADPH regeneration system (1.3 mM $NADP^+$, 3.3 mM glucose-6-phosphate, 3.3 mM $MgCl_2$, 0.4 U/mL glucose-6-phosphate dehydrogenase) and 1.0 mM EDTA in 50 mM potassium phosphate buffer (pH = 7.5) at 37 °C for 0, 5, 10, 20, 40, and 60 min. Negative control incubations were performed with the negative control Supersome (Corning, Cat. No. 456200) in the incubation samples. At the end of each incubation time point, the reactions were terminated with three volumes of ice-cold mixture of 9:1 (v/v) MeCN:MeOH containing tolbutamide and labetalol. The mixtures were extracted and analyzed with LC−MS/MS. The elimination rate constant (K_e) was calculated by fitting the concentration of **PIPE-791** at time t as a function of incubation time to the first order decay equation using Prism (GraphPad). The half-life ($T_{1/2}$) was calculated by dividing 0.693 by K_e. The study was performed at Wuxi AppTec (Cranbury, NJ, USA).

CYP Induction Assessment

The potential of **PIPE-791**, at testing concentrations ranging from 0.1 to 50 μM, to induce human CYP enzymes was determined using cryopreserved plateable human hepatocytes. The solubility of **PIPE-791**, at a nominal testing concentration of 50 μM, in InVitroGro

https://doi.org/10.1021/acs.jmedchem.6c01049
J. Med. Chem. 2026, 69, 15888−15927

hepatocyte incubation medium (BioIVT, Cat. No. Z990012) supplemented with Torpedo antibiotic mix (BioIVT, Cat. No. Z990008), hence known as *Incubation Media*, was determined by visual observations and by LC−MS/MS analysis. The stability of **PIPE-791**, at a nominal testing concentration of 50 μM, after incubating at 37 °C under a 5% CO_2 atmosphere for 4 h with plated human hepatocytes (BioIVT, Cat. No. M00995-9, Lot No. PDC) in *Incubation Media* at a seeding density of 1×10^6 viable cells/mL, was determined by LC−MS/MS analysis. The effect of **PIPE-791**, at a nominal testing concentration of 50 μM, on the viability of plated human hepatocytes (BioIVT, Cat. No. M00995-P, Lot No. PDC) in *Incubation Media* seeded at a density of 1×10^6 viable cells/mL, was evaluated using a CellTiter-Glo Cell Viability Assay kit (Promega, Cat. No. G7571) as per manufacturer's instructions after 3 days of incubation at 37 °C under a 5% CO_2 atmosphere. The CYP induction studies were performed by incubating **PIPE-791**, at testing concentrations ranging from 0.1 to 50 μM, with plated human hepatocytes from three separate donors in *Incubation Media* seeded at a density of 1×10^6 viable cells/mL (BioIVT, Cat. No. M00995-P, Lot No. GKJ and ZEY; BioIVT, Cat. No. F00995−P, Lot No. WKF) for 3 days at 37 °C under a 5% CO_2 atmosphere. At the end of each incubation day, the spent media was replaced with freshly prepared dosing solutions of **PIPE-791** in *Incubation Media* at the respective nominal testing concentrations (final DMSO concentration of 0.1%). At the end of the experiment, the CYP induction effect was assessed by measuring the mRNA expression levels of CYP 1A2, 2B6, 2C8, 2C9, and 3A4, as well as the enzyme activities of CYP2C19. To measure the mRNA expression levels, the RNA samples of each treated human hepatocytes were isolated and purified using the SV96 Total RNA Isolation System (Promega, Z3505) per manufacturer's instructions. The target gene expression levels of each RNA sample were monitored (Taqman CYP1A2 probes and primers, Life Technologies, Cat. No. 4351370; Taqman CYP2B6 probes and primers, Life Technologies, Cat. No. 4351370; Taqman CYP2C8 probes and primers, Life Technologies, Cat. No. 4331182; Taqman CYP2C9 probes and primers, Life Technologies, Cat. No. 4331182; Taqman CYP3A4 probes and primers, Life Technologies, Cat. No. 4351370) and normalized against GADPH mRNA expression level (Taqman GADPH probes and primers, Life Technologies, Cat. No. 4331182) of the same sample. The fold induction potential of **PIPE-791** on the various CYP isozymes was then calculated by using the normalized CYP mRNA expression of vehicle-treated hepatocytes as the baseline. The CYP2C19 activity at the end of the experiment was determined by quantifying the amount of *S*-mephenytoin 4′-hydroxylation metabolite formed from adding *S*-mephenytoin to the treated human hepatocytes by LC−MS/MS. Where appropriate, the regression lines and their associated EC_{50} and E_{max} values were obtained for each treated human hepatocytes by fitting the dose concentration responses (the fold induction) of **PIPE-791** to a nonlinear sigmoidal regression model using Prism (GraphPad). The study was performed at Wuxi AppTec (Cranbury, NJ, USA).

Direct and Time-Dependent CYP Inhibition Assessment

The potential of **PIPE-791**, at testing concentrations ranging from 0.1 to 100 μM, to directly and time-dependently inhibit CYP1A2-mediated *O*-deethylation of phenacetin (50 μM), CYP2B6-mediated hydroxylation of bupropion (50 μM), CYP2C8-mediated *N*-deethylation of amodiaquine (2 μM), CYP2C9-mediated 4′-hydroxylation of diclofenac (5 μM), 2C19-mediated 4′-hydroxylation of *S*-mephenytoin (20 μM), CYP2D6-mediated 1′-hydroxylation of bufuralol (5 μM), CYP3A4-mediated 1′-hydroxylation of midazolam (2 μM), and CYP3A4-mediated 6β-hydroxylation of testosterone (50 μM), was determined using LC−MS/MS. For these evaluations, the incubation concentrations of marker substrates used were within or below their previously established K_m values (Wuxi AppTec, Cranbury, NJ, USA). To study direct inhibition, incubation mixtures containing 0.1 mg/mL of HLM (Corning, Cat. No. 452117), **PIPE-791**, and the specific marker substrate were gently shaken in 50 mM phosphate-buffered saline (pH = 7.4) and 1 mM EDTA at 37 °C for 5 min. The reactions were then initiated by the addition of an NADPH regenerating system (1.3 mM $NADP^+$, 3.3 mM glucose-6-phosphate, 3.3 mM $MgCl_2$, 0.4 U/mL glucose-6-phosphate dehydrogenase). After 10 min of incubation at 37 °C, the reactions were quenched with the addition of two volumes of cold MeCN containing the appropriate internal standards prior to analysis by LC−MS/MS. To study time-dependent inhibition, incubation mixtures containing 0.1 mg/mL of HLM, **PIPE-791**, and NADPH regenerating system were first gently shaken in 50 mM phosphate-buffered saline (pH = 7.4) and 1 mM EDTA at 37 °C for 30 min. The specific marker substrate was then added, and the resulting sample was incubated at 37 °C for an additional 10 min before quench. The extent of CYP activity inhibited by **PIPE-791** for each isoform was quantified as the percentage decrease in the amount of marker metabolite formed when compared to vehicle control. IC_{50} was generated by fitting the dose concentration responses (% CYP activity inhibition) of **PIPE-791** to a nonlinear sigmoidal regression model using Prism (GraphPad). The study was performed at Wuxi AppTec (Cranbury, NJ, USA).

MDR1 and BCRP Permeation Inhibition Assays

The inhibitory potential of **PIPE-791**, at 3 and 30 μM, on the activities of MDR1 and BCRP was evaluated in permeation inhibition assays using transfected MDCKII cells stably expressing the individual human efflux transporters (SOLVO Biotechnology). These cells were seeded onto the porous membrane inserts of Milicell 24-well plates (Millipore, Cat. No. PSMW010R5) to facilitate the formation of a monolayer with tight junctions that effectively separated the two solute compartments, above and below the cell layer, corresponding to apical and basolateral sides of a pharmacological barrier, respectively. The bidirectional, either apical-to-basolateral or basolateral-to-apical, P_{app} of an appropriate probe substrate ([^{3}H]-digoxin diluted in 1 μM digoxin for MDR1; [^{3}H]-prazosin diluted in 1 μM prazosin for BCRP) was determined by applying the probe substrate to either the apical or basolateral side of the cell monolayer and monitoring its transport from the dosing compartment to the receiving compartment. The efflux ratio (ER) was then determined from the bidirectional P_{app}. The inhibitory potential of **PIPE-791** at the chosen testing concentrations was determined by comparing the ER of probe substrates in the absence and presence of **PIPE-791**. Experimentally, the dosing compartment was charged a prewarmed solution (37 °C) of the probe substrate in HBSS (pH = 7.4) supplemented with 10 mM HEPES in the presence or absence of **PIPE-791** (final DMSO concentration of 0.5%). The receiving compartment was instead charged a prewarmed solution of HBSS (pH = 7.4) supplemented with 10 mM HEPES in the presence or absence of **PIPE-791** (final DMSO concentration of 0.5%). The experiment was initiated by placing the apical plate on the corresponding basolateral plate, and the setup was incubated at 37 °C for either 120 min (MDR1 permeation assay) or 60 min (BCRP permeation assay). An aliquot was sampled from the dosing chamber at the start and the end of the incubation period, and from the receiving chamber at the end of the incubation period. The amount of radiolabeled probe substrate in each aliquot was determined using a MicroBeta2 microplate counter (PerkinElmer) 30 min after the addition of an appropriate amount of MicroScint 20 liquid scintillation cocktail (PerkinElmer, Cat. No. 6013621) in the dark. The study was performed at Wuxi AppTec (Cranbury, NJ, USA).

MATE1, MATE2-K, OAT1, OAT3, OATP1B1, OATP1B3, OCT1, and OCT2 Cellular Uptake Inhibition Assays

The inhibitory potential of **PIPE-791**, at testing concentrations ranging from 0.1 to 30 μM, on the activities of MATE1, MATE2-K, OAT1, OAT3, OATP1B1, OATP1B3, OCT1, and OCT2 was determined by monitoring the intracellular accumulation of their corresponding radiolabeled probe substates ([^{14}C]-metformin diluted in 2 μM metformin for MATE1; [^{14}C]-metformin diluted in 10 μM metformin for MATE2-K; [^{3}H]-*p*-aminohippuric acid diluted in 0.4 μM *p*-aminohippuric acid for OAT1; [^{3}H]-estrone-3-sulfate diluted in 1 μM estrone-3-sulfate for OAT3; [^{3}H]-estradiol-17β-glucuronide diluted in 1 μM of estradiol-17β-glucuronide for OATP1B1; [^{3}H]-cholecystokinine-8 diluted in 0.1 μM of cholecystokinine-8 for OATP1B3; [^{14}C]-tetraethylammonium diluted in 5 μM of tetraethylammonium for OCT1 and OCT2) in transfected cells stably expressing these uptake

https://doi.org/10.1021/acs.jmedchem.6c01049
J. Med. Chem. 2026, 69, 15888−15927

transporters (SOLVO Biotechnology; CHO for OAT1, OCT1, and OCT2; HEK293 for OATP1B1 and OATP1B3; MDCKII for OAT3). The requisite cells were rinsed twice with prewarmed KHB assay buffer (pH = 7.4 for OAT1, OAT3, OATP1B1, OATP1B3, OCT1, and OCT2; pH = 8.0 for MATE1 and MATE2-K) and preincubated with an additive when deemed necessary (OAT3 transfected cells were preincubated with 5 mM of glutaric acid in KHB (pH = 7.4) for 20 min; OATP1B1 and OATP1B3 transfected cells were preincubated with **PIPE-791** or DMSO vehicle control for 30 min). The experiment was initiated with the addition of a prewarmed KHB assay buffer containing the appropriate probe substrate in the presence or absence of **PIPE-791** (final DMSO concentration of 2%). After incubating at 37 °C for the requisite amount of time (15 min for MATE1 and MATE2-K; 3 min for OAT1, OAT3, OATP1B1, and OATP1B3; 10 min for OCT1; 5 min for OCT2), the media were aspirated. The remaining cells were rinsed twice with the appropriate ice-cold KHB assay buffers and then lysed in 0.1 N aqueous sodium hydroxide. The amount of radiolabeled probe substrate in the lysed cells was determined using a MicroBeta2 microplate counter (PerkinElmer) 30 min after the addition of an appropriate amount of MicroScint 20 liquid scintillation cocktail (PerkinElmer, Cat. No. 6013621) in the dark. The percent inhibition of transporter activity at a given testing concentration of **PIPE-791** was calculated using the following equation

$$\Big(1 - \Big\{[\text{Radioactivity with } \mathbf{PIPE-791}]_{\text{transportertransfectedcells}} - [\text{Radioactivity with } \mathbf{PIPE-791}]_{\text{parentalcells}}\Big\} / \Big\{[\text{Radioactivity with DMSO}]_{\text{transportertransfectedcells}} - [\text{Radioactivity with DMSO}]_{\text{parentalcells}}\Big\}\Big) \times 100\%$$

The study was performed at Wuxi AppTec (Cranbury, NJ, USA).

BSEP Vesicular Transport Inhibition Assay

The inhibitory potential of **PIPE-791**, at testing concentrations ranging from 0.1 to 30 μM, on the activity of BSEP was evaluated using inside-out membrane vesicles (Corning, Cat. No. 453802). The requisite membrane vesicles (50 μg) were combined with freshly prepared vesicle assay mix (75 μL, containing 2 mM HEPES-Tris, 100 mM KNO_3, 10 mM $Mg(NO_3)_2$, and 50 mM sucrose), radiolabeled probe substate ([^{3}H]-taurocholate diluted in 2 μM of taurocholate), and **PIPE-791** on a plate incubator shaker. After 15 min of preincubation at 37 °C, the reaction was initiated with either the addition of Mg-ATP (4 mM final incubation concentration) or AMP, with the latter serving as baseline control. The assay plate was incubated at 37 °C for 5 min and then quenched with the addition of ice-cold washing solution (75 μL, containing 10 mM Tris−HCl, 100 mM KNO_3, and 50 mM sucrose). The quenched samples were then filtered and washed further (5 × 75 μL) with ice-cold washing solution. The amount of radiolabeled probe substrate in the thoroughly washed solid was determined using a MicroBeta2 microplate counter (PerkinElmer) 30 min after the addition of MicroScint 20 liquid scintillation cocktail (PerkinElmer, Cat. No. 6013621) in the dark. The percent inhibition of BSEP activity at a given testing concentration of **PIPE-791** was calculated using the following equation

$$\Big(1 - \{[\text{Radioactivity with } \mathbf{PIPE-791}]_{\text{ATP}} - [\text{Radioactivity with } \mathbf{PIPE-791}]_{\text{AMP}}\} / \{[\text{Radioactivity with DMSO}]_{\text{ATP}} - [\text{Radioactivity with DMSO}]_{\text{AMP}}\}\Big) \times 100\%$$

The study was performed at Wuxi AppTec (Cranbury, NJ, USA).

GENERAL AND CHOLESTATIC DILI ASSESSMENT

The ability of imatinib (50 μM, general hepatotoxic positive control), troglitazone (75 μM, cholestatic hepatotoxic positive control), and **PIPE-791** (1, 3, 10, and 30 μM) to induce LDH leakage or ATP depletion in SCHH was evaluated. SCHH were prepared on BioCoat 96-well Cell Culture Plate (Corning, Cat. No. 354407) using Transporter Certified cryopreserved hepatocytes (BioIVT, Cat. No, M00995-TCERT) and maintained in QualGro Hepatocyte Culture Medium (BioIVT). On day 4 of culture, SCHH were treated with QualGro Sensitization Medium (BioIVT, contains 250 μM bile acid mixture for the assessment of cholestatic hepatotoxicity risk) or QualGro Human Culture Medium (BioIVT, for the assessment of general hepatotoxicity risk) containing 0.1% DMSO (solvent control), imatinib, troglitazone, or **PIPE-791**. Following 24 h of exposure to the test article at the chosen final testing concentration, cellular ATP content was determined using the CellTiter-Glo Assay Kit (Promega, Cat. No. G9681) and LDH leakage into the culture media was determined using the CytoTox-ONE Assay Kit (Promega, Cat. No. G7890), as per manufacturer's instructions. The study was performed at BioIVT (Durham, CO, USA).

BACTERIAL REVERSE MUTATION (AMES) ASSAY

An in vitro GLP bacterial reverse mutation (Ames) assay was conducted to evaluate the mutagenic potential of **PIPE-791** at 100, 250, 500, 1000, 2500, and 5000 μg/plate in four histidine-requiring strains of *S. typhimurium* (TA98, TA100, TA1535, and TA1537) and one tryptophan-requiring strain of *E. coli* (WP2 *uvrA*) in the presence or absence of exogenous metabolic activation (phenobarbital/5,6-benzoflavone-induced rat liver S9) using the plate incorporation method. **PIPE-791** was prepared as a stock formulation in DMSO at 50 mg/mL and this stock was serially diluted in DMSO to 1, 2.5, 5.0, 10, and 25 μg/mL. Sterile 12 × 75 mm test tubes were place into heating blocks at approximately 46 °C and the following items were added in stepwise manner: (1) 2.00 mL top agar supplemented with 10% of a 0.5 mM histidine/biotin/tryptophan solution, (2) 0.10 mL indicator organisms, (3) 0.10 mL DMSO (vehicle control) or **PIPE-791** stock (in DMSO) for evaluation of mutagenic potential at doses of 0, 100, 250, 500, 1000, 2500, and 5000 μg/plate, and (4) 0.50 mL metabolic activation mixture (with S9 activation assay conditions) or phosphate-buffered saline (without metabolic activation assay conditions). The tube contents were gently mixed and then poured onto minimal glucose plates. The top agar was allowed to set, and the plates were incubated at 36 to 38 °C for 2 days. Mutagenicity testing was performed at each concentration with and without a phenobarbital/5,6-benzoflavone-induced rat liver S9 metabolic activation system. For each strain and metabolic activation condition, mutagenicity was assessed by evaluation of mean revertant colony counts in **PIPE-791**-treated plates compared with those in vehicle control treated-plates. This study was performed at Charles River Laboratories (Skokie, IL, USA and Mattawan, MI, USA).

GSH TRAPPING ASSAY

50 μM of **PIPE-791** was incubated at 37 °C with 1 mg/mL of human liver microsomes (Corning, Cat. No. 452117) and glutathione (5 mM) in the presence of NADPH (1 mM) for 60 min. The reaction was quenched with 150 μL of 15% aqueous TFA, vortexed (5 min at 1000 rpm), and then centrifuged (10 min at 16,100*g*, 4 °C). The centrifuged samples were subsequently loaded onto a preconditioned Oasis HLB μElution plate (Waters, Cat. No. 186001828BA) and the resulting cartridge was washed first with water (200 μL, to remove proteins and salts) and then eluted with MeOH (100 μL). The

https://doi.org/10.1021/acs.jmedchem.6c01049
J. Med. Chem. 2026, 69, 15888−15927

eluent was analyzed by LC−MS/MS for the detection of GSH adducts (using constant neutral loss scan of 129 Da and a negative precursor scan of 272 Da), if any. The study was performed at Pharmaron (Ningbo, China).

28 DAY TOXICITY STUDY IN SPRAGUE−DAWLEY RATS

The repeat-dose toxicity and toxicokinetic (TK) of oral **PIPE-791** were evaluated in a 28 day GLP toxicology study in rats. Male and female Sprague−Dawley rats (n = 10/sex/group) were administered **PIPE-791** once daily by oral gavage (10 mL/kg) for 28 consecutive days at 0 (vehicle: aqueous 1% HPMC/0.1% Tween 80), 30, 100, or 1000 mg/kg/day. Blood samples were collected from satellite TK animals (n = 3/sex/group for vehicle, n = 6/sex/group for **PIPE-791** at all dose levels) on Days 1 and 28 at predose (Day 28 only), and 0.5, 1, 2, 4, 8, and 24 h postdose for assessment of **PIPE-791** plasma concentrations. Ophthalmic examinations were conducted on Day 23. The persistence, reversibility, or progression of findings was evaluated following a 28 day recovery period for animals in the vehicle and 1000 mg/kg/day groups (n = 6/sex/group). Toxicity was assessed by mortality, clinical observations, body weight, food consumption, ophthalmology, hematology, coagulation, clinical chemistry, urinalysis, organ weights, and macroscopic and microscopic examinations. In addition, the potential of **PIPE-791** to induce micronuclei in polychromatic erythrocytes (as an indication of genotoxic potential) was evaluated in bone marrow that was harvested between 18 and 24 h after the last dose. This study was conducted at Charles River Laboratories (Ashland, OH, USA and Mattawan, MI, USA) and performed following the protocols evaluated and approved by the Charles River Laboratory Ashland IACUC (Protocol # 01780001).

28 DAY TOXICITY STUDY IN GÖTTINGEN MINIPIGS

The repeat-dose toxicity and toxicokinetic (TK) of oral **PIPE-791** were evaluated in a 28 day GLP toxicology study in minipigs. Male and female Göttingen minipigs (n = 3/sex/group) were administered **PIPE-791** once daily by oral gavage (5 mL/kg) for 28 consecutive days at 0 (vehicle: aqueous 1% HPMC/0.1% Tween 80), 30, 100, or 1000 mg/kg/day. Blood samples were collected from animals on Days 1 and 28 at predose (Day 28 only), and 0.5, 1, 2, 4, 8, and 24 h postdose for assessment of **PIPE-791** plasma concentrations. Cardiovascular effects of **PIPE-791** were evaluated by electrocardiogram (ECG) on Days −5, 1, and 24 (males) or Days −8, 1, and 26 (females) by standard limb-lead. The persistence, reversibility, or progression of findings was evaluated following a 28 day recovery period for animals in the vehicle and 1000 mg/kg/day groups (n = 2/sex/group). Toxicity was assessed by mortality, clinical observations, body weight, ophthalmology, ECG measurements, hematology, coagulation, clinical chemistry, urinalysis, organ weights, and macroscopic and microscopic evaluations. This study was conducted at Charles River Laboratories (Mattawan, MI, USA) and performed following the protocols evaluated and approved by the Charles River Laboratories Mattawan IACUC (Protocol # 3137-024).

ASSOCIATED CONTENT

Supporting Information

The Supporting Information is available free of charge at https://pubs.acs.org/doi/10.1021/acs.jmedchem.6c01049.

Molecular formula string and in vitro biological data (CSV)

Mean potencies, purity, SEM and biological replicates of all final compounds; **PIPE-791** (**47**) reaction phenotyping study using recombinant CYP enzymes; transporter-mediated efflux and accumulation of **PIPE-791** (**47**); NMR and LC−MS data for **14**, **15**, **21**, **44**, **45**, **PIPE-791** (**47**), **48**, **49**, **50**, **51**, and **52**; preclinical species PK curves for **PIPE-791** (**47**); graphical summary of Eurofins SAFETYscan E/IC_{50} ELECT Data for **21** and **PIPE-791** (**47**); EIC from HLM and RLM incubation studies with **15** and **PIPE-791** (**47**); stability assessment of **47-Hep-M8** in potassium phosphate buffer (PDF)

AUTHOR INFORMATION

Corresponding Author

Austin Chen − *Contineum Therapeutics, San Diego, California 92121, United States*; orcid.org/0009-0005-1749-5622; Email: achen@contineum-tx.com

Authors

Christopher Baccei − *Contineum Therapeutics, San Diego, California 92121, United States*

Jill Baccei − *Contineum Therapeutics, San Diego, California 92121, United States*

Alexander Broadhead − *Contineum Therapeutics, San Diego, California 92121, United States*

Kym I. Lorrain − *Contineum Therapeutics, San Diego, California 92121, United States*

Michael M. Poon − *Contineum Therapeutics, San Diego, California 92121, United States*

Jeffrey Roppe − *Contineum Therapeutics, San Diego, California 92121, United States*

Thomas O. Schrader − *Contineum Therapeutics, San Diego, California 92121, United States*; orcid.org/0000-0003-3468-9566

Karin J. Stebbins − *Contineum Therapeutics, San Diego, California 92121, United States*

Lino Valdez − *Contineum Therapeutics, San Diego, California 92121, United States*

Yifeng Xiong − *Contineum Therapeutics, San Diego, California 92121, United States*

Daniel S. Lorrain − *Contineum Therapeutics, San Diego, California 92121, United States*

Complete contact information is available at: https://pubs.acs.org/10.1021/acs.jmedchem.6c01049

Author Contributions

All authors have given approval to the final version of the manuscript.

Funding

Funding was provided by Contineum Therapeutics, who employed all authors at the time this research was conducted.

Notes

The authors declare no competing financial interest.

ACKNOWLEDGMENTS

John Atkins, Danxi Li, Yu Xue, and Rong Zhang are gratefully acknowledged.

ABBREVIATIONS

BALF, bronchoalveolar lavage fluid; BAST, bis(2-methoxyethyl)aminosulfur trifluoride; BCRP, breast cancer resistance protein; BSEP, bile salt export pump; CDI, 1,1′-carbonyldiimidazole; CNR, cannabinoid receptor; CPhos, 2-dicyclohexylphosphino-2′,6′-bis(*N*,*N*-dimethylamino)-biphenyl; cpm, counts per minute; DILI, drug-induced liver injury; DMEM, Dulbecco's modified Eagle medium; EDG, endothelial differentiation gene(s); EIC, extracted ion chromatogram; FBS, fetal bovine serum; f_u, fraction unbound; FVC, forced vital capacity; GADPH, glyceraldehyde-3-phosphate dehydrogenase; GLP, good laboratory practice; GSH, glutathione; HBSS, Hank's balanced salt solution; HEPES, 4-(2-hydroxyethyl)-1-piperazineethanesulfonic acid; HPMC, hydroxypropyl methylcellulose; HtrA, high-temperature requirement factor A; IACUC, institutional animal care and use committee; IDT, idiosyncratic drug toxicity; IPF, idiopathic pulmonary fibrosis; KHB, Krebs-Henseleit buffer; $K_{p,uu,brain}$, unbound brain-to-plasma partition coefficient; LDH, lactate dehydrogenase; LM, liver microsome(s); LPA, lysophosphatidic acid(s); LPAR, lysophosphatidic acid receptor(s); LPC, lysophosphatidylcholine; LSCS, lumbar spinal canal stenosis; MATE, multidrug and toxin extrusion; MDCK, Madin−Darby canine kidney; nAChR, nicotinic acetylcholine receptor; OAT, organic anion transporter; OATP, organic anion transporting polypeptide; OCT, organic cation transporter; P_{app}, apparent permeability; PDE, phosphodiesterase; PLA, phospholipase A; rh, recombinant human; SCHH, sandwich-cultured human hepatocyte(s); TDI, time-dependent inhibition; TK, toxicokinetic; XantPhos, 4,5-bis(diphenylphosphino)-9,9-dimethylxanthene; XPhos, 2-dicyclohexylphosphino-2′4′6′-triisopropylbiphenyl; UDPGA, UDP glucuronic acid; UGT, UDP-glucuronosyltransferase.

REFERENCES

(1) (a) Noguchi, K.; Herr, D.; Mutoh, T.; Chun, J. Lysophosphatidic acid (LPA) and its receptors. *Curr. Opin. Pharmacol.* **2009**, *9*, 15−23. (b) Choi, J. W.; Herr, D. R.; Noguchi, K.; Yung, Y. C.; Lee, C. W.; Mutoh, T.; Lin, M. E.; Teo, S. T.; Park, K. E.; Mosley, A. N.; Chun, J. LPA receptors: subtypes and biological actions. *Annu. Rev. Pharmacol. Toxicol.* **2010**, *50*, 157−186. (c) Yung, Y. C.; Stoddard, N. C.; Chun, J. LPA receptor signaling: pharmacology, physiology, and pathophysiology. *J. Lipid Res.* **2014**, *55*, 1192−1214.

(2) Fukushima, N.; Chun, J. The LPA receptors. *Prostag. Other Lipid Mediat.* **2001**, *64*, 21−32.

(3) Aoki, J.; Inoue, A.; Okudaira, S. Two pathways for lysophosphatidic acid production. *Biochim. Biophys. Acta Gen. Subj.* **2008**, *1781*, 513−518.

(4) Michalczyk, A.; Budkowska, M.; Dolegowska, B.; Chlubek, D.; Safranow, K. Lysophosphatidic acid plasma concentrations in healthy subjects: circadian rhythm and associations with demographic, anthropometric and biochemical parameters. *Lipids Health Dis.* **2017**, *16*, 140.

(5) Bese, T.; Barbaros, M.; Baykara, E.; Guralp, O.; Cengiz, S.; Demirkiran, F.; Sanioglu, C.; Arvas, M. Comparison of total plasma lysophosphatidic acid and serum CA-125 as a tumor marker in the diagnosis and follow-up of patients with epithelial ovarian cancer. *J. Gynecol. Oncol.* **2010**, *21*, 248−254.

(6) Watanabe, N.; Ikeda, H.; Nakamura, K.; Ohkawa, R.; Kume, Y.; Aoki, J.; Hama, K.; Okudaira, S.; Tanaka, M.; Tomiya, T.; Yanase, M.; Tejima, K.; Nishikawa, T.; Arai, M.; Arai, H.; Omata, M.; Fujiwara, K.; Yatomi, Y. Both plasma lysophosphatidic acid and serum autotaxin levels are increased in chronic hepatitis C. *J. Clin. Gastroenterol.* **2007**, *41*, 616−623.

(7) Sasagawa, T.; Suzuki, K.; Shiota, T.; Kondo, T.; Okita, M. The significance of plasma lysophospholipids in patients with renal failure on hemodialysis. *J. Nutri. Sci. Vitaminol. (Tokyo)* **1998**, *44*, 809−818.

(8) Tager, A. M.; LaCamera, P.; Shea, B. S.; Campanella, G. S.; Selman, M.; Zhao, Z.; Polosukhin, V.; Wain, J.; Karimi-Shah, B. A.; Kim, N. D.; Hart, W. K.; Pardo, A.; Blackwell, T. S.; Xu, Y.; Chun, J.; Luster, A. D. The lysophosphatidic acid receptor LPA1 links pulmonary fibrosis to lung injury by mediating fibroblast recruitment and vascular leak. *Nat. Med.* **2008**, *14*, 45−54.

(9) Montesi, S. B.; Mathai, S. K.; Brenner, L. N.; Gorshkova, I. A.; Berdyshev, E. V.; Tager, A. M.; Shea, B. S. Docosatetetraenoyl LPA is elevated in exhaled breadth condensate in idiopathy pulmonary fibrosis. *BMC Pulm. Med.* **2014**, *14*, 5.

(10) Neighbors, M.; Li, Q.; Zhu, S. J.; Liu, J.; Wong, W. R.; Jia, G.; Sandoval, W.; Tew, G. W. Bioactive lipid lysophosphatidic acid species are associated with disease progression in idiopathic pulmonary fibrosis. *J. Lipid Res.* **2023**, *64*, 100375.

(11) Jian, D.; Ju, W.; Wu, X.; Zhan, X. Elevated lysophosphatidic acid levels in the serum and cerebrospinal fluid in patients with multiple sclerosis: therapeutic response and clinical implication. *Neurol. Res.* **2018**, *40*, 335−339.

(12) Hayakawa, K.; Kurano, M.; Ohya, J.; Oichi, T.; Kano, K.; Nishikawa, M.; Uranbileg, B.; Kuwajima, K.; Sumitani, M.; Tanaka, S.; Aoki, J.; Yatomi, Y.; Chikuda, H. Lysophosphatidic acids and their substrate lysophospholipids in cerebrospinal fluid as objective biomarkers for evaluating the severity of lumbar spinal stenosis. *Sci. Rep.* **2019**, *9*, 9144.

(13) Arun, P.; Wilder, D. M.; Morris, A. J.; Sabbadini, R.; Long, J. B. Cerebrospinal fluid levels of lysophosphatidic acids can provide suitable biomarkers for blast-induced traumatic brain injury. *J. Neurotrauma* **2023**, *40*, 2289−2296.

(14) (a) Benesch, M. G. K.; Tang, X.; Brindley, D. N.; Takabe, K. Autotaxin and lysophosphatidate signaling: prime targets for mitigating therapy resistance in cancer. *World J. Oncol.* **2024**, *15*, 1−13. (b) Simonetti, J.; Ficili, M.; Sgalla, G.; Richeldi, L. Experimental autotaxin inhibitors for the treatment of idiopathic pulmonary fibrosis. *Expert Opin. Invest. Drugs* **2024**, *33*, 133−143. (c) Liu, Y.; Luo, D.; Leng, H.; Gu, C.; Ding, Q.; Zhao, L.; Chao, X.; Wang, H.; He, Y.; Zhu, S.; Ai, G.; Peng, W. Design and bioactivity evaluation of a novel autotaxin inhibitor with anti-hepatic fibrosis effects. *Sci. Rep.* **2025**, *15*, 11092.

(15) (a) Delik, A.; Ülger, Y. Phospholipase inhibitors as cancer therapy in hepatocellular carcinoma. *Phospholipases Physiol. Pathol.* **2023**, *5*, 173−179. (b) Nikolaou, A.; Kokotou, M. G.; Vasilakaki, S.; Kokotos, G. Small-molecule inhibitors as potential therapeutics and as tools to understand the role of phospholipase A. *Biochim. Biophys. Acta Mol. Cell Biol. Lipids* **2019**, *1864*, 941−956.

(16) (a) Taneja, A.; Jentsch, G.; Delage, S.; Randall, M. J.; van den Blink, B.; Bauer, Y.; Namour, F. ISABELA Studies: Plasma exposure and target engagement do not explain the lack of efficacy of Ziritaxestat in patients with idiopathic pulmonary fibrosis. *Clin. Pharmacol. Ther.* **2024**, *115*, 606−615. (b) Trachalaki, A.; Lindahl, A. L.; Petrarulo, S.; Margaritopoulos, G. A. "Regression to the truth": lessons learned from negative IPF trials. *Breathe* **2025**, *21*, 240260. (c) Maher, T.; Song, J. W.; Kramer, M. R.; Lancaster, L.; Corte, T. J.; Yun, J.; Kim, K.-J.; Cho, J.; Sather, L. F.; George, P. M.; Devaraj, A.; Jung, J.-H.; Jung, S. Phase 2 study design and analysis approach for BBT-877: an autotaxin inhibitor targeting idiopathic pulmonary fibrosis. *BMJ. Open Respir. Res.* **2025**, *12*, No. e003038.

(17) Geraldo, L. H. M.; de Sampaio Spohr, T. C. E.; do Amaral, R. F. D.; da Fonseca, A. C. C.; Garcia, C.; de Almeida Mendes, F.; Freitas, C.; dosSantos, M. F.; Lima, F. R. S. Role of lysophosphatidic acid and its receptors in health and disease: novel therapeutic strategies. *Signal Transduct. Target. Ther.* **2021**, *6*, 45.

(18) Palmer, S. M.; Snyder, L.; Todd, J. L.; Soule, B.; Christian, R.; Anstrom, K.; Luo, Y.; Gagnon, R.; Rosen, G. Randomized, double-blind, placebo-controlled, Phase 2 trial of BMS-986020, a lysophosphatidic acid receptor antagonist for the treatment of idiopathic pulmonary fibrosis. *Chest* **2018**, *154*, 1061−1069.

https://doi.org/10.1021/acs.jmedchem.6c01049
J. Med. Chem. 2026, 69, 15888−15927

(19) Corte, T. J.; Behr, J.; Cottin, V.; Glassberg, M. K.; Kreuter, M.; Martinez, F. J.; Ogura, T.; Suda, T.; Wijsenbeek, M.; Berkowitz, E.; Elpers, B.; Kim, S.; Watanabe, H.; Fischer, A.; Maher, T. M. Efficacy and safety of Admilparant, an LPA_1 antagonist, in pulmonary fibrosis: a Phase 2 randomized clinical trial. *Am. J. Respir. Crit. Care Med.* **2025**, *211* (2), 230−238.
(20) Gill, M. W.; Murphy, B. J.; Cheng, P. T. W.; Sivaraman, L.; Davis, M.; Lehman-McKeeman, L. Mechanism of hepatobiliary toxicity of the LPA_1 antagonist BMS-986020 developed to treat idiopathic pulmonary fibrosis: Contrasts with BMS-986234 and BMS-986278. *Toxicol. Appl. Pharmacol.* **2022**, *438*, 115885.
(21) (a) Ueda, H.; Neyama, H. LPA1 receptor involvement in fibromyalgia-like pain induced by intermittent psychological stress, empathy. *Neurobiol. Pain* **2017**, *1*, 16−25. (b) Ueda, H.; Neyama, H.; Nagai, J.; Matsushita, Y.; Tsukahara, T.; Tsukahara, R. Involvement of lysophosphatidic acid-induced astrocyte activation underlying the maintenance of partial sciatic nerve injury-induced neuropathic pain. *Pain* **2018**, *159*, 2170−2178. (c) Gao, L.; Shi, H.; Sherchan, P.; Tang, H.; Peng, Li.; Xie, S.; Liu, R.; Hu, X.; Tang, J.; Xia, Y.; Zhang, J. H. Inhibition of lysophosphatidic acid receptor 1 attenuates neuro-inflammation via PGE2/EP2/NOX2 signalling and improves the outcome of intracerebral hemorrhage in mice. *Brain, Behav., Immun.* **2021**, *91*, 615−626.
(22) Cheng, P. T. W.; Corte, J. R. Lysophosphatidic acid receptor 1 (LPA_1) antagonists. *Med. Chem. Rev.* **2025**, *60*, 167−193.
(23) Cheng, P. T. W.; Kaltenbach, R. F., III.; Zhang, H.; Shi, J.; Tao, S.; Li, J.; Kennedy, L. J.; Walker, S. J.; Shi, Y.; Wang, Y.; Dhanusu, S.; Reddigunta, R.; Kumaravel, S.; Jusuf, S.; Smith, D.; Krishnananthan, S.; Li, J.; Wang, T.; Heiry, R.; Sum, C. S.; Kalinowski, S. S.; Hung, C.-P.; Chu, C.-H.; Azzara, A. V.; Ziegler, M.; Burns, L.; Zinker, B. A.; Boehm, S.; Taylor, J.; Sapuppo, J.; Mosure, K.; Everlof, G.; Guarino, V.; Zhang, L.; Yang, Y.; Ruan, Q.; Xu, C.; Apedo, A.; Traeger, S. C.; Cvijic, M. E.; Lentz, K. A.; Tirucherai, G.; Sivaraman, L.; Robl, J.; Ellsworth, B. A.; Rosen, G.; Gordon, D. A.; Soars, M. G.; Gill, M.; Murphy, B. J. Discovery of an oxycyclohexyl acid lysophosphatidic acid receptor 1 (LPA_1) antagonist BMS-986278 for the treatment of pulmonary fibrotic diseases. *J. Med. Chem.* **2021**, *64*, 15549−15581.
(24) Qian, Y.; Hamilton, M.; Sidduri, A.; Gabriel, S.; Ren, Y.; Peng, R.; Kondru, R.; Narayanan, A.; Truitt, T.; Hamid, R.; Chen, Y.; Zhang, L.; Fretland, A. J.; Sanchez, R. A.; Chang, K.-C.; Lucas, M.; Schoenfeld, R. C.; Laine, D.; Fuentes, M. E.; Stevenson, C. S.; Budd, D. C. Discovery of highly-selective and orally active lysophosphatidic acid receptor-1 antagonists with potent activity on human lung fibroblasts. *J. Med. Chem.* **2012**, *55*, 7920−7939.
(25) Sato, T.; Sugimoto, K.; Inoue, A.; Okudaira, S.; Aoki, J.; Tokuyama, H. Synthesis and biological evaluation of optically active Ki16425. *Bioorg. Med. Chem. Lett.* **2012**, *22*, 4323−4326.
(26) Neyama, H.; Dozono, N.; Sahara, Y.; Nishikawa, K.; Ueda, H. A novel lysophosphatidic acid receptor 1 antagonist with high brain penetrability has a curative effect in the empathic pain-related fibromyalgia model. *J. Pharm. Sci.* **2025**, *158*, 139−142.
(27) Tang, D. T.; Du, Z.; Yang, K. S.; Bestvater, B. P.; Kaplan, J.; Neubig, M. E.; Olen, C. L.; Phillips, B.; Wang, P.; Hudson, T.; Marchand, B.; Chan, J.; Sharma, M.; Hu, Y.; Matles, M.; Nejati, E.; Chojnacka, M.; Adams, C.; Pong, C.; Holsapple, K.; Budas, G.; Tsui, V.; Venkataramani, C.; Lazerwith, S. E.; Notte, G. T.; Watkins, W. J.; McGlinchey, E.; Zagorska, A.; Farand, J. Discovery of GS-2278, a potent and selective LPAR1 antagonist for the treatment of idiopathic pulmonary fibrosis. *J. Med. Chem.* **2025**, *68*, 5152−5169.
(28) Giuliani, M.; Rizzi, A.; Pagano, M.; Raveglia, L. F.; Saccani, F.; Di Lascia, M. R.; Interlandi, M.; Nardella, T. S.; Marchini, G.; Murgo, A.; Tigli, L.; Pappani, A.; Capelli, A. M.; Fernandez, S. X.; Puccini, P.; Villetti, G.; Civelli, M.; Beato, C.; Moro, E.; Mundi, C.; Remelli, R.; Armani, E. Novel cyclohexyl amido acid antagonists of lysophosphatidic acid type 1 receptor for the treatment of pulmonary fibrosis. *ACS Med. Chem. Lett.* **2025**, *16*, 317−326.
(29) An, S.; Li, C.; Zhou, G.; Huang, C. Compound as antagonist of lysophosphatidic receptor, composition, and use thereof. WO 2012100436 A1, Aug 2, 2012.
(30) Sandiego, C.; Boscutti, G.; Wells, L.; Baccei, C.; Lorrain, D.; Chen, A. Evaluation of [^{18}F]-OPC3497 to image lysophosphatidic acid receptor 1 in brain and lungs of non-human primate. In *XXXIIrd International Symposium on Cerebral Blood Flow, Metabolism and Function & XVIth International Conference on Quantification of Brain Function with PET (Brain & Brain PET 2025)*, Seoul, Republic of Korea, 2025.
(31) Contineum Therapeutics. PET Study of PIPE-791 in Healthy Volunteers and Volunteers with PrMS and IPF. ClinicalTrials.gov identifier: NCT06683612. https://clinicaltrials.gov/study/NCT06683612 (Accessed February 23rd, 2026).
(32) Terakado, M.; Suzuki, H.; Hashimura, K.; Tanaka, M.; Ueda, H.; Hirai, K.; Asada, M.; Ikura, M.; Matsunaga, N.; Saga, H.; Shinozaki, K.; Karakawa, N.; Takada, Y.; Minami, M.; Egashira, H.; Sugiura, Y.; Yamada, M.; Nakade, S.; Takaoka, Y. Discovery of a slow tight binding LPA1 antagonist (ONO-0300302) for the treatment of benign prostatic hyperplasia. *ACS Med. Chem. Lett.* **2017**, *8*, 1281−1286.
(33) Sakamoto, K.; Noguchi, Y.; Ueshima, K.; Yamakuni, H.; Ohtake, A.; Sato, S.; Ishizu, K.; Hosogai, N.; Kawaminami, E.; Takeda, M.; Masuda, N. Effect of ASP6432, a novel type 1 lysophosphatidic acid receptor antagonist, on urethral function and prostate cell proliferation. *J. Pharmacol. Exp. Ther.* **2018**, *366*, 390−396.
(34) (a) Bolli, M.; Brotschi, C.; Lescop, C.; Williams, J. T. Alkoxy-substituted pyridinyl derivatives as LPA1 receptor antagonists and their use in the treatment of fibrosis. WO 2019234115, Dec 12 2019. (b) Bolli, M.; Brotschi, C.; Lescop, C. Pyrdin-3-yl derivatives. WO 2020254408 A1, Dec 24 2020. (c) Birker, M.; Lescop, C. Combination of an azetidine LPA1 receptor antagonist with pirfenidone and/or nintedanib for use in the treatment of fibrotic diseases. WO 2021110805 A1, June 10 2021. (d) Lescop, C.; Brotschi, C.; Williams, J. T.; Sager, C. P.; Birker, M.; Morrison, K.; Froidevaux, S.; Delahaye, S.; Nayler, O.; Bolli, M. H. Discovery of Novel, Orally Active, Selective LPA Receptor Type 1 Antagonist, 4-(4-(2-Isopropylphenyl)-4-((2-emethoxy-4-methylphenyl)carbamoyl)piperidin-1-yl)-4-oxobutanoic Acid, with a Distinct Molecular Scaffold. *J. Med. Chem.* **2024**, *67*, 2379−2396.
(35) (a) Lescop, C.; Birker, M.; Brotschi, C.; Bürki, C.; Morrison, K.; Froidevaux, S.; Delahaye, S.; Nayler, O.; Bolli, M. H. Discovery of Novel, Orally Active, and Selective LPA1 Receptor Antagonist ACT-1016−0707 as a Preclinical Candidate for the Treatment of Fibrotic Diseases. *J. Med. Chem.* **2024**, *67*, 2397−2424. (b) Birker-Robaczewska, M.; Boucher, M.; Ranieri, G.; Poirey, S.; Studer, R.; Freti, D.; Schnoebelen, M.; Froidevaux, S.; Morrison, K.; Wyss, C.; Scherer, J.; Lescop, C.; Brotschi, C.; Bolli, M. H.; Kramberg, M.; Di Stefano, S.; Rey, M.; Iglarz, M.; Delahaye, S.; Vezzali, E.; Sieber, P.; Schäfer, A.; Caimi, S. L.; Hesse, C.; Nayler, O. The novel lysophosphatidic acid receptor 1-selective antagonist, ACT-1016−0707, has unique binding properties that translate into effective antifibrotic and anti-inflammatory activity in different models of pulmonary fibrosis. *J. Pharmacol. Exp. Ther.* **2025**, *392*, 103396.
(36) Davenport, R.; Masse, F.; Prud'homme, A.; Bürki, C.; Doerrwaechter, P.; Künzli, M.; D'Aiuto, F.; Bolli, M. H.; Schäfer, G. Large-Scale Synthesis of LPA1-Receptor Antagonist ACT-1016−0707. *Org. Process Rev. Dev.* **2024**, *28*, 577−587.
(37) Roppe, J. R.; Chen, A. C.-Y.; Xiong, Y.; Schrader, T.; Valdez, L. LPAR1 antagonists and uses thereof. WO 2023014908 A1, Feb 09, 2023.
(38) (a) Tummino, P. J.; Copeland, R. A. Residence time of receptor-ligand complexes and its effect on biological function. *Biochemistry* **2008**, *47*, 5481−5492. (b) Knochenhauer, K. E.; Copeland, R. A. The importance of binding kinetics and drug-target residence time in pharmacology. *Br. J. Pharmacol.* **2024**, *181*, 4103−4116.
(39) Bhattarai, P.; Trombley, T. A.; Altman, R. A. Metabolic Stability of Fluorinated Small Molecules: A Physical Organic Chemistry Perspective. *J. Med. Chem.* **2026**, *69*, 1916−1941.
(40) Hansch, C.; Leo, A.; Taft, R. W. A survey of Hammett substituent constants and resonance and field parameters. *Chem. Rev.* **1991**, *91*, 165−195.

https://doi.org/10.1021/acs.jmedchem.6c01049
J. Med. Chem. 2026, 69, 15888−15927

(41) Feng, B.; West, M.; Patel, N. C.; Wager, T.; Hou, X.; Johnson, J.; Tremaine, L.; Liras, J. Validation of human MDR1-MDCK and BCRP-MDCK cell lines to improve prediction of brain penetration. *J. Pharm. Sci.* **2019**, *108*, 2476−2483.
(42) Bowes, J.; Brown, A. J.; Hamon, J.; Jarolimek, W.; Sridhar, A.; Waldron, G.; Whitebread, S. Reducing safety-related drug attrition: the use of in vitro pharmacological profiling. *Nat. Rev. Drug Discovery* **2012**, *11*, 909−922.
(43) Kirichok, A. A.; Tkachuk, H.; Kozyriev, Y.; Shablykin, O.; Datsenko, O.; Granat, D.; Yegorova, T.; Bas, Y. P.; Semirenko, V.; Pishel, I.; Kubyshkin, V.; Lesyk, D.; Klymenko-Ulianov, O.; Mykhailiuk, P. K. 1-Azaspiro[3.3]heptane as a bioisostere of piperidine. *Angew. Chem., Int. Ed.* **2023**, *62*, No. e202311583.
(44) Obach, R. S.; Lombardo, F.; Waters, N. J. Trend analysis of a database of intravenous pharmacokinetic parameters in humans for 670 drug compounds. *Drug Metab. Dispos.* **2008**, *36*, 1385−1405.
(45) Calculated using CDD Vault at pH 7.4.
(46) Broccatelli, F.; Aliagas, I.; Zheng, H. Why decreasing lipophilicity alone is often not a reliable strategy for extending IV half-life. *ACS Med. Chem. Lett.* **2018**, *9*, 522−527.
(47) Caldwell, G. W.; Masucci, J. A.; Yan, Z.; Hageman, W. Allometric scaling of pharmacokinetic parameters in drug discovery: can human CL, Vss and $t_{1/2}$ be predicted from in-vivo rat data? *Eur. J. Drug Metab. Pharmacokinet.* **2004**, *29*, 133−143.
(48) Kelder, J.; Grootenhuis, P. D.; Bayada, D. M.; Delbressine, L. P.; Ploemen, J. P. Polar molecular surface as a dominating determinant for oral absorption and brain penetration of drugs. *Pharm. Res.* **1999**, *16*, 1514−1519.
(49) Bull, J. A.; Croft, R. A.; Davis, O. A.; Doran, R.; Morgan, K. F. Oxetanes: recent advances in synthesis, reactivity, and medicinal chemistry. *Chem. Rev.* **2016**, *116*, 12150−12233.
(50) Luo, X.; Deng, Y.; Li, X.; Zhang, Y.; Deng, C.; Zhang, W. Application of carboxylic acid bioisosteres in drug structure optimization to enhance BBB penetration. *Eur. J. Med. Chem.* **2026**, 118104.
(51) Weidolf, L.; Wilson, I. Minimizing the DILI potential of carboxylic acid-containing drugs: a perspective. *Med. Chem. Res.* **2023**, *32*, 2034−2047.
(52) Sawamura, R.; Okudaira, N.; Watanabe, K.; Murai, T.; Kobayashi, Y.; Tachibana, M.; Ohnuki, T.; Masuda, K.; Honma, J.; Kurihara, A.; Okazaki, O. Predictability of idiosyncratic toxicity risks for carboxylic acid-containing drugs based on the chemical stability of acyl glucuronide. *Drug Metab. Dispos.* **2010**, *38*, 1857−1864.
(53) Che, M.; Borlak, J.; Tong, W. A model to predict severity of drug-induced liver injury in humans. *Hepatology* **2016**, *64*, 931−940.
(54) Zhong, S.; Jones, R.; Lu, W.; Schadt, S.; Ottaviani, G. A new rapid in vitro assay for assessing reactivity of acyl glucuronide. *Drug Metab. Dispos.* **2015**, *43*, 1711−1717.
(55) (a) Marion, T. L.; Leslie, E. M.; Brouwer, K. L. R. Use of sandwich-cultured hepatocytes to evaluate impaired bile acid transport as a mechanism of drug-induced hepatotoxicity. *Mol. Pharmaceutics* **2007**, *4*, 911−918. (b) Swift, N.; Pfeifer, N. D.; Brouwer, K. L. Sandwich-cultured hepatocytes: an in vitro model to evaluate hepatobiliary transporter-based drug interactions and hepatotoxicity. *Drug Metab. Rev.* **2010**, *42*, 446−471.
(56) Funk, C.; Pantze, M.; Jehle, L.; Ponelle, C.; Scheuermann, G.; Lazendic, M.; Gasser, R. Troglitazone-induced intrahepatic cholestasis by an interference with hepatobiliary export of bile acids in male and female rats. *Toxicology* **2001**, *167*, 83−98.
(57) Poon, M. M.; Lorrain, K. I.; Stebbins, K. J.; Edu, G. C.; Broadhead, A. R.; Lorenzana, A. O.; Paulson, B. E.; Baccei, C. S.; Roppe, J. R.; Schrader, T. O.; Valdez, L. J.; Xiong, Y.; Chen, A. C.; Lorrain, D. S. Discovery of a brain penetrant small molecule antagonist targeting LPA1 receptors to reduce neuroinflammation and promote remyelination in multiple sclerosis. *Sci. Rep.* **2024**, *14*, 10573.
(58) Poon, M.; Lorrain, K.; Broadhead, A.; Stebbins, K.; Bagnol, D.; Edu, G.; Joseph, G.; Baccei, C.; Roppe, J.; Schrader, T.; Valdez, L.; Xiong, Y.; Chen, A.; Lorrain, D. The LPAR1 antagonist, PIPE-791 produces antifibrotic effects in models of lung fibrosis. *Respir. Res.* **2025**, *26*, 265.
(59) Hama, A.; Baccei, C.; Chen, A.; Poon, M.; Stebbins, K.; Okamoto, K.; Itani, Y.; Kosugi, T.; Matsushita, M.; Nozawa, K.; Natsume, T.; Takamatsu, H.; Lorrain, D. S. Reduced activation of pain-related brain regions with lysophosphatidic acid receptor subtype-1 antagonist PIPE-791 in a nonhuman primate model of chronic peripheral neuropathy. *J. Neuropharm.* **2025**, *280*, 110647.
(60) Kocherlakota, S.; Nicol, A.; Locri, F.; Stebbins, K. J.; Lorrain, D. S.; Tribble, J. R.; Williams, P. A. Pharmacological blockade of LPAR1 does not provide neuroprotection in a rate model of ocular hypertensive glaucoma. *Transl. Vis. Sci. Technol.* **2026**, *15*, 11.
(61) Yadav, N. D.; Bhide, R. S.; Bora, R. O.; Gunaga, P.; Panda, M.; Priestley, E. S.; Richter, J. Substituted nitrogen containing compounds as ROMK inhibitors and their preparation. WO 2018222795 A1, Dec 6 2018.
(62) Baker-Glenn, C.; Chambers, M.; Chan, B. K.; Estrada, A.; Sweeney, Z. K. 2-(Phenyl or pyridine-3-yl) aminopyrimidine derivatives as kinase LRRK2 modulators for the treatment of Parkinson's disease. WO 2013079495 A1, June 6, 2013.
(63) Lal, G. S.; Pez, G. P.; Pesaresi, R. J.; Prozonic, F. M.; Cheng, H. Bis(2-methoxyethyl)aminosulfur trifluoride: a new broad-spectrum deoxofluorinating agent with enhanced thermal stability. *J. Org. Chem.* **1999**, *64*, 7048−7054.
(64) Miyazaki, S.; Inui, M.; Kurosaki, Y.; Yamamoto, Y.; Izumi, M.; Soma, K.; Pinkerton, A.; Kishida, M. Preparation of sulfonamide compounds having TNAP inhibitory activity. WO 2018119444 A1, June 28 2018.
(65) Kamer, P. C. J.; van Leeuwen, P. W. N. M.; Reek, J. N. H. Wide bite angle diphosphines: XantPhos ligands in transition metal complexes and catalysis. *Acc. Chem. Res.* **2001**, *34*, 895−904.
(66) Perrie, J. A.; Harding, J. R.; Holt, D. W.; Johnston, A.; Meath, P.; Stachulski, A. V. Effective synthesis of 1-α-acyl glucuronides by selective acylation. *Org. Lett.* **2005**, *7*, 2591−2594.
(67) Abbot, N. J. Blood-brain barrier structure and function and the challenges for CNS drug delivery. *J. Inherit. Metab. Dis* **2013**, *36*, 437−449.
(68) Yang, F.; Zhang, Y.; Liang, H. Interactive association of drugs binding to human serum albumin. *Int. J. Mol. Sci.* **2014**, *15*, 3580−3595.
(69) Lillethorup, I. A.; Hemmingsen, A. V.; Qvortrup, K. Prodrugs and their activation mechanisms for brain drug delivery. *RSC Med. Chem.* **2025**, *16*, 1037−1048.
(70) Puris, E.; Fricker, G.; Gynther, M. Targeting transporters for drug delivery to the brain: can we do better? *Pharm. Res.* **2022**, *39*, 1415−1455.
(71) Sidduri, A.; Budd, D. C.; Fuentes, M. E.; Lambros, T.; Ren, Y.; Roongta, V.; Schoenfeld, R. C.; Gillespie, P.; Stevenson, C. S.; Truitt, T.; Qian, Y. Discovery of novel non-carboxylic acid 5-amino-4-cyanopyrazole derivatives as potent and highly selective LPA1R antagonists. *Bioorg. Med. Chem. Lett.* **2014**, *24*, 4450−4454.
(72) **NCT05983939:** Study evaluation safety and tolerability of escalating single and multiple doses of PIPE-791 and food effect in healthy volunteers. **NCT06683612:** PET study of PIPE-791 in healthy volunteers and volunteers with PrMS and IPF.
(73) Howard, J. H.; Seiders, T. J.; Wang, B.; Arruda, J. M.; Roppe, J. R.; Parr, T. Polycyclic antagonists of lysophosphatidic acid receptors. WO 2010141761 A2, Dec 09, 2010.

https://doi.org/10.1021/acs.jmedchem.6c01049
J. Med. Chem. 2026, 69, 15888−15927